Norges miljø- og
biovitenskapelige
universitet

Master's Thesis 2021 60 ECTS
Faculty of Chemistry, Biotechnology and Food Sciences

CMV-specific Immune Responses Induced by Dendritic Cell Vaccines in Glioblastoma patients

And Clinical Benefit

Synne Halvorsen Hougsnæs
Master of Science in Biotechnology

ACKNOWLEDGEMENTS

This research was conducted with the Translational Research Unit at the Department of Cellular Therapy, Oslo University Hospital (Radiumhospitalet), in the period between August 2020 and June 2021. Else Marit Inderberg supervised the project, with Dzung Diep as my internal supervisor.

First, I would like to thank my supervisor, Else Marit Inderberg, and Sébastien Wälchli, for giving me the unique opportunity to work on this project, and for excellent guidance, advice and feed-back during this study. It has been so inspiring, interesting, and exciting to work with you and learn from you.

Second, I would like to thank Hedvig Vidarsdotter Juul, Solveig Mjelstad Olafsrud, and Birthe Mikkelsen Saberniak for giving me great training in the different immunomonitoring techniques, and for always being there if I needed assistance. And everybody else at the Translational Research Unit deserve a big thank you for your help, assistance, advice, good mood, and great humor. It has truly been amazing to be a part of your team. I couldn't have done it without you.

Last, I wish to thank my friends, family, and my boyfriend, for your support and encouraging words.

ABSTRAKT

Glioblastom (GBM) er en WHO-grad IV malign gliom og er den vanligst primære hjernesvulsten. GBM har en av de dårligste prognosene av alle krefttyper, med en median overlevelse på <15 måneder, til tross for standard terapi med kirurgi, strålebehandling og cellegiften temozolomid. Terapier som skal øke pasientens immunsystem, som vaksinebaserte immunterapier, har vist lovende resultater i å forlenge progresjonsfri og total overlevelse i mange kreftformer, inkludert GBM.

Seks pasienter diagnostisert med GBM mottok dendrittisk celle vaksinasjoner mot CMVpp65 protein, telomerase revers transkriptase (hTERT) peptider og survivin peptider i tidsperioden 2014-2016. Immunresponser mot disse peptidene ble undersøkt ved å teste perifere mononukleære blodceller (PBMC) fra tidspunkter før og etter vaksinene i proliferasjonstester og ELISpot, og ved å se på T celle aktivering og funksjon ved hjelp av flow cytometri. PBMC og tumorinfiltrerende lymfocytter ble også analysert ved hjelp av massecytometri for å undersøke lokal immunaktivitet. Dette ble undersøkt for å se om immunresponser kunne bli indusert ved hjelp av vaksinene og om dette påvirket overlevelse.

Alle pasientene viste induserte immunresponser mot minst et av vaksineantigenene i enten proliferasjonstest eller ELISpot. De sterkeste responsene var mot CMVpp65 proteinet, og en av pasientene viste også økt IFN-γ produksjon mot hTERT peptidmiks i ELIspot testen. Intracellulær farging etterfulgt av flow cytometri viste at T cellene produserte TNF-α og/eller IFN-γ i respons til deres spesifikke antigen, og det var en blanding av $CD4^+$ og $CD8^+$ T celler som produserte cytokinene avhengig av pasienten og antigenet. Massecytometri av PBMC og tumorinfiltrerende lymfocytter, der det var tilgjengelig, viste også at cellene uttrykte ulike markører som indikerte at cellene var aktiverte eller hadde blitt eksponert for antigen. Selv om det var for få pasienter i dette studiet til å konkludere, tyder resultatene på at immunresponser ble indusert av DC vaksinene. En av pasientene hadde en total overlevelse på 40 måneder, og denne pasienten hadde også flest detekterbare responser, spesielt mot CMVpp65 protein, og det høyeste antallet DC vaksiner.

ABSTRACT

Glioblastoma multiforme (GBM) is a WHO grade IV malignant glioma and is the most common primary brain tumor. It has one of the poorest prognoses of all cancers, with a median survival of <15 months despite standard therapy with maximal surgical resection followed by radiotherapy and temozolomide treatment. Therapies intended to boost the patient's immune system, such as vaccine-based immunotherapies, have shown promising results in prolonging progression free survival and overall survival in many cancers, including GBM.

Six patients diagnosed with GBM who received dendritic cell (DC)-vaccinations against CMVpp65 protein, telomerase reverse transcriptase (hTERT) peptides, and survivin peptides were tested for immune responses before and after each vaccination to see if immune responses could be induced by the vaccines and if it had an impact on the survival. This was investigated by proliferation assays, ELISpot assays, and flow cytometry looking at T cell activation and function. Peripheral blood mononuclear cells (PBMCs) and tumor-infiltrating lymphocytes (TILs) were analyzed by mass cytometry to investigate local immune activity.

All patients showed induced immune responses against at least one of the vaccine antigens in either proliferation assays or IFN-γ ELISpot assays. The strongest responses in the patients were against the CMVpp65 protein, and one patient also showed increased IFN-γ production against hTERT peptide mix in the ELISpot assay. Intracellular staining followed by flow cytometry showed that the T cells produced TNF-α and/or IFN-γ in response to their cognate antigen, and there was a mix of cytokine producing $CD8^+$ and $CD4^+$ T cells, depending on the patient and antigen. Mass cytometry of PBMCs and TILs, where available, also showed expression of different markers indicative of activation and/or previous exposure to antigens. Although there were too few patients included in this study to conclude, the results suggest that immune responses were induced by DC vaccines. One of the patients had an overall survival of 40 months, and this patient had the most detectable responses, especially against CMVpp65 protein, and the highest amount of DC vaccines.

TABLE OF CONTENTS

1 INTRODUCTION

Glioblastoma

Glioblastoma multiforme (GBM) is the most common primary brain tumor and has one of the poorest prognoses of all cancers. The current standard therapy is surgical resection followed by radiotherapy and temozolomide chemotherapy, but this is rarely curative for GBM and the median survival is <15 months. (Reap et al., 2018; Vik-Mo et al., 2013). This poor survival rate has been attributed in part to intratumoral heterogeneity, glioma cancer stem cells (GSCs), and several mechanisms of immunosuppression (Cuoco et al., 2018). Novel therapies are urgently needed, and clinical trials of vaccine-based immunotherapies have shown promising results in prolonging progression-free survival (PFS) and overall survival (OS) (Cuoco et al., 2018; Reap et al., 2018; Vik-Mo et al., 2013).

Gliomas arise from glial cells, i.e. supporting cells, of the central nervous system (CNS). Histologically, gliomas are categorized based on similarity to their cell of origin and they vary in aggressiveness from benign to highly malignant. GBM is WHO grade IV (Jackson et al., 2019) and the defining histopathologic features of glioblastoma are microvascular proliferation and necrosis. Other signs of malignancy are anaplasia, high mitotic rates, and invasiveness. Immunohistochemical markers are often assessed to ascertain the diagnosis of GBM, like Ki-67 to aid quantification of proliferation, and isocitrate dehydrogenase 1(IDH-1) mutations. IDH mutations occur in about 5-10% of all GBMs and are associated with younger age and better outcome whereas IDH wild-type glioblastoma is associated with older age and poor prognosis. Furthermore, an even worse prognosis is expected with IDH wild-type and human telomerase reverse transcriptase (hTERT) promoter mutation (Wirsching et al., 2016).

T cells and the immune system

The immune system is divided into the innate and adaptive immune system. The innate immune system is the first line of defense and neutralizes foreign pathogens at the invasion site in a non-specific manner with the help of macrophages, neutrophils, natural killer (NK) cells, and antigen-presenting cells (APCs). The adaptive immune system, however, provides targeted and potentially lifelong immunity against foreign pathogens. The effector cells of the adaptive immune system are the T and B lymphocytes (Wilcox et al., 2018).

T cells are defined as lymphocytes that contain T cell receptor (TCR); complexes composed of CD3 subunits and ζ chains and two variable chains responsible for antigen recognition (Santana & Esquivel-Guadarrama, 2006). A T cell is activated by a foreign antigen to

proliferate and differentiate into effector cells when the antigen is displayed on the surface of an APC, usually a dendritic cell (DC). DCs display the antigen in a complex with major histocompatibility complex (MHC) proteins on its surface, referred to as peptide-MHC complexes. There are two main classes of MHC proteins – class I MHC and class II MHC. Class I MHC present foreign peptides to TCRs on cytotoxic (T_C) T cells, whereas class II MHC present foreign peptides to TCRs on helper (T_H) and regulatory T cells (T_{reg}) (Alberts et al., 2015). The specific binding of the cognate antigen to the TCR, with the appropriate affinity, triggers T cell activation. T lymphocytes are divided into T_C $CD8^+$ cells and T_H $CD4^+$ cells (Wilcox et al., 2018). $CD8^+$ T_C have the capacity to directly kill tumor cells. The development of such antitumor $CD8^+$ T cells depends on help from $CD4^+$ T cells. $CD4^+$ T cells also have the ability to directly kill tumor cells (Richardson et al., 2021).

There are different subsets of $CD4^+$ T cells. The main subsets are T_H1, T_H2, T_H9, T_H17, T_H22, T_{reg} and follicular helper (T_{FH}) cells. Three dominant cytokines interleukin (IL)-12, IL-23, and transforming growth factor (TGF)-β have been proposed to control the fate of the $CD4^+$ T cells. When it comes to antitumor T cell immunity, mainly T_H1, T_H2, T_H17, and T_{regs} have been characterized. Differentiation into T_H1 cells is induced by IL-12 and interferon (IFN)-γ. T_H1 cells produce IFN-γ, which together with IL-2 and tumor necrosis factor (TNF), activates the innate immune system and the recruitment, expansion, and functions of T_C $CD8^+$ cells (Richardson et al., 2021). T_H2 cells promote antibody-mediated responses by secreting IL-4, IL-5, IL-9, IL-10, and IL-13 (Wilcox et al., 2018). T_H17 cells are important for immunity against extracellular pathogens, like bacteria and fungi, while T_{reg} cells are responsible for down-regulating the immune responses when needed by releasing immunosuppressive TGF-β and IL-10. T_{reg} also express inhibitory checkpoint molecules like Cytotoxic T-lymphocyte associated protein-4 (CTLA-4) or T cell immunoreceptor with immunoglobulin and ITIM domains (TIGIT) that can contribute to inhibition of immune effector cells (Richardson et al., 2021). The quantity and the quality of effector T cells are essential to an effective immune response. Polyfunctional T_H1 cells, i.e. cells that produce IFN-γ, TNF-α, and IL-2, appear to have better effector functions than monofunctional cells, and they produce more IFN-γ on a per-cell basis than single-cytokine producing cells (Seder et al., 2008).

DCs are the most potent APCs in the human immune system and they are able to activate both naïve and memory immune responses (Sabado et al., 2017). DCs are present in an immature state in most tissues and they are important for immunosurveillance as they monitor their surrounding tissues for antigens and danger signals (van Willigen et al., 2018). Immature

DCs are unable to stimulate T cells because they lack proteins such as CD40, CD56, and CD80 on their surface, which are all necessary for T cell activation. However, immature DCs are very well equipped to capture antigens by receptor-mediated endocytosis, phagocytosis or macropinocytosis. As soon as the DC has captured an antigen, it becomes activated. Its skills to capture antigens decline, and MHC molecules and T-cell stimulatory functions increase, and there is a shift in the chemokine receptor profile (Banchereau & Steinman, 1998; Constantino et al., 2016). Because of the modification of chemokine receptors, i.e. C-X-C chemokine receptor (CXCR) type 4 (CXCR4) and C-C chemokine receptor (CCR) type 7 (CCR7)(Constantino et al., 2016), the activated DCs can migrate to lymph nodes where they present the foreign antigens to T cells using the MHC proteins on the DC surface (Banchereau & Steinman, 1998).

Differentiation of T cells

T cells are released from the thymus as mature, naïve T (T_N) cells with a given epitope specificity following positive and negative selection. T_N cells proliferate and differentiate into effector cells when they encounter their specific antigen presented by a professional APC, and the activated T cells migrate to peripheral tissues and inflamed sites to facilitate the destruction of infected targets. Most of the effector T cells die after antigen clearance while some T cells develop into memory T cells. There are dozens of memory T cell subsets, which express different combinations of surface and intracellular markers, and with diverse cellular functions (Mahnke et al., 2013). Compared with their naïve counterparts, these memory T cells do not have as many requirements for activation, they have an increased proliferative capacity, and a more effective effector response (Pennock et al., 2013). Human T_N and memory T cells can be separated in subclasses based on differential expression of surface molecules (Mahnke et al., 2013) as listed in **Table 1**.

T_N cells express high levels of CD62L and CCR7, the lymph-node homing receptor, and CD45RA (Mahnke et al., 2013). CCR7 and CD62L are also expressed by stem cell memory T (T_{SCM}) and central memory T (T_{CM}) cells, meaning that they home to lymphoid tissues in search of their specific antigen presented by APCs. T_{CM} cells have limited effector functions. Effector memory T (T_{EM}) cells, however, are negative for CCR7 and CD62L, and they patrol peripheral tissues and blood and produce effector molecules, such as IL-4, IL-5 and in IFN-γ, efficiently in response to antigen encounter (Mousset et al., 2019). T_{CM} and T_{EM} are the two main subclasses of memory T cells.

T_{SCM} cells are a different subset of T cells with multiple stem-like properties. T_{SCM} are a relatively rare memory population with a phenotype resembling that of T_N cells, being $CD45RA^+CCR7^+CD62L^+CD27^+CD28^+$. However, T_{SCM} cells express $CD95^+$, which is not expressed by T_N cells. T_{SCM} cells can self-renew and they can generate all memory subsets (Mahnke et al., 2013).

Terminal effector (T_{TE}) cells express markers of senescence, for example CD57, and have low proliferative and functional capacity. This T cell subset is $CD45RA^+CCR7^-CD62L^-$ and generally also negative for CD27 and CD28 (Mahnke et al., 2013).

Table 1: Table of extracellular markers used to differentiate T cell subsets

	T_N	T_{SCM}	T_{CM}	T_{EM}	T_{TE}
CD45RA	+	+	-	-	+
CD45RO	-	-	+	+	-
CCR7	+	+	+	-	-
CD62L	+	+	+	-	-
CD27	+	+	+	+/-	-
CD28	+	+	+	+/-	-
CD57	-	-	-	+/-	+
CD95	-	+	+	+	+

T cells, B cells, and natural killer (NK) cells often infiltrate tumor tissues and are called tumor-infiltrating lymphocytes (TILs) (Lin et al., 2020). The TILs in the T cell compartment consist of T_H $CD4^+$ cells and T_C $CD8^+$ cells, and they are considered to have a higher specific immunological reactivity against tumor than non-infiltrating lymphocytes (Badalamenti et al., 2019).

Immunotherapy in glioblastoma

The goal of cancer immunotherapy is to generate a tumor-specific immune response capable of eliminating cancer cells. The number of clinical trials for immune-based therapies has exploded in recent years and immunotherapies have shown great responses in several solid and hematologic malignancies (Wilcox et al., 2018).

Glioblastoma is a genetically heterogeneous disease with a relatively low mutational burden compared to other tumor types, such as melanoma (**Figure 1**) (Alexandrov et al., 2013).

Cancers with many mutations are associated with increased foreign neoantigen, i.e. mutated antigens only expressed by tumor cells and not normal cells, exposure and therefore, increased immunogenicity. Tumors with high mutational loads are characterized by less immunosuppression and better response to immune checkpoint inhibitors (Wilcox et al., 2018).

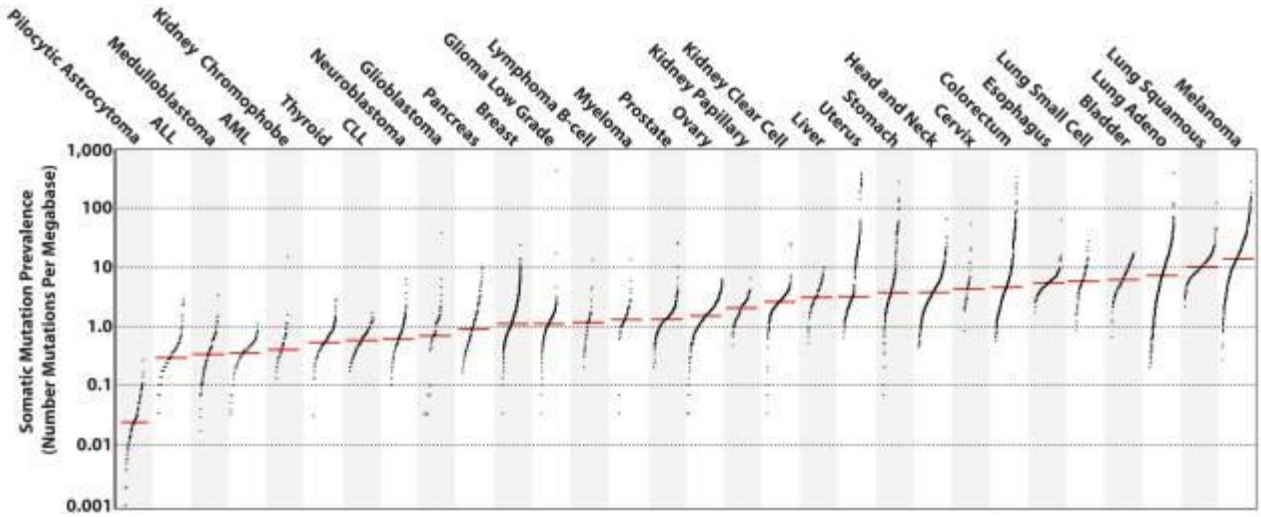

Figure 1 The prevalence of somatic mutations in different cancer types. Every dot represents a sample while the red line is the median number of mutations in the respective cancer types. Glioblastoma have a relatively low mutational burden compared to other tumor types, such as melanoma (Alexandrov et al., 2013)

GBM rarely metastasizes to distant sites, however, resected tumors often recur from cells that infiltrate surrounding brain tissue despite adjuvant chemotherapy and radiotherapy. Glioma stem cells (GSCs) are thought of as drivers of this form of resistance. GSCs harbor robust DNA-repair mechanisms, and they can self-renew and differentiate into stromal and vascular structures that support tumor growth (Jackson et al., 2019).

The Cancer-Immunity Cycle

The Cancer-Immunity Cycle is a series of stepwise events that must be initiated and allowed to proceed and expand repeatedly, for an anticancer immune response to lead to effective killing of cancer cells. The Cancer-Immunity Cycle involves 7 steps (Chen & Mellman, 2013).

In the first step, DCs capture and process neoantigens created by oncogenesis. For an anticancer T cell response to occur, it is important that this step is followed by immunogenic signals, such as pro-inflammatory cytokines, that specify immunity. In step two, DCs present the captured antigens on class I and class II MHC molecules to T cells, which result in the priming and activation of effector T cell responses against the cancer-specific antigens (step

3). This is followed by trafficking of the activated effector T cells to the tumor site (step 4), and the infiltration of the T cells into tumor (step 5). In the tumor, the T cells specifically recognize and bind to cancer cells through the interaction between its TCR and its cognate antigen bound to class I MHC molecules (step 6). The final step is the killing of the target cancer cell. Killing of the cancer cell releases additional tumor-associated antigens, and the cycle is repeated (Chen & Mellman, 2013).

There are many obstacles during the Cancer-Immunity Cycle in cancer patients, and in GBM patients, which prevents an effective anticancer immune response. Tumor antigens may not be detected by DCs or T cells, DCs and T cells may treat antigens as self instead of foreign and create T_{reg} responses rather than effector responses, T cells may not traffic to tumors or be inhibited from infiltrating the tumor, or the tumor microenvironment might release immunosuppressive factors that inhibit the effector cells (Chen & Mellman, 2013). There are also several mechanisms within the glioblastoma microenvironment that facilitate the tumor's evasion of the immune response. GBM tumors express many potent immunosuppressive factors, such as prostaglandin E2 (PGE2) and TGF-β, and the expression of immune checkpoint molecules and recruitment of immunosuppressive cells such as T_{reg} cells can contribute to immune evasion (Preusser et al., 2015).

Immune checkpoints

The term immune checkpoint refers to a group of inhibitory or stimulatory molecules expressed on immune cells, APCs, tumor cells, or other types of cells, which mostly mediate the progress of the adaptive and innate immune system and T cells (**Figure 2**)(Zhang & Zheng, 2020). The effector T cells must pass these immune checkpoints to use their full effector functions. Immune checkpoints have become increasingly used as targets in immunotherapy because of their roles in immune escape, their abnormal expression on different tumor types, and their role in tumor biology (Zhang & Zheng, 2020). CTLA-4, programmed cell death protein-1 (PD-1), lymphocyte-activation gene-3 (LAG-3), TIGIT, and T cell immunoglobulin domain and mucin domain-3 (TIM-3) suppress immune activation. These immune checkpoint pathways are exploited by tumor cells to evade immune detection and can be target for therapies (Preusser et al., 2015).

PD-1 becomes expressed by all T cells during initial antigen-mediated activation, i.e. it is a marker of effector T cells, but it can also be associated with T cell exhaustion, i.e. that the T cells are dysfunctional and loses their effector functions. PD-1 has an essential role in

balancing protective immunity and immunopathology, homeostasis and tolerance, and the receptor acts as a natural brake to prevent over-activation of T cell responses by several mechanisms; inhibiting T cell proliferation, activation, and cytokine production to name some. PD-1 expression levels decrease on responding T cells if the antigen is cleared, and the expressions sustain if the antigen is not cleared, for example during chronic infections and cancer. The ligands for PD-1 is PDL-1 and PDL-2. PDL-1 is expressed by many different cell types, including T cells, B cells and DCs, while PDL-2 is more restricted and is generally expressed by DCs, B cells and macrophages. Both ligands can also be expressed by cancer cells, however expression of PDL-1 if the most common. Expression of the PD-1 ligands are often associated with ongoing inflammatory responses, but mutated cancer cells can also have increased PDL-1 expression. Cytokines regulate the expression of PDL-1 and PDL-2. (Sharpe & Pauken, 2018).

PD-1 expression alone is not enough to indicate if a T cell is exhausted. To determine if a T cell is exhausted, it has to express a number of other cell surface inhibitory molecules, for example LAG-3, TIM-3, CTLA-4 and TIGIT (Wherry & Kurachi, 2015). TIGIT plays a critical role in limiting adaptive and innate immunity and participates in a complex network involving many inhibitory receptors. TIGIT is expressed by activated $CD4^+$ and $CD8^+$ T cells, and is weakly expressed by naïve T cells (Chauvin & Zarour, 2020). The pattern of the co-expression of these checkpoints and the number of receptors being expressed simultaneously affect how dysfunctional the T cells are. However, blocking these receptors using ICIs, as mentioned previously, can undo this exhaustion, and activate the T cells again (Wherry, 2011). ICIs inhibiting PD-1 and CTLA-4, for example, have been approved by the FDA in the treatment of other tumors such as melanoma and non-small-cell lung cancer, but none have yet been approved for GBM (Preusser et al., 2015).

All these features make GBM a cancer that is hard to beat, and novel therapeutic strategies are under investigation.

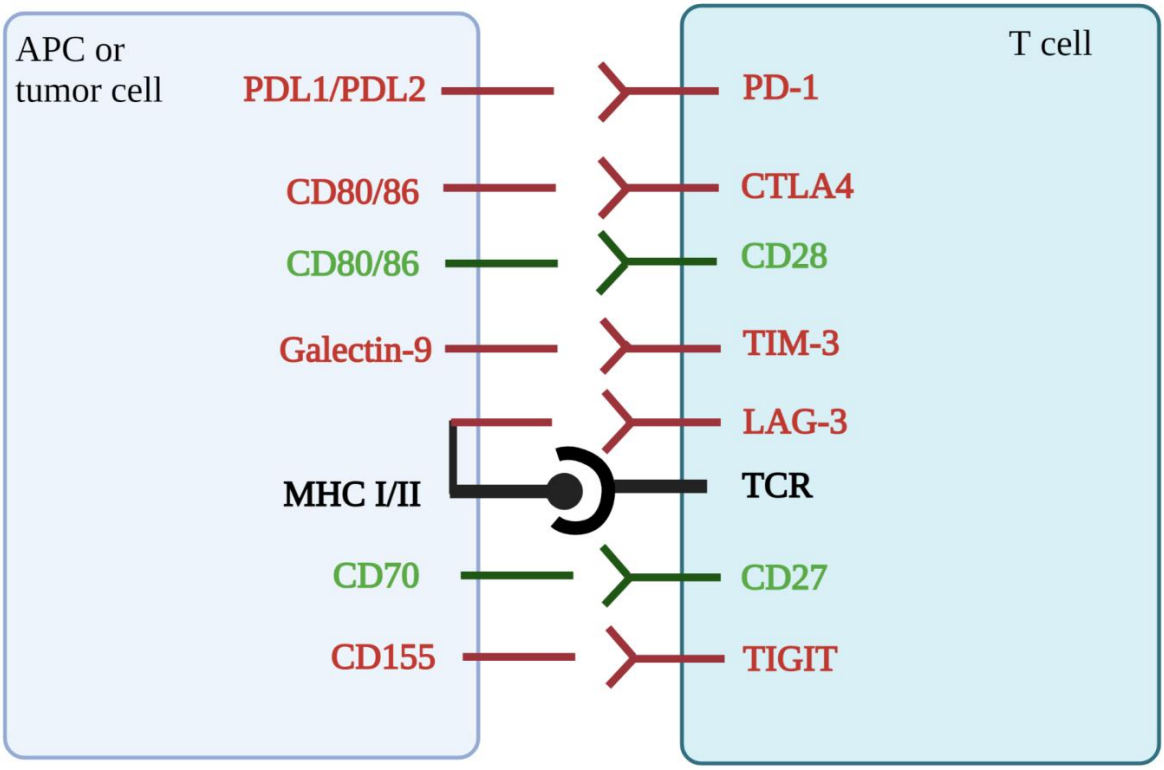

Figure 2 Expression of some of the inhibitory or co-stimulatory receptors on T cells and their respective ligands on an APC or tumor cell. Several ligands on APCs or tumor cells regulate the quality and duration of the immune response. Receptor-ligand interactions that amplify responses (green color) are for example CD28-CD80, or CD28-CD86, and CD27-CD70. Receptor-ligand interactions that suppress immune responses (red color) are for example PD-1-PDL-1/2, CTLA4-CD80/86, TIM3-Galectin-9, TIGIT-CD155. The figure was created using Biorender.com.

Cytomegalovirus

Epstein-Barr virus (EBV) and *human papillomavirus* (HPV) are examples of viruses that have been implicated in human malignancies. Recently, the role of *cytomegalovirus* (CMV) in oncogenic progression has emerged. CMV is a β-herpesvirus that infects 50-70% of the human population, and it establishes a latent infection that lasts for the entire lifetime of the host after the initial infection. CMV is mostly known for causing high morbidity and mortality in fetuses and immunocompromised patients (Brune & Andoniou, 2017; Crough et al., 2012). Studies have reported the presence of the immunogenic CMV antigens IE (immediate early)-1 and pp65 in GBM but not in normal brain tissue (Reap et al., 2018), while others have not detected CMV in GBM (Lau et al., 2005). The exact role of CMV in GBM pathogenesis is uncertain, but there are evidence that suggests CMV infection can promote oncogenic progression, for example by dysregulating key transcription factors, tumor suppressor proteins, or intracellular signaling pathways (Lucas et al., 2011). Nevertheless, the

most important implication of the CMV protein expression in GBM is that the CMV encoded proteins can be targeted for immune-based therapies (Crough et al., 2012).

Telomerase reverse transcriptase

Telomerase reverse transcriptase (TERT) is a component of the cellular enzyme telomerase. Telomerase synthesizes the 5'-TTAGGG-3' repeats of telomeric DNA, which prevents DNA shortening at the chromosomal ends after DNA replication, by reverse transcription of its own RNA template. (Zanetti, 2017)

TERT is a self-antigen that is constitutively expressed in human tumors of various histological types. Approximately 85-90% of all human tumors express high telomerase activity (Kim, 1997) and it is expressed at every stage of the cancer process, making it an attractive target for immunotherapies. TERT expression is regulated by mutations in the promoter region, and these mutations are the most frequent mutations in the cancer genome. GBM is among the cancers that are associated with TERT promoter mutations. (Dosset et al., 2020).

Survivin

Survivin is a member of the inhibitor of apoptosis family and plays a major role in cell division and the inhibition of apoptosis. Overexpression of survivin has been detected in many malignancies, including glioblastoma, while it is minimally expressed in normal healthy tissues. Uematsu et al. found that 85% of GBM cells were immunoreactive to survivin (Uematsu et al., 2005). The overexpression of survivin correlates with tumor aggressiveness, cancer relapse, resistance to therapies, and poor clinical outcome. (Shojaei et al., 2019). Survivin is therefore a potential target in glioblastoma immunotherapy.

Dendritic cell vaccines

Because DCs are highly efficient in generating robust immune responses and maintaining tolerance to self or foreign antigens, DCs are an attractive tool for the design of immunotherapeutic approaches. DCs are primarily used to boost the immune system during cancer treatment and several clinical trials are ongoing across a wide range of malignancies, for example prostate cancer and melanoma. Overall survival is viewed as one of the most relevant outcomes to measure therapeutic benefits (Constantino et al., 2016).

Generation of DC based vaccines

There are several different methodologies used to produce DC-based antitumor vaccines. Ex vivo manipulation of DCs is the most used strategy, and it requires obtaining DCs or DC precursors from patients, manipulate the DCs by inducing maturation and loading antigens, and reinjecting the DCs into the patient (**Figure 3**) (Constantino et al., 2016). For the patients in this thesis, two different procedures involving DC maturation have been used to generate the DC vaccines.

The protocol begins by harvesting peripheral blood mononuclear cells (PBMCs) from the patient by leukapheresis. Monocytes are enriched by elutriation before being cultured in CellGro DC medium supplemented with granulocyte-macrophage-colony-stimulating factor (GM-CSF) and IL-4 for 5 days in Teflon bags. Immature DCs are then cultured for two more days with IL-1β, IL-6, TNF-α, and prostaglandin E2 (PGE2) for maturation (Vik-Mo et al., 2013). This is also called the Jonuleit cocktail.

The second protocol only takes 3 days instead of 7 days as the first protocol and is called the Munich protocol. PBMCs are collected by leukapheresis and monocytes are enriched using elutriation. Monocytes are cultured in RPMI 1640 medium with low endotoxin plus human AB serum supplemented with GM-CSF and IL-4 for 40-72 hours. TNF-α, IL-1β, IFN-γ, PGE2 and the toll-like receptor (TLR) agonist R848 are added to the culture medium for another 20-26 hours for maturation (Lichtenegger et al., 2020; Subklewe et al., 2014).

For both the protocols, three different batches of DCs are transfected with hTERT, survivin and CMVpp65 mRNA, and cryopreserved until use. The vaccines are given intradermally (Subklewe et al., 2014).

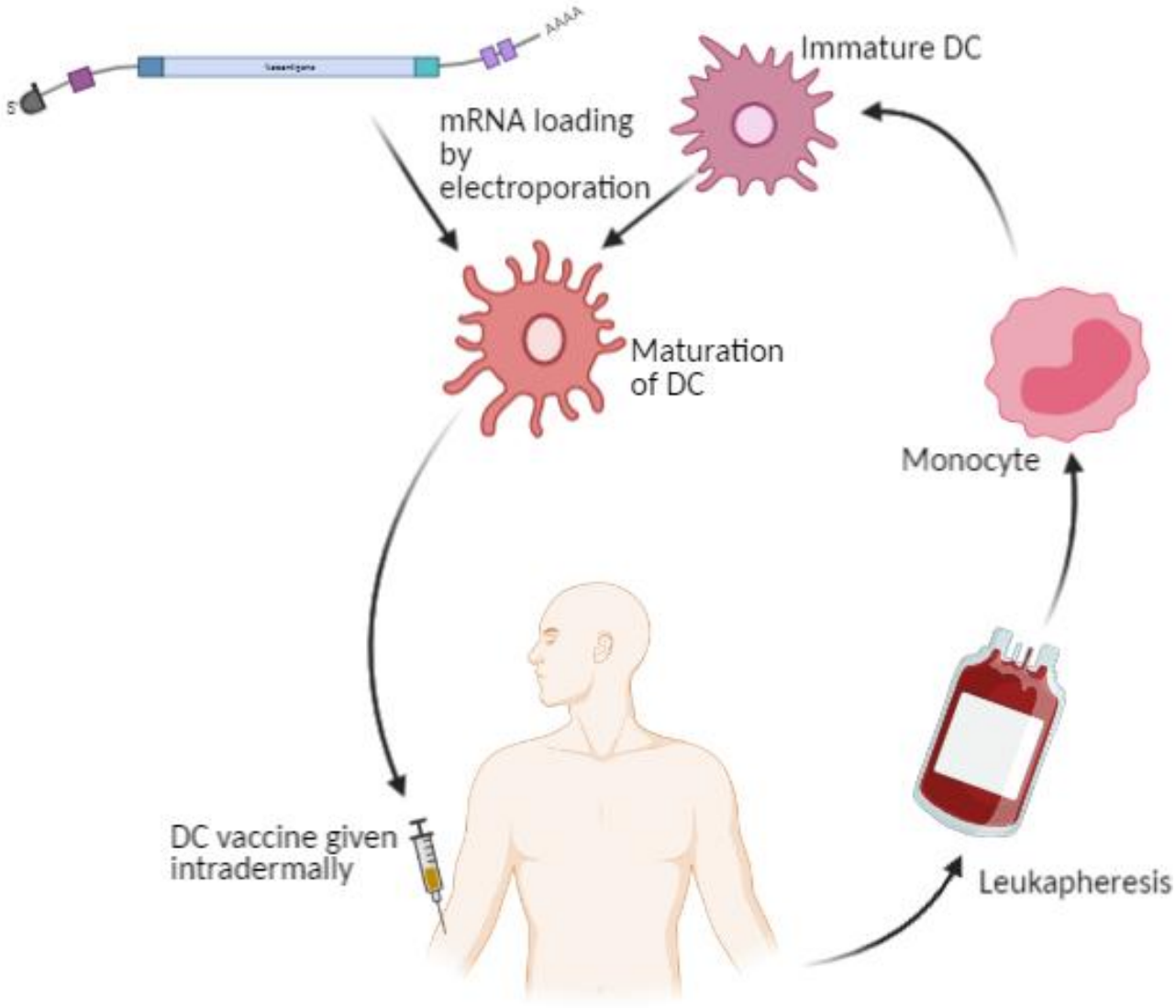

Figure 3 Overview of the production of DCs loaded with hTERT, survivin and CMVpp65. PBMCs are harvested by leukapheresis. Monocytes are enriched by elutriation and cultured to differentiate into immature DCs. The immature DCs are then cultured with a maturation cocktail. The DCs are transfected with hTERT, survivin, and CMVpp65 mRNA either in the immature or mature state. The DCs are injected back into the patient intradermally. The figure was created with Biorender.com. *DC*: Dendritic cell

2 AIM OF THE PROJECT

The main goal of this project was to investigate if we could induce immune responses in glioblastoma patients with dendritic cell vaccines transfected with hTERT and survivin peptides, and CMVpp65 protein, and if the vaccination influenced the survival of the patients. This was investigated by proliferation assays, ELISpot assays and flow cytometry looking at T cell activation and function. As a secondary goal was to investigate if there was a bias towards $CD8^+$ or $CD4^+$ T cell responses. In addition, peripheral blood mononuclear cells (PBMCs) and TILs, where available, were characterized by mass cytometry to assess local immune activity.

3 MATERIAL AND METHODS

Patient selection

6 patients diagnosed with glioblastoma received dendritic cell vaccines against hTERT peptides, survivin peptides, and CMVpp65 protein in 2014-2016. Some of the patients also received vaccines against autologous tumor. The patients received different amounts of vaccines, but blood samples were collected for each patient prior to vaccination and after each vaccine boost. PBMCs from these blood samples were isolated by centrifugation over Lymphoprep (Axis-Shield, Oslo, Norway) and frozen for storage in liquid nitrogen until this project started in August 2020. **Table 2** shows an overview of the patient selection, which dendritic cell vaccine protocol they received, and how many vaccines they received in total. All patients were diagnosed with primary glioblastoma and they were all negative for IDH-1 mutations.

Table 2: Overview of patients, protocols, and peptides used in the vaccination

Patient ID	Protocol	Number of vaccinations	Peptides
CoU-GBM #019	Fast DC (Jonuleit), transfected on mature DCs	8	hTERT, Survivin and CMV
CoU-GBM #027	Munich protocol, transfected on mature DCs	20	hTERT, Survivin, and CMV
CoU-GBM #028	Munich protocol, transfected on mature DCs	10	hTERT. survivin. and CMV
CoU-GBM #035	Munich protocol, transfected on mature DCs	5	hTERT, Survivin, CMV, and autologous
CoU-GBM #038	Munich protocol, transfected on mature DCs	7	hTERT, Survivin, CMV, and autologous
CoU-GBM #044	Munich protocol, transfected on immature DCs	4	hTERT, Survivin, CMV, and autologous

Thawing and counting of cells

Tubes containing 10 ml of DC medium were prepared. Vials from liquid nitrogen were thawed in a water bath while gently swirling the vial in the water until only a small piece of ice was left. The thawed cells were transferred to the tube and 1 ml of medium was used to thaw the remaining piece of ice. When all the ice was thawed, the cells were transferred to the tube. The cells were centrifuged at 700RPM for 5 minutes and resuspended in the medium used for further experiments.

Cell counting was performed using Trypan Blue (Gibco), which enters dead cells. 10µl of Trypan Blue was mixed with 10µl cell suspension in a 96-well U-bottomed microtiter plate. 10µl of this mix was then transferred to a cell counting chamber slide (NanoEnTek) and the cells were counted using Countess II (Invitrogen). The cell counting and viability of the cells after thawing are shown in the supplementary material.

Freezing of cells

The whole procedure was carried out cold. Freezing solutions were prepared in advance to cool down and were kept on cooling blocks for the entire freezing process. Cryo,tubes were labeled and put in the freezer beforehand. $10x10^6$ cells were frozen down per vial. There are different freezing solutions for PBMCs and T cells, and cell lines.

PBMCs and T cells:

Solution 1: 10% HSA (stock of 20% diluted 1:2) in RPMI

Solution 2: 10% HSA + 20% in RPMI

DMSO and RPMI were mixed first to avoid precipitation of HSA.

Cell lines (EBV-LCL):

Solution 1: 50% FBS in RPMI

Solution 2: 50% FBS + 20% DMSO in RPMI

Cells were counted and spun down, and resuspended in half of the final volume of solution 1. Cells were kept on a cooling block for a few minutes to cool down. The same volume of solution 2 as solution 1 were added and mixed well. 1 mL of the cell suspension was aliquoted into cryo tubes immediately, and the vials were kept in -80°C freezer. The vials were transferred to liquid N_2 within one week.

Analysis of antigen-specific T cell responses *in vitro*

PBMCs were isolated from peripheral blood by centrifugation over Lymphoprep (Axis-Shield, Oslo, Norway) and frozen for storage at liquid nitrogen. Thawed PBMCs from different time points were counted and plated in 24-well plates, 2×10^6 cells/well in 1 mL medium, and prestimulated with either 10µL/mL CMVpp65 (Miltenyi Biotec), 10 µM hTERT-mix (CordenPharma and ProImmune Ltd) or 10 µM survivin-mix (ProImmune Ltd). An overview of the peptides is shown in **Table 3**.

After three days, 500 µl of medium containing 60 U/mL IL-2 (Gibco) and 15 ng/mL IL-7 (R&D) were added to the wells. Cells were split or added together when necessary, and medium with a standard concentration of 20 U/mL IL-2 and 5 ng/mL IL-7 was changed the subsequent days.

All PBMCs/T cells were cultured in CellGro DC medium (CellGenix) supplemented with 630 µL gentamycin (Gibco), 5 mL Hepes (BioWest) and 4 mL Mucomyst (Meda AS).

Table 3: List of peptides used to generate T cell responses in vitro and in proliferation assay. *NA*: Not applicable

Name	Peptide sequence	Vendor/catalog nr
Survivin 16-30	DHRISTFKNWPFLEG	ProImmune Ltd/CPD58360
Survivin 86-100	FLSVKKQFEELTLGE	ProImmune Ltd/CPD65315
Survivin 96-110	LTLGEFLKLDRERAK	ProImmune Ltd/CPD6012
Survivin 128-142	AKKVRRAIEQLAAMD	ProImmune Ltd/CPD4791
hTERT 719-20	ALFSVLNYERARRPGLLGASVLGLDDIH RA	CordenPharma-Sveits/30729
hTERT 725	RTFVLRVRAQDPPPE	CordenPharma-Sveits/30730
hTERT 728	AERLTSRVKALFSVL	CordenPharma-Sveits/DP-05-262
GV1001	EARPALLTSRLRFIPK	ProImmune Ltd/CPD54857
UPC2	KSVWSKLQSIGIRQH	ProImmune Ltd/CPD55055
UPC4	SLCYSILKAKNAGMS	ProImmune Ltd/CPD55056
CMVpp65 recombinant protein	NA	Miltenyi Biotec/51909224018 5181126062
Staphylococcus enterotoxin C_3	NA	Toxin Technologies/32801RC

Generation of autologous B lymphoblastoid cell lines by EBV (EBV-LCLs)

One vial of PBMCs was thawed and counted as described earlier. 2-3×10^6 cells were resuspended in 1 mL RPMI with 10 % FCS. 1 mL of Epstein Barr virus (EBV) supernatant B95.8, which comes from a monkey cell line infected with EBV, was added to the 15 mL tubes. The cells were incubated in 37°C, 5 % CO_2 overnight.

The following day, the cells were centrifuged and resuspended in 2 mL RPMI/10 % FCS and 0,2 µg/mL cyclosporin A (Sandoz, Holzkirchen, Germany). Cyclosporin A inhibits growth of T cells and the EBV-infected B cells will be selected. The cells were plated in a 26-well plate. 1 mL of medium containing 10 % FCS and cyclosporin A was changed every three days. The cells were cultured with cyclosporin A for one week. After two weeks, the cells were transferred to a 25 cm^2 flask. Medium was changed and cells were split when necessary. When the volume of the flask reached 20 mL, the cultures were transferred to a 75 cm^2 flask. Medium was changed and cells were split when necessary. When the volume reached 60 mL,

20 mL were transferred to a second 75 cm^2 flask, while 20 mL were frozen down. The cells were kept in culture until further use.

T cell proliferation assay

T cells were seeded in 96-well U-bottomed microtiter plates, at 5×10^4 cells/well. Autologous DCs were irradiated (30Gy) and used as APCs at an APC:T cell ratio of 1:1. Negative controls with T cells and APCs, and positive controls with T cells, APCs, and 0,1 µg/mL *Staphylococcus enterotoxin C3*(SEC_3; Toxin Technologies) were included. T cells were tested for proliferation at each time point and peptide stimuli, i.e 10 µL/mL CMVpp65 protein, survivin-mix and hTERT-mix as listed in Table 3, at a concentration of 10 µM. 20 µL [^{3}H] Thymidine (Montebello Diagnostics, Oslo, Norway), which will be incorporated into chromosomal DNA during cell divisions, was added to each well after two days. The cells were harvested and transferred to a glass fiber filter plate the following day using a Filtermate Harvester and 25 µL of MicroScint (Perkin Elmer) was added to the wells after 1,5 hours of drying in 45°C. The cells were counted by TopCount NXT (Perkin Elmer), a beta-counter that determines the extent of cell divisions by measuring the radioactivity in DNA from the cells, and analyzed by GraphPad Prism 8 software. The assay was performed in triplicates. Stimulatory index (SI), defined as proliferation with peptide divided by proliferation without peptide, was calculated. $SI \geq 2$ is considered a positive response.

Human IFN-γ Single-Color Enzymatic ELISPOT assay

Antigen-specific T cells were counted and 5×10^4 cells/well were added to the precoated wells. Irradiated, autologous PBMCs, or harvested EBV-LCL were used as APCs at an APC:T cell ratio of 1:1. Medium alone was used as negative control, and T cells, APCs and 0,1 µg/mL SEC_3 were used as positive control. 10 µL/mL CMVpp65 or peptide-mix was added to the wells of each time point to a final concentration of 10 µM. All cells were plated in CTL-Test™ Medium (Cellular Technology Limited) supplemented with 1 % fresh L-glutamine (Thermo Fisher). The assay was performed using the manufacture's procedure (CTL, Human IFN-γ Single-Color Enzymatic ELISPOT assay).

In brief, after 24 hours of incubation at 37°C with 5 % CO_2 in a humidified incubator, the plates were washed two times with PBS and then two times with PBS containing 0,05 % Tween. Anti-Human INF-γ (Biotin) Detection Antibody was diluted 4:1000 in Diluent B, and 80 µL of this solution was added to each well. The plate was incubated at room temperature for two hours. 80 µL of Streptavidin-AP, diluted 1:1000 in Diluent C, was added to each well

after three repeated washings with 0,05 % Tween-PBS. The plate was incubated at room temperature for 30 minutes, followed by two washings in 0,05 % Tween-PBS and then two washings in distilled water. 80 µL of Blue Developer Solution was added to each well and incubated in the dark at room temperature for 15 minutes. To stop the reaction, the membrane was gently rinsed with tap water three times. The plate was scanned and counted using Immunospot® Analyzer and software after minimum 24 hours of air-drying. The assay was performed in triplicates.

Phenotyping of PBMCs and TILs using mass-cytometry (CyTOF)

To prevent clumping of cells from patient samples, DNase I (Roche/Sigma) was added during cell thawing. 100 µL of 2 mg/mL DNase was added to 10 mL of pre-warmed RPMI with 10% FCS. PBMCs from different time points and TILs were thawed and counted, and 1-3×10^6 cells per sample were used. The cells were washed and resuspended in Maxpar Cell Staining Buffer (SB, Fluidigm). 0,5 mL of SB was added to the cisplatin aliquot and 250 µL of this 2x solution was added to the samples to be able to separate dead cells from live cells, followed by 5 minutes of incubation in room temperature. The samples were washed to remove excess cisplatin and resuspended in 50 µL SB. Fc-receptor blocking solution was added to the samples to prevent unspecific binding of the antibodies. 50 µL extracellular antibody mix from **Table 4** or **Table 5** was then added to the samples followed by incubation for 30 minutes in the dark. The samples were washed and fixated in 1,6 % PFA, and then washed again. The cells were resuspended in residual volume and 1 mL of ice-cold methanol was added drop wise. The cells were stored in -80°C freezer overnight.

The following day, the methanol was removed by centrifugation, and the cells were washed in SB. Meanwhile, the intercalator was prepared by adding 15 µL SB to the intercalator aliquot to make a 1000x solution. 1 µL of this solution was then added to 0,5 mL SB to make a 2x solution. 100 µL SB and 100 µL of 2x intercalator were added to the samples to separate singlets from doublets. After 20 minutes of incubation, the cells were washed in SB followed by one wash in Cell Acquisition Solution, and the cells were left pelleted until CyTOF analysis.

The samples were resuspended in Cell Acquisition Solution (Fluidigm) and 10% Calibration Beads (Fluidigm). Each sample was prepared just before acquisition on a Helios mass cytometer (Fluidigm) followed by analysis using Cytobank software (Cytobank Inc., Santa Clara, CA, USA).

Table 4: Extracellular antibodies used in staining of PBMCs for mass cytometry

Extracellular antibody panel PBMCs			
n	**Antigen**	**Tag**	**Catalog nr.**
1	CD45	89Y	3089003B
2	CD196 (CCR6)	141Pr	3141014A
3	CD19	142Nd	*3142001B*
4	CD45RA	143Nd	3143006B
5	CD11b	144Nd	*3144001B*
6	CD4	145Nd	3145001B
7	CD8	146Nd	3146001B
8	CD20	147Sm	3147001B
9	CD274 (PDL1)	148Nd	3148017B
10	CD25	149Sm	3149010B
11	LAG-3 (CD223)	150Nd	3150030B
12	CD103	151Eu	3153004B
13	CD66b	152Sm	*3152011B*
14	CD62L	153Eu	3153004B
15	TIGIT	154Sm	3154016B
16	CD27	155Gd	3155001B
17	CD14	156Gd	*3156019B*
18	CD137	158Gd	3158013B
19	CD197 (CCR7)	159Tb	3159003A
20	CD39	160Gd	3160004B
21	CTLA4	161Dy	3161004B
22	CD69	162Dy	3162001B
23	CD183 (CXCR3)	163Dy	3163004B
24	CD161	164Dy	3164009B
25	CD127	165Ho	3165008B
26	NKG2D	166Er	3166016B
27	CD38	167Er	3167001B
28	CD73	168Er	3168015B
29	CD33	169Tm	3169010B
30	CD3	170Er	3170001B
31	CD185 (CXCR5)	171Yb	3171014B
32	CD57/PDL2	172Yb	3172009B/ 3172014B
33	CD184 (CXCR4)	173Yb	3173001B
34	HLA-DR	174Yb	3174001B
35	CD279 (PD1)	175Lu	3175008B
36	CD56	176Yb	3176008B
37	CD16 (FcgRIII)	209Bi	3209002B

Table 5: Extracellular antibodies used for staining of TILs for mass cytometry

Extracellular antibody panel TILs			
n	**Antigen**	**Tag**	**Catalog nr.**
1	CD45	89Y	3089003B
2	CD196 (CCR6)	141Pr	3141014A
3	CD19	142Nd	3142001B
4	CD45RA	143Nd	3143006B
5	CD11b	144Nd	3144001B
6	CD4	145Nd	3145001B
7	CD8	146Nd	3146001B
8	CD20	147Sm	3147001B
9	CD274 (PDL1)	148Nd	3148017B
10	CD25	149Sm	3149010B
11	LAG-3 (CD223)	150Nd	3150030B
12	CD103	151Eu	3153004B
13	CD66b	152Sm	3152011B
14	CD62L	153Eu	3153004B
15	TIGIT	154Sm	3154016B
16	CD27	155Gd	3155001B
17	CCR5	156Gd	3156015A
18	CD137	158Gd	3158013B
19	CD197 (CCR7)	159Tb	3159003A
20	CD39	160Gd	3160004B
21	CTLA4	161Dy	3161004B
22	CD69	162Dy	3162001B
23	CD183 (CXCR3)	163Dy	3163004B
24	CD161	164Dy	3164009B
25	CD127	165Ho	3165008B
26	NKG2D	166Er	3166016B
27	CD38	167Er	3167001B
28	CD73 (AD2)	168Er	3168015B
29	TIM3	169Tm	3169028B
30	CD3	170Er	3170001B
31	CD185 (CXCR5)	171 Yb	3171014B
32	CD57	172Yb	3172009B
33	CD184 (CXCR4)	173Yb	3173001B
34	HLA DR	174Yb	3174001B
35	CD279 (PD1)	175Lu	3175008B
36	CD56	176Yb	3176008B
37	CD16 (FcgRIII)	209Bi	3209002B

After running the samples on CyTOF, an FSC file was generated and uploaded to Cytobank. The following gating strategy was used to find the alive, single cells (

Figure 4):

- Exclude the calibration beads by plotting two channels positive for the beads on the x- and y-axis.
- Choosing the population negative for the beads and further excluding dead cells by plotting CD45 vs cisplatin. The live cells are positive for CD45 and negative for cisplatin.
- Exclude the doublets by plotting the intercalator on the x-axis and event length on the y-axis. The singlets are positive for the intercalator.

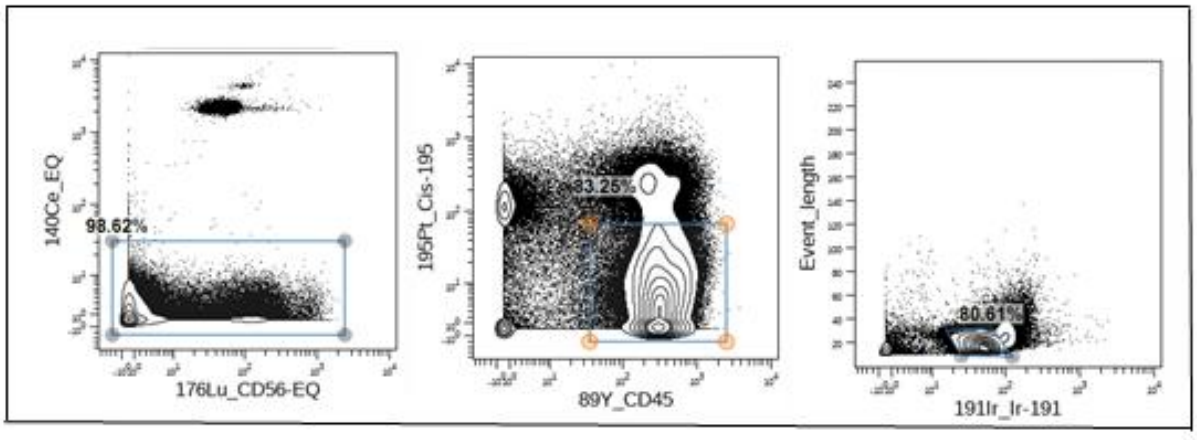

Figure 4 Gating strategy used in Cytobank to find live, single cells. First, the beads are excluded, then the dead cells, and last the doublets are excluded.

Stimulation of TILs

One vial of TILs was thawed and counted as described previously. The cell density was adjusted to 1×10^6 cells/mL. Autologous EBV-LCL were harvested and counted to get as many cells as needed. EBV-LCL were irradiated at 100Gy (300kW, 10mA, 21minutes and 30 seconds), centrifuged and the cell density was adjusted to 1×10^6 cells/mL. 1×10^6 TILs and 1×10^6 EBV-LCL were added to each well on a 26-well plate. 20 µL of CMVpp65 recombinant protein was added to each well, and the cells were incubated in 37°C, 5% CO_2.

On day 2, 50 U/mL of IL-2 was added to each well. Cells were split and medium was changed when necessary. The TILs were cultured for 7 days.

The TILs were cultured in CellGro DC medium (CellGenix) supplemented with 630 µL gentamicin (Gibco), 5 mL Hepes (BioWest), 4 mL Mucomyst (Meda AS) and 5% human serum (TSC Biosciences).

Intracellular cytokine staining

Antigen-specific T-cells were activated with target cells (monocytes/PBMCs/EBV-LCL) *in vitro* at a target:effector ratio of 2:1.

Target cells were thawed (monocytes/PBMCs) or harvested (EBV-LCL) and the cell density was adjusted to 2×10^6 cells/mL in medium. 10 µL/mL of CMVpp65 protein or peptide mix was added to the target cells to a final concentration of 10µM. Harvested EBV-LCLs were incubated with peptide(s) over night.

Effector cells were thawed or harvested, and the cell density was adjusted to 1×10^6 cells/mL in medium. 100 µL of target cell suspension and 100 µL effector cell suspension were added per well in a 96-well plate. 0,2 µL of the protein transport inhibitors BD GolgiStop and BD Golgiplug (BD Biosciences) were added to prevent the cells from secreting the cytokines produced. Negative controls with T cells and target cells, and positive controls with T cells, target cells, 1µM Ionomycin (Sigma-Aldrich) and 50ng/mL PMA (Sigma-Aldrich) were included. The plates were incubated at 37°C and 5% CO_2 overnight.

The next day, the cells were resuspended in 100% serum (FBS) and centrifuged. The cells were stained according to the manufacture's protocol (Beckman Coulter, PerFix-nc Kit). Briefly, the supernatant was removed by blotting the tubes on tissue and 2,5 µL Fixative Reagent (Beckman Coulter) was added followed by 15 minutes of incubation in room temperature. During the incubation, an antibody mix using the conjugated antibodies listed in **Table 6** was made. 2.5 µL of anti-CD3(Invitrogen), -CD4 (BioLegend) and -CD8 (Invitrogen), 5 µL of anti-IFNγ (Invitrogen) and 10 µL of anti- TNFα (BD Pharmingen) were used per tube. 150 µL of Permeabilizing Reagent (Beckman Coulter) was then added to the tubes while mixing well followed by 22.5 µL of the antibody mix. After 15-30 minutes of incubation, 1 mL of 1x Final Solution (Beckman Coulter) was added to the tubes. The tubes were centrifuged and resuspended in 300 µL of 1x final solution. Compensation tubes were made by mixing one drop of BD CompBeads negative control with Final Solution as unstained sample, and one and one antibody with 1x Final Solution and one drop of BD CompBeads Anti-mouse Igk. The samples were analyzed by FACSCanto II flow cytometer and FlowJo™ software (BD).

Table 6 Antibodies and fluorochromes used to stain antigen-specific T cells

Antibody	Fluorochrome	Volume/tube	Catalog nr.	Vendor/lot#
Anti-CD4	BV421	2.5 µL	317434	Biolegend/#B329450
Anti-CD8	PE-Cy7	2.5 µL	25-0088-42	Invitrogen/#2189811
Anti-CD3	APC	2.5 µL	17-0037-42	Invitrogen/#2181732
Anti-TNFα	PE	10 µL	559321	BD Pharmingen/#0042328
Anti-IFNγ	FITC	5 µL	11-7319-82	InVitrogen/#2204969

Staining of TILs

CMV-stimulated TILs were stained for CD3, CD4, CD8, TIGIT and PD-1 to see if TIGIT and PD-1 expression was upregulated by CMV-stimulated TILs.

Autologous EBV-LCL were harvested and the cell density was adjusted to $2x10^6$ cells/mL in medium. 10 µL/mL CMVpp65 protein was added to the tube and the cells were incubated overnight.

The next day, pre-stimulated TILs were harvested, and the cell density was adjusted to $1x10^6$ cells/mL in medium. 100 µL TILs and 100 µL EBV-LCL were added per well in a 96-well plate. Unstimulated TILs, and TILs, EBV-LCL and 1µM Ionomycin (Sigma-Aldrich) and 50ng/mL PMA (Sigma-Aldrich) were included. The plates were incubated at 37°C and 5% CO_2 overnight.

The following day, the cells were transferred to FACS tubes, spun down, and resuspended in 1 mL flow buffer (2 % FCS in PBS). 5 µL aggregated γ-globulin was added to each tube and 25 µL of a master mix containing the antibodies listed in **Table 7** were added to the tubes, followed by 30 minutes of incubation. The cells were washed in 1 mL flow buffer and resuspended in 300 µL flow buffer. Isotype controls were included to see if there were any unspecific binding of the antibodies. The samples were analyzed by FACSCanto II flow cytometer and FlowJo™ software (BD).

Table 7 Antibodies and isotypes used to stain CMV-specific T cells

Antibody	Fluorochrome	Catalog nr	Volume/tube	Vendor/lot#
Anti-CD4	BV421	317434	5 µL	BioLegend/#B329450
Anti-CD8	FITC	MHCD0801	5 µL	Life Technologies
Anti-CD3	BV605	563219	5 µL	BD Horizon
Anti-TIGIT	PE-Cy7	25-9500-42	5 µL	Life Technologies
Anti-PD-1	PE	12-2799-42	5 µL	eBioScience
Mouse IgG1, κ isotype control	PE	559320	5 µL	BD Pharmingen
Mouse IgG1, κ isotype control	PE-Cy7	25-4714-73	5 µL	eBioScience

Statistical analyses

All experiments were done in triplicates, and standard deviation and p-values were calculated using GraphPad Prism 8 software and two-tailed t tests. SI values were calculated in Excel.

Table 8 Table of reagents

Name	Vendor / Batch #	Catalog nr.	Lot # / Batch # / Initials
CellGro DC medium	CellGenix	0020-801-0500	0295Z 0402Z
Mucomyst 200mg/ml	Meda AS	78859	1929429
HEPES 1M	BioWest	L0180-100	S18431L0180
Gentamycin	Fisher Scientific AS	15750-037	2141621 /#324/HVJ 2819290/#342/BMS
rhIL7 2µg/ml	R&D	207-IL-205	AY1318062/#327/BMS
Trypan Blue Stain 0,4%	Life Technologies	15250061	2188980
FBS	Gibco	10500	08F7582K/#346/SJ
PerFix-nc Buffer 1 Fixative reagent	Beckman Coulter	B31168	200070 200071
PerFix-nc Buffer 2 Permeabilizing Reagent	Beckman Coulter	B31168	200070 200071
PerFix-nc Buffer 3 Final 10x Solution	Beckman Coulter	B31168	200070 200071
IL2	Novartis	004184	801313AL/#320/NM 801313BF/#357/CF
RPMI	BioWest	L0500-500	MS00NM1005 MS00P6100H
PMA (500µg/ml)	Sigma-Aldrich	P8139-1MG	MKCG6946 /#270
Ionomycin (1mM)	Sigma-Aldrich	I2909-1ML	098M4026V/#271
BD GolgiStop Protein transport inhibitor	BD Biosciences	554724	8033974
BD GolgiPlug Protein Transport Inhibitor	BD Biosciences	555029	8114699
CMVpp65 recombinant protein	Miltenyi Biotec	130-091-824	51909224018 5181126062
BD CompBeads negative control	BD Biosciences	51-90-9001291	8087701
BD CompBeads Anti-mouse Igk	BD Biosciences	51-90-9001229	8087701
DNase I (2mg/ml)	Roche/Sigma	DN25-100MG	10104159001/#256/EMI
PBS	Lonza	17-512F/12	0000718527
Diluent B	CTL	hIFNgp-2M/5(96-well,	10730JEW

		5 plate kit)	
Diluent C	CTL	hIFNgp-2M/5(96-well, 5 plate kit)	10730JEW
Blue Developer Solution (Blue substrate component 1, Blue substrate component 2, Blue substrate component 3)	CTL	hIFNgp-2M/5(96-well, 5 plate kit)	10730JEW
Streptavidin AP	CTL	hIFNgp-2M/5(96-well, 5 plate kit)	10730JEW
CTL Test-Medium	CTL	hIFNgp-2M/5(96-well, 5 plate kit)	
Maxpar Cell Staining Buffer	Fluidigm	201068	P20F0602
Sterile water	Fresenius Kabi		13PCP231
PFA 4% in PBS	Alfa Aesar, Thermo Fisher	AAJ61899-AK	N08E501K9 /#183
Cisplatin (5mM)	Fluidigm	201195	
Intercalator (125µM)	Fluidigm	201192B	
Maxpar Cell Acquisition Solution	Fluidigm	201240	P20F2503
Calibration beads	Fluidigm	201078	P20C1612
CS&T beads	Puls Medical Devices AS	655051	
Methanol	Sigma-Aldrich	34860-2.5L-R	
3H-Thymidine	Montebello Diagnostics	MT6035	181218/#322/BMS
MicroScint	Perkin Elmer	6013611	86-19361
B95.8 Epstein Barr Virus (EBV) supernatant	Produced in-house	NA	160717 EMI
Human serum (HS)	TCS Biosciences	QUO00570	200168/#316/PD
PHA (40µg/ml)	Thermo Fisher Diagnostics	R30852801	2350062/#222/HVJ
L-glutamine (200mM)	Thermo Fisher	25030081	2091403/#333/BMS
Human Serum Albumin (HSA)	Octapharma	54376	P018A6865

200 mg/ml			
DMSO	Sigma-Aldrich	D5879-1L-M	SHBL1941

4 RESULTS

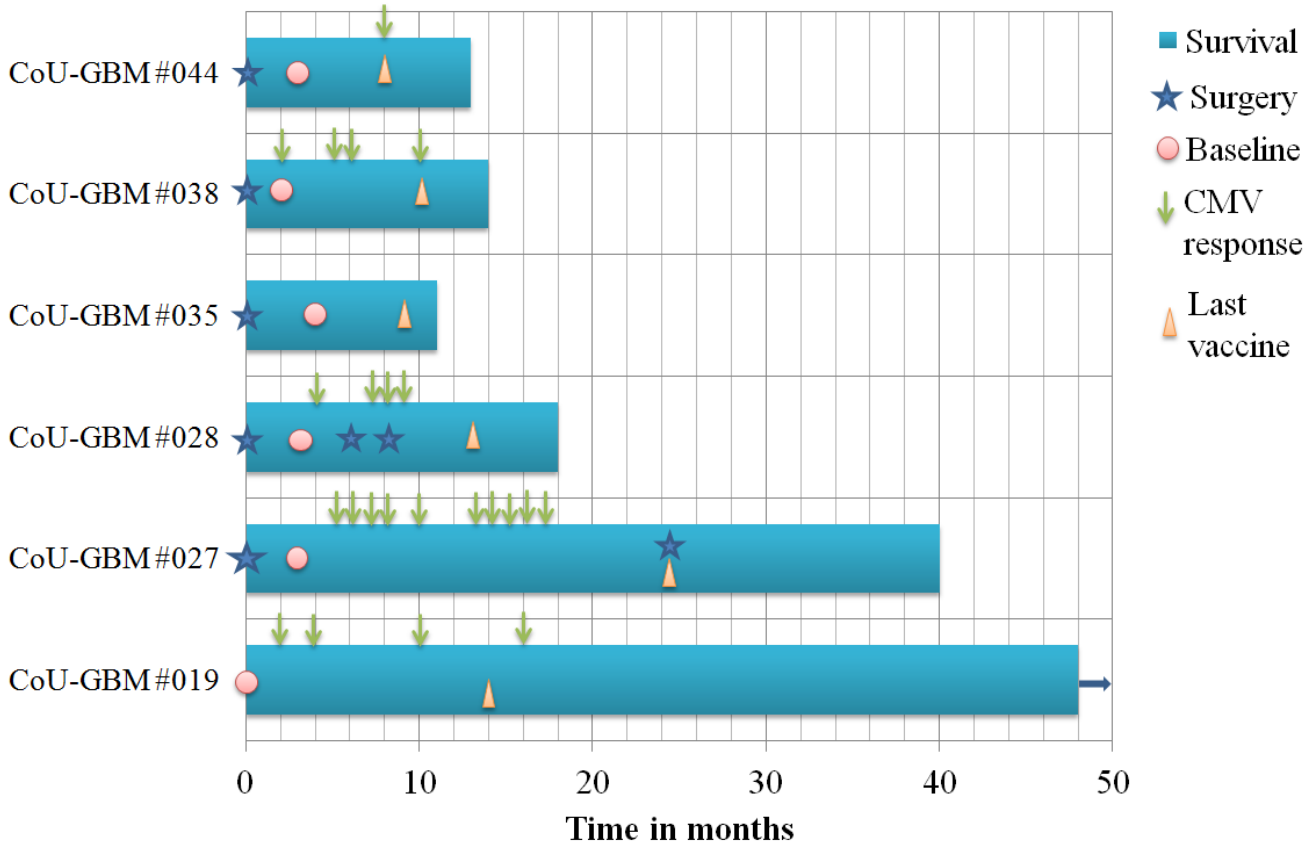

Figure 5 Swimmer plot. Each bar represents the survival of each patient in months from diagnosis/first surgery. *Blue* star: surgery, *red circle*: baseline; *green arrow*: time of CMV response; *orange triangle*: last vaccination.

In this study, six patients diagnosed with GBM who received DC-vaccinations against CMVpp65 protein, hTERT peptides, survivin peptides, (and some autologous tumor mRNA), were tested for immune responses against the three defined antigens before and after each vaccination. The proteins and peptides included CMVpp65 protein, the hTERT peptides 719-20, 725, 728, UPC2, UPC4, and GV1001, and the survivin peptides 16-30, 86-100, 96-110, and 128-142 (**Table 3**). These peptides were selected based on previous experiences in vaccine development and frequency of recognition in a large number of patients (Inderberg-Suso et al., 2012; Wang et al., 2008). All patients, except CoU-GBM #019, received DC vaccines made with the Munich protocol. **Table 2** shows an overview of the patients and what kind of vaccine they received. The patient cohort was 83% male and 17% female. Patients were diagnosed with primary GBM, and none had IDH1-mutations. An overview of the survival of the patients from diagnosis, when they were vaccinated and when responses

against CMVpp65 were seen are depicted in **Figure 5**. CoU-GBM #019 is still alive and received 8 DC vaccines against CMVpp65, hTERT peptides, and survivin peptides in 2015. Therefore, those time points were in focus here and the Swimmer plot is not completely representative for that patient. After the 8 CMVpp65 protein DC vaccines, the patient continued to receive transfected DC vaccines against hTERT and survivin peptides.

After surgery, the patients received standard of care treatment, i.e. radiotherapy and temozolomide, and DC vaccines. The vaccination program was terminated for most patients due to recurrent cancer or because they started treatment with Medrol, a corticosteroid used to decrease inflammation or swelling of the brain. Medrol suppresses/dampens immune responses and therefore inhibits the function of the vaccine. After vaccination termination, the patients went back to standard of care treatment.

To measure immune responses in peripheral blood and tumor infiltrating lymphocytes, where available, proliferation assays, ELISpot, flow and mass cytometry were used.

CoU-GBM #027, except CoU-GBM #019, had the highest OS with 40 months.

Immune response

Lymphocyte proliferation assay measures the ability of lymphocytes in culture to undergo proliferation when stimulated in vitro by a foreign antigen. This response only happens if the patient has been primed to that antigen. The proliferation responses were measured based upon stimulation of pre- and post-vaccination samples by CMVpp65 protein, hTERT- and survivin peptide mixes. In four out of six patients, in vitro lymphocyte proliferation was found upon stimulation with CMVpp65 protein. This included CoU-GBM #019 (**Figure 6A**), CoU-GBM #028 **Figure 6B**), CoU-GBM #027 (**Figure 6C**) and CoU-GBM #038 (**Figure 6E**). Especially CoU-GBM #027 showed a great increase in response towards CMVpp65 protein after vaccination. CoU-GBM #035 (**Figure 6D**) did not show responses against CMVpp65, but a response against survivin-mix was seen at one time point. CoU-GBM #019 and #038 also showed responses against hTERT-mix in addition to CMVpp65 protein. The responses against hTERT- and survivin peptide mixes were in general low, but the responses against CMVpp65 protein were much higher and clearly vaccine induced as they were not detectable in pre-treatment samples except in one patient (CoU-GBM #038), but increased post-vaccination. The only patient who did not show responses in the proliferation assays against any of the peptides or CMV protein was CoU-GBM #044 (**Figure 6F**).

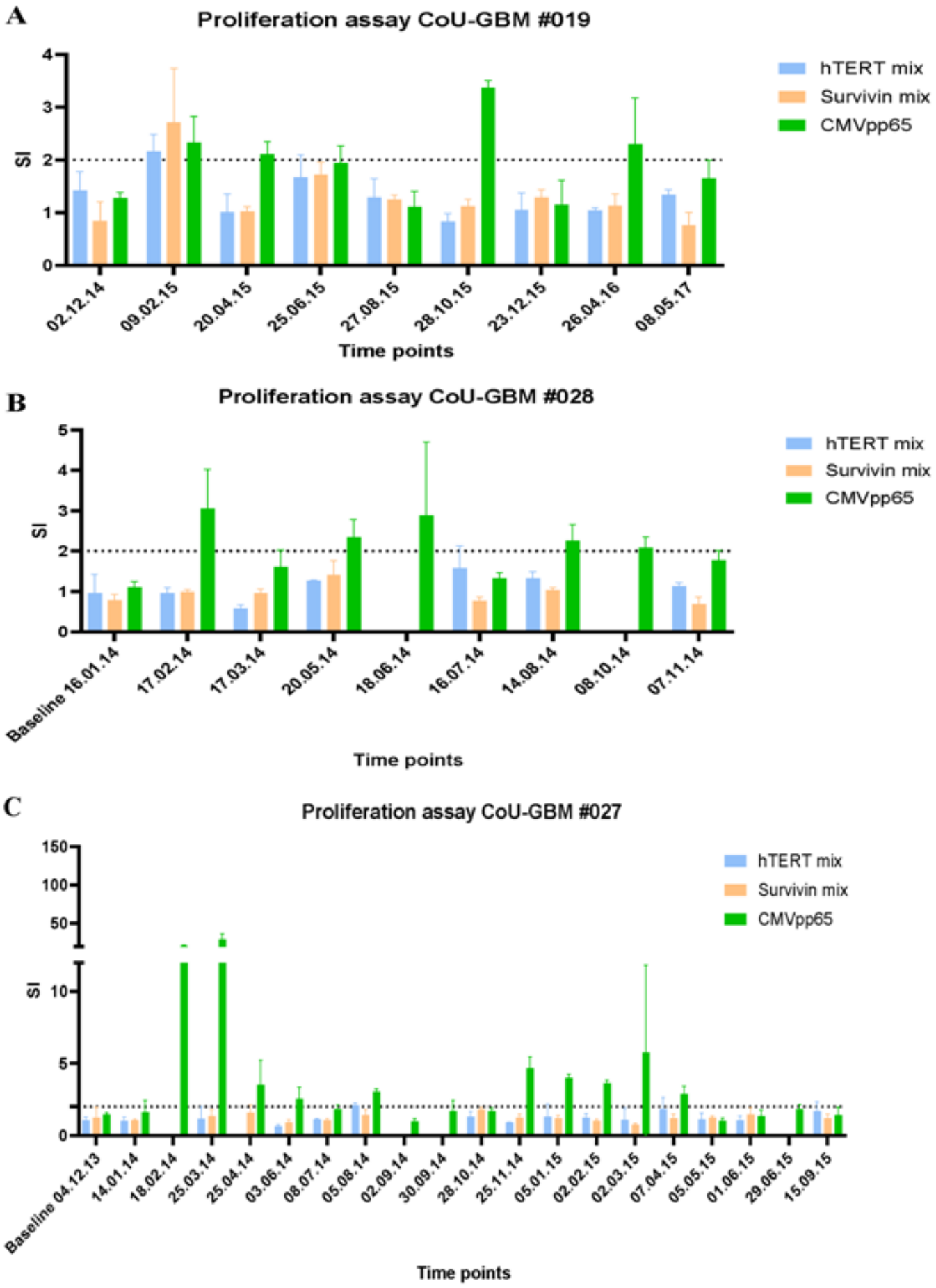
A
Proliferation assay CoU-GBM #019
hTERT mix
Survivin mix
CMVpp65
SI
0
1
2
3
4
02.12.14
09.02.15
20.04.15
25.06.15
27.08.15
28.10.15
23.12.15
26.04.16
08.05.17
Time points
B
Proliferation assay CoU-GBM #028
hTERT mix
Survivin mix
CMVpp65
SI
0
1
2
3
4
5
Baseline 16.01.14
17.02.14
17.03.14
20.05.14
18.06.14
16.07.14
14.08.14
08.10.14
07.11.14
Time points
C
Proliferation assay CoU-GBM #027
hTERT mix
Survivin mix
CMVpp65
SI
0
5
10
50
100
150
Baseline 04.12.13
14.01.14
18.02.14
25.03.14
25.04.14
03.06.14
08.07.14
05.08.14
02.09.14
30.09.14
28.10.14
25.11.14
05.01.15
02.02.15
02.03.15
07.04.15
05.05.15
01.06.15
29.06.15
15.09.15
Time points

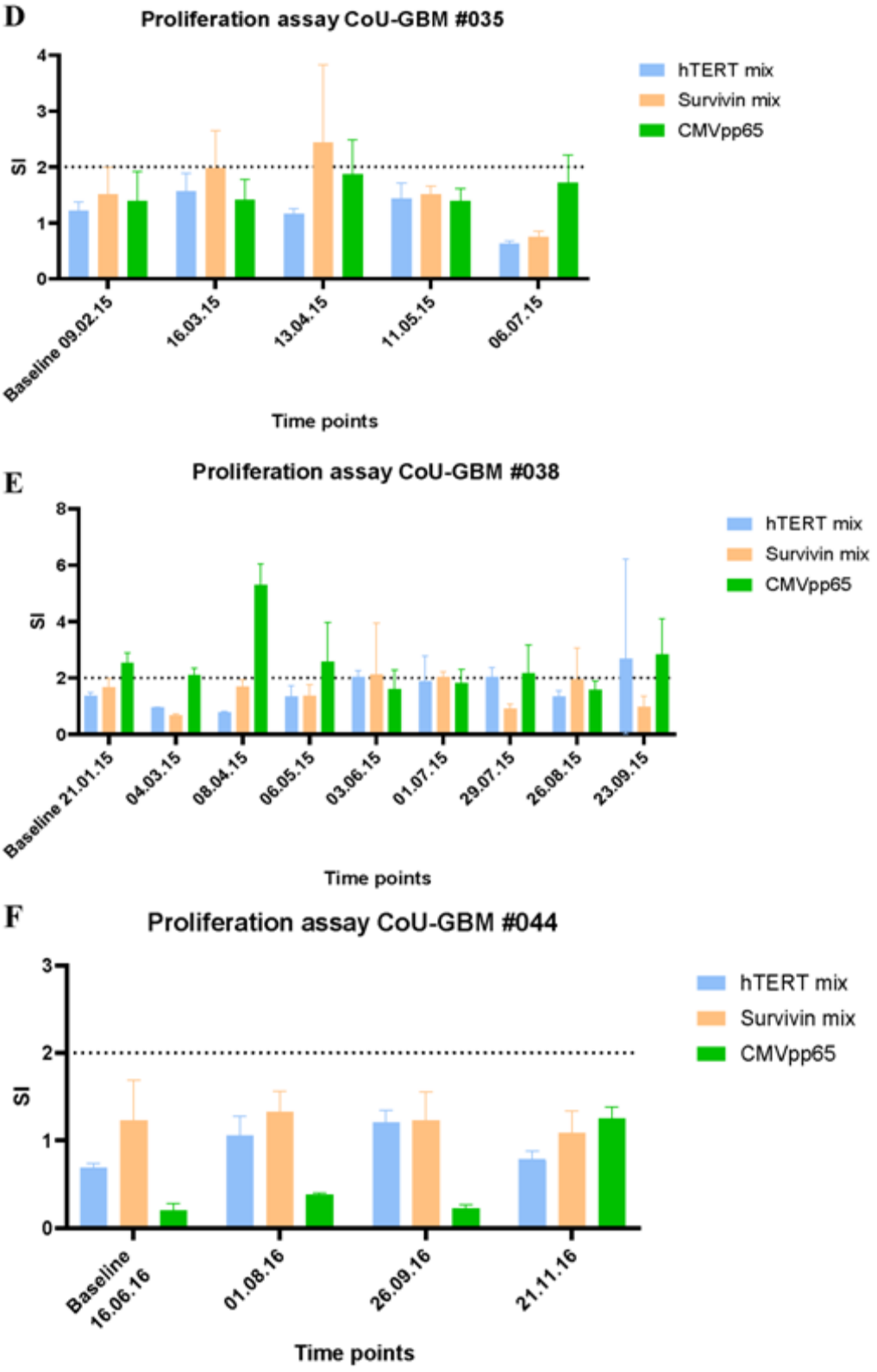

Figure 6 Proliferation assays for each patient using ^{3}H-Thymidine incorporation. Each plot represents one patient and the colored bars represents SI for each peptide mix. APCs and T cells were seeded in a 96-well plate alone, with peptide, or sec-3 (0,1µg/mL) as positive control, at an effector:target ratio of 1:1. CMVpp65 protein (10 µL/mL), the hTERT peptides 719-20, 725, 728, UPC2, UPC4, and GV1001, and the survivin peptides 16-30, 86-100, 96-110, and 128-142 were used, at a final concentration of 10 µM. After two days of incubation, ^{3}H-Thymidine was added to the wells followed by incubation overnight, harvesting the following morning and counting by a β-counter. The assay was

done in triplicates, and the SI value with standard deviation are shown for each time point in the plots. Stimulation Index (SI) ≥2 was considered a positive response (indicated by dotted line). A positive response to CMVpp65 protein, hTERT peptide mix and/or survivin peptide mix was seen in five out of six patients. *SI*: Stimulation index.

If there were enough antigen-specific T cells left after the proliferation assay set up, the remaining T cells were used in an IFN-γ ELISPOT assay as described in the methods chapter (Human IFN-γ Single-Color Enzymatic ELISPOT assay). CMV-stimulated T cells from CoU-GBM #019, #035, #038, and #044, and hTERT-stimulated T cells from CoU-GBM #035 were tested. All the CMV-stimulated T cells produced IFN-γ in response to CMVpp65 (**Figure 7**), suggesting that the T cells were activated and pro-inflammatory, compared to the unstimulated cells. The highest number of IFN-γ producing cells were in patients #035 and #044, which did not show responses in the proliferation assay. The hTERT-stimulated T cells from CoU-GBM #035 (**Figure 8**) also produced IFN-γ in response to hTERT-mix.

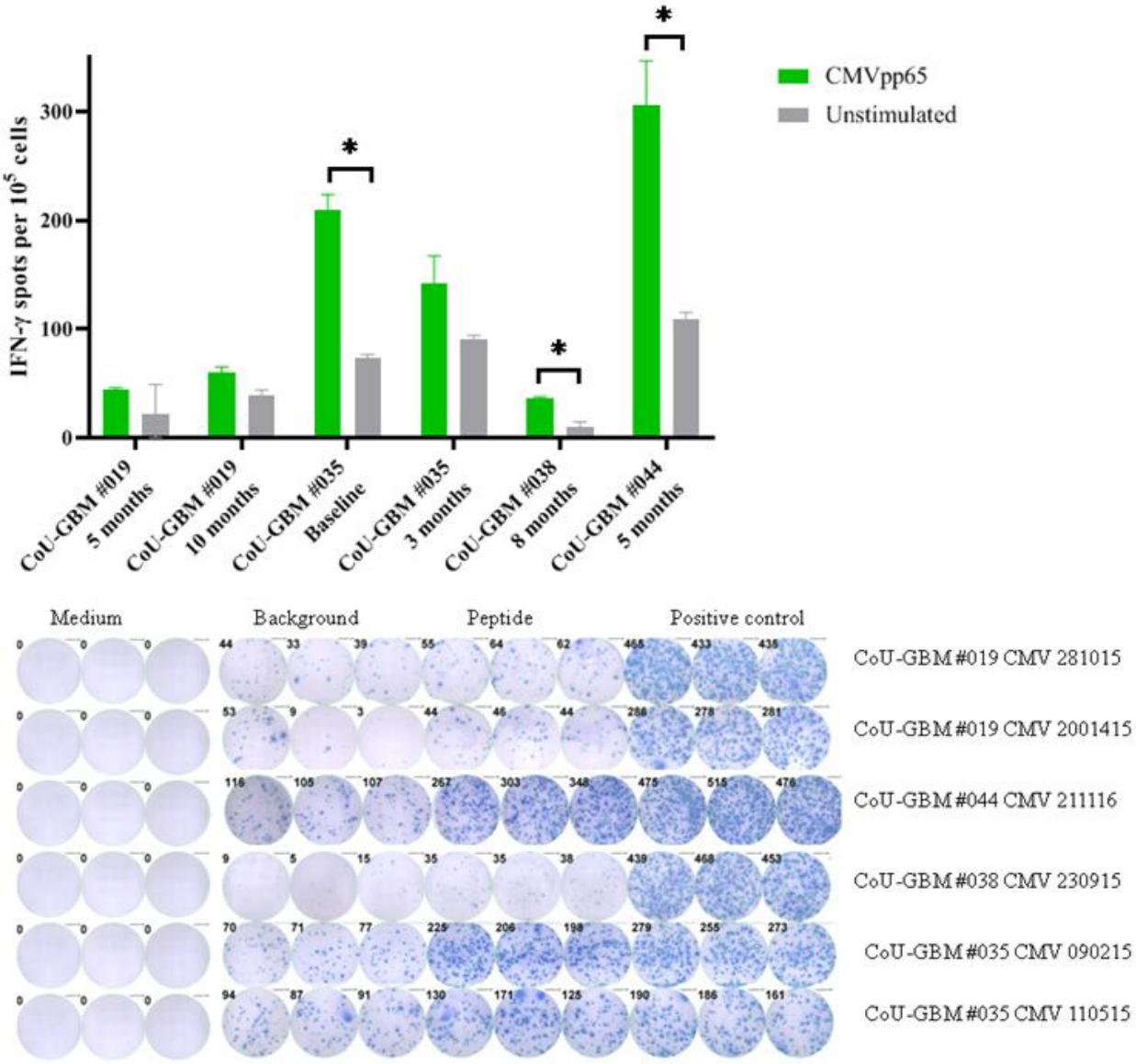

Figure 7 CMV-stimulated T cell responses were assessed by IFN-γ ELISpot assay. APCs and T cells were seeded in a pre-coated ELISpot plate in an effector:target ratio of 1:1. The cells were plated alone (background/unstimulated), with CMVpp65 (10µL/mL), or with 0,1 µg/mL sec-3 (positive control). Medium alone was used as negative control. The cells were incubated for 24 hours, followed by the procedure according to the manufacturer's protocol. The number of spots were counted and quality controlled using the Immunospot analyzer and CTL software. Compared to the background (unstimulated cells), all T cells showed increased IFN-γ production in response to CMVpp65, indicating that the T cells are activated in response to CMVpp65. Statistical significance was calculated by a two-tailed paired t test in GraphPad Prism. *, $P<0.05$.

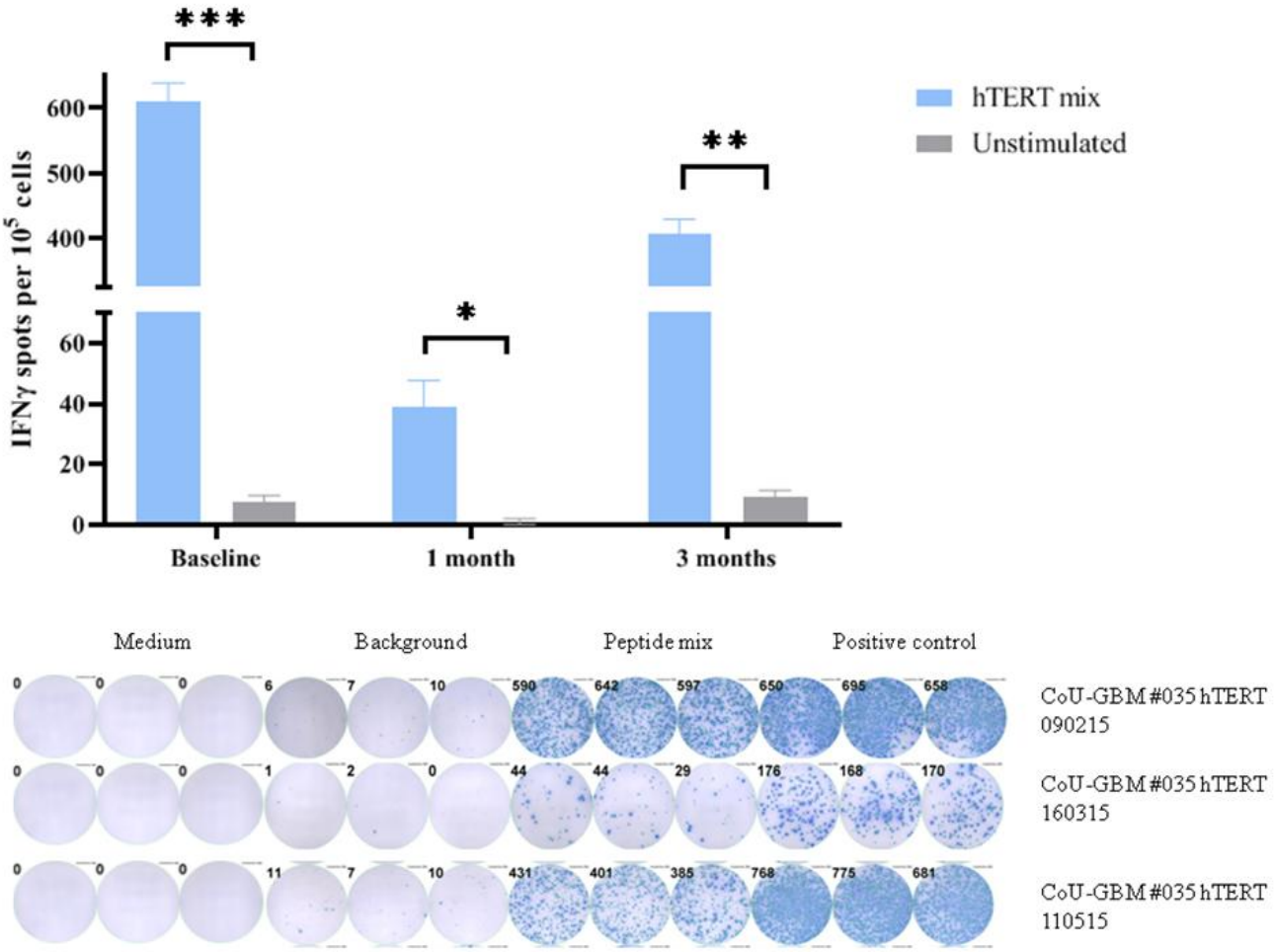

Figure 8 hTERT-stimulated T cell responses were assessed by IFN-γ ELISPOT assays. T cells and APCs were seeded in a 96-well pre-coated ELISpot plate alone (background), with hTERT mix (10µM), or 0,1µg/mL sec-3 (positive control). Medium alone was used as negative control. The plate was incubated for 24 hours, followed by the procedure using the manufacturer's protocol. The plate was scanned and counted using an Immunospot analyzer. Only T cells from CoU-GBM #035 were available. There was increased IFN-γ production in all time points when stimulated with hTERT-mix, compared to the unstimulated cells. Statistical significance was calculated by a two-tailed paired t test in GraphPad Prism. *, P<0.05; **, P<0.002; ***, P<0.001.

Staining of antigen-stimulated T cells from PBMCs

The results from ELISpot showed that the antigen-stimulated T cells produced IFN-γ in response to CMVpp65 protein and hTERT mix. So, we wanted to investigate by flow cytometry if the antigen-stimulated T cells were cytotoxic CD8 T cells or T_H1 CD4 cells, and if the T cells also produced the cytokine TNF-α in response to their antigen. As mentioned previously, the quantity and quality of effector T cells are essential for an effective immune response, and multifunctional T cells are associated with better effector functions. Patients #019, #027, #038 and #044 had enough CMV-stimulated T cells, and only CoU-GBM #027 had enough hTERT- and survivin-stimulated T cells. After overnight incubation with

peptide(s) and monocytes, where available, or irradiated PBMCs, the cells were stained for CD3, CD4, CD8, TNF-α and IFN-γ.

CoU-GBM #019, CoU-GBM #027 and CoU-GBM #044 had more CMV-specific $CD4^+$ T cells than $CD8^+$ T cells, while CoU-GBM #038 had more CMV-specific $CD8^+$ T cells. CoU-GBM #027 had the highest percentage of $CD4^+$ T cells and CoU-GBM #038 had the highest percentage of $CD8^+$ T cells **(Figure 9**). The percentages of $CD4^+$ T cells also remained relatively stable over time, in contrast to the $CD8^+$ T cell populations. The general gating strategy used to find the populations is shown in **Figure 10.**

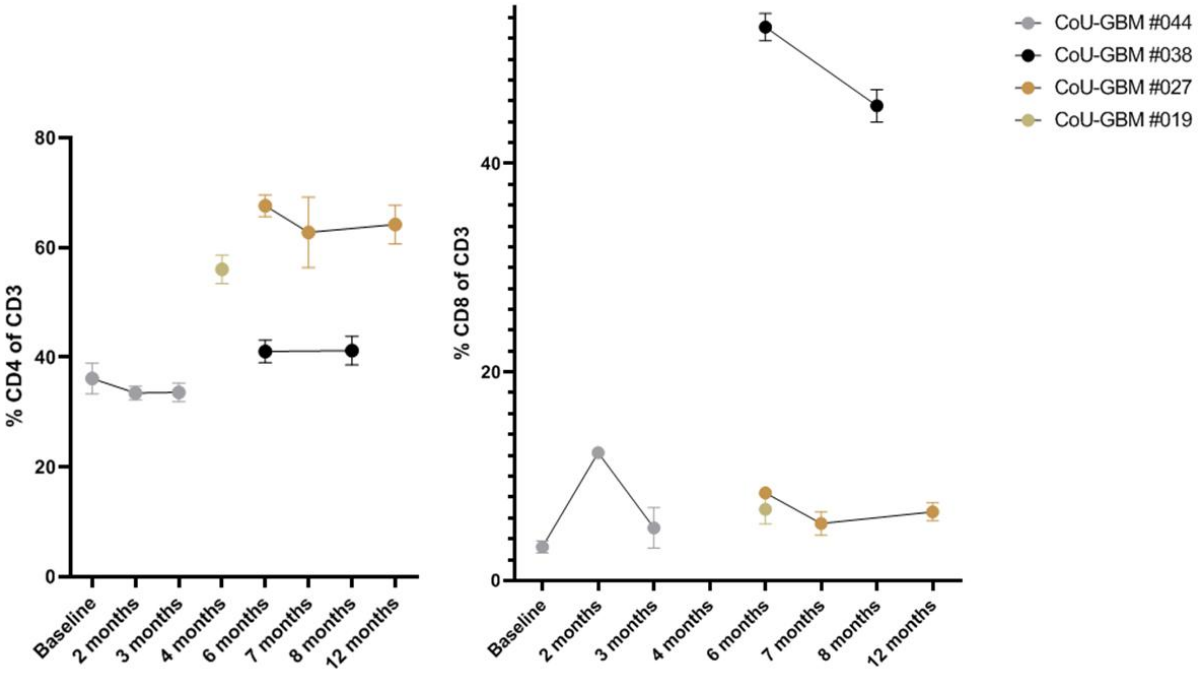

Figure 9 CMV-stimulated T cells from four different patients and different time points were seeded in a 96-well plate with APCs at an target:effector ratio of 2:1. T cells and APCs alone, and T cells, APCs, and PMA+ionomycin were used as negative and positive control, respectively. Protein transport inhibitors were added to the wells to prevent the cytokines from being secreted. After overnight incubation, the cells were stained for CD3, CD4, CD8, TNF-α, and IFN-γ according to the manufacturer's protocol, and analyzed by flow cytometry. The plots show the percentages of $CD4^+$ (left) and $CD8^+$ (right) T cells in each patient at different time points. Each color represents a patient and the dots represents time points. CoU-GBM #027 had the highest percentage of $CD4^+$ T cells, whereas CoU-GBM #044 had the lowest percentage. The frequency of the $CD4^+$ T cells remained stable over time. CoU-GBM #038 had a much higher percentage of $CD8^+$ T cells compared to the other three patients.

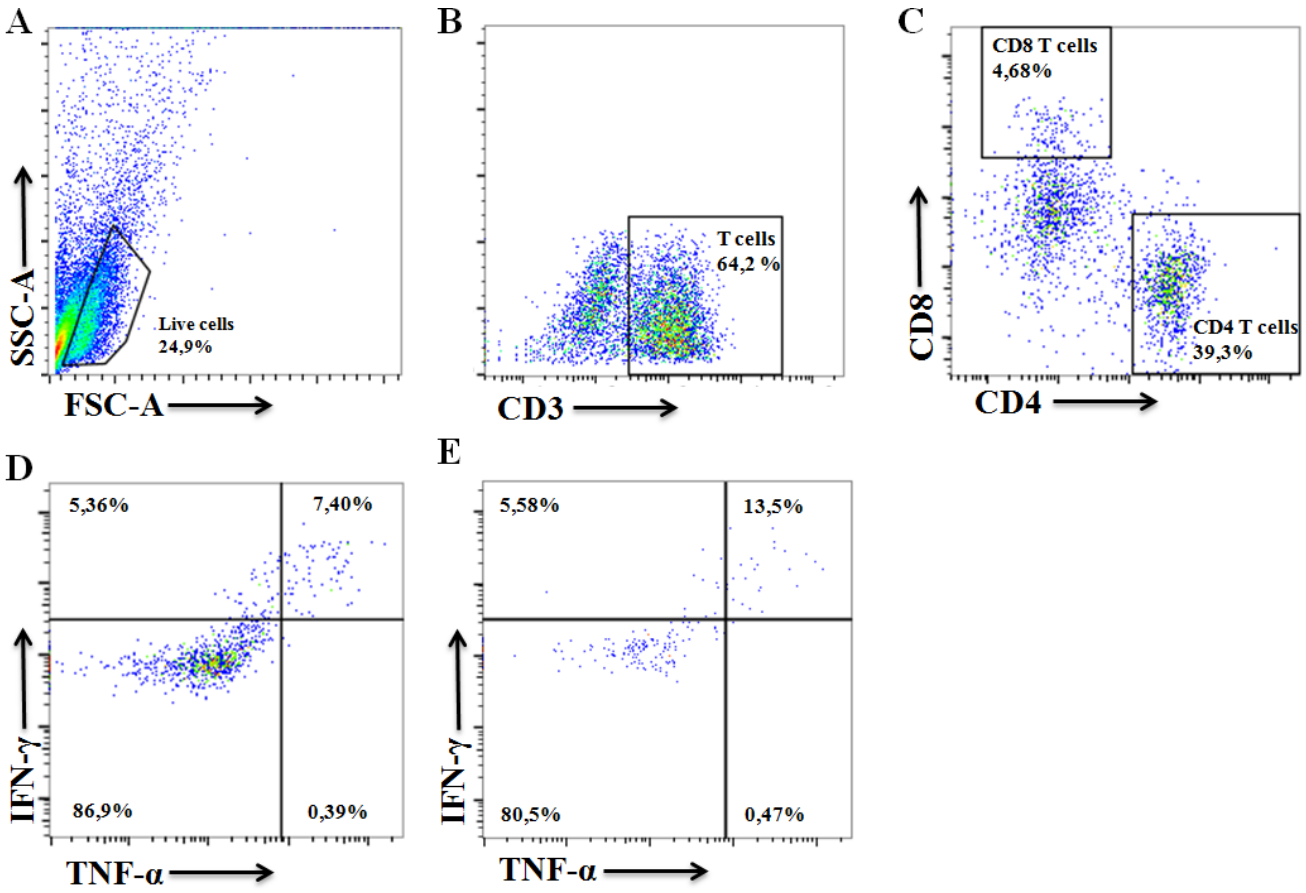

Figure 10 Gating strategy of CMV-stimulated T cells from baseline of CoU-GBM #044. **A**. SSC-A and FSC-A plot used to generate the live cell gate. Debris and dead cells are excluded. **B.** CD3 plot to gate the T cells and exclude the APCs. **C**. $CD4^+$ and $CD8^+$ T cell populations. **D**. Plot of the $CD4^+$ cytokine producing T cells. **E**. Plot of the $CD8^+$ cytokine producing T cells. In both the $CD4^+$ and $CD8^+$ T cell populations, production of TNF-α and IFN-γ together, or IFN-γ alone, were the most common in response to CMVpp65 protein.

It was mainly the $CD4^+$ T cells that produced cytokines in response to antigen presentation in CoU-GBM #027. The hTERT-specific $CD4^+$ T cells produced IFN-γ (**Figure 11**), while the T cells stimulated with CMVpp65 protein were either polyfunctional, or produced IFN-γ alone (**Figure 13**). There were few $CD8^+$ cytokine producing T cells in the hTERT and CMV compartment, however, among the survivin-stimulated T cells, $CD4^+$ and $CD8^+$ TNF-α and/or IFN-γ producing cells were present (**Figure 12**).

The percentages of cytokine producing cells were low in CoU-GBM #038 and there was a mix of $CD4^+$ and $CD8^+$ T cells that produced IFN-γ or TNF-α (**Figure 14**). In CoU-GBM #044, however, the percentages of cytokine producing T cells were relatively high, and $CD4^+$ and $CD8^+$ T cells producing IFN-γ and/or TNF-α were present, with the highest percentages

in polyfunctional $CD8^+$ T cells (**Figure 15**). So, the vaccine induced both CD4 and CD8 effector functions in the patients, although to different degrees.

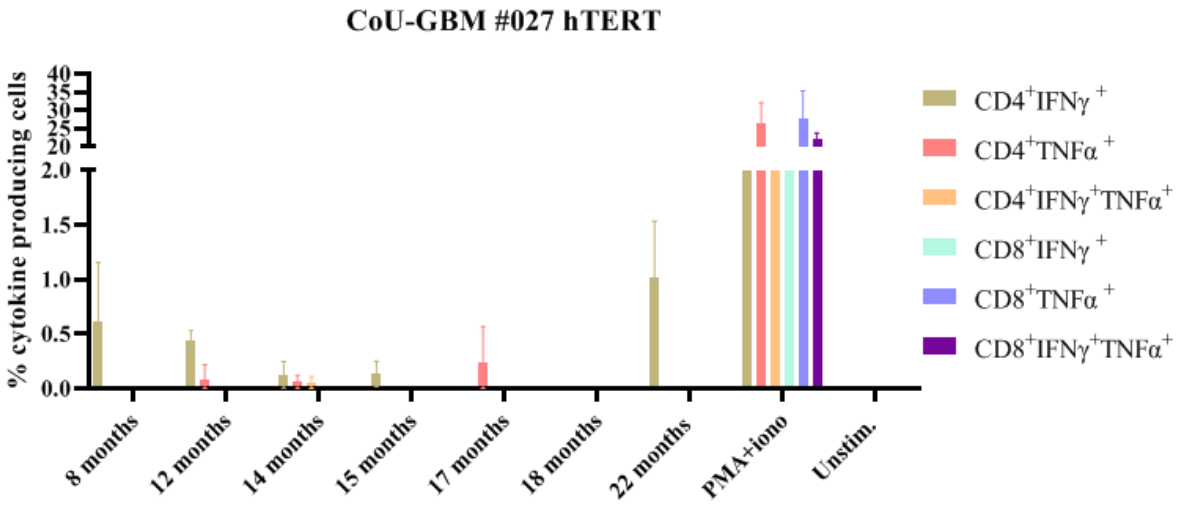

Figure 11 Intracellular cytokine staining of hTERT-stimulated T cells from different time points from CoU-GBM #027. hTERT stimulated T cells from 7 different time points were seeded in a 96-well plate with monocytes at an target:effector ratio of 2:1. T cells and monocytes alone, and T cells, monocytes, and PMA+ionomycin were used as negative and positive control, respectively. Protein transport inhibitors were added to the wells to prevent the cytokines from being secreted. After overnight incubation, the cells were stained for CD3, CD4, CD8, TNF-α, and IFN-γ according to the manufacturer's protocol, and analyzed by flow cytometry. Each colored bar represents a T cell population and cytokine production. It was predominantly $CD4^+$ T cells that produced IFN-γ in response to hTERT mix.

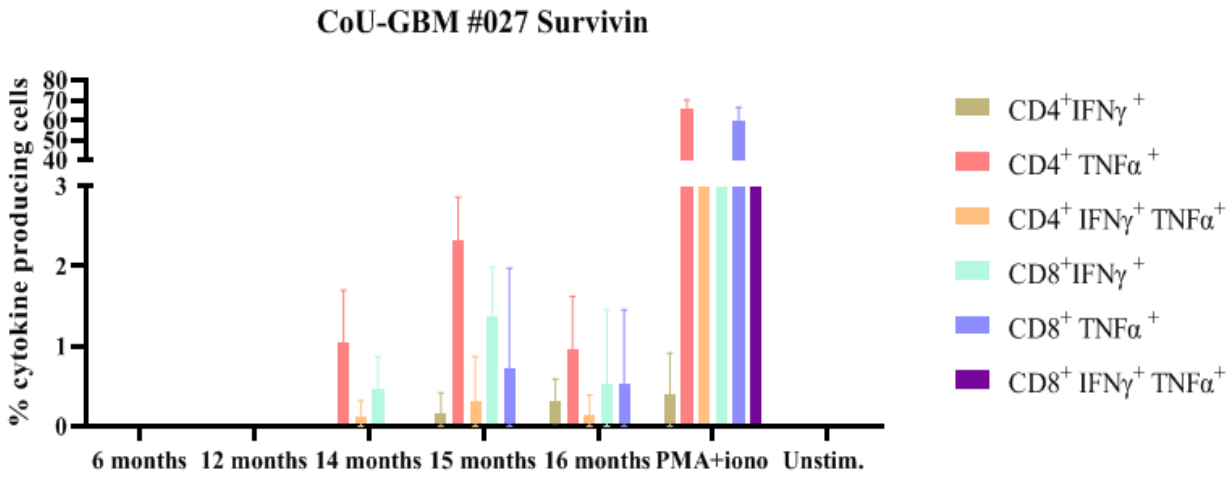

Figure 12 Intracellular cytokine staining of survivin-stimulated T cells from different time points from CoU-GBM #027. Survivin stimulated T cells from 5 different time points were seeded in a 96-well plate with monocytess at an target:effector ratio of 2:1. T cells and monocytes alone, and T cells, monocytes, and PMA+ionomycin were used as negative and positive control, respectively. Protein transport inhibitors were added to the wells to prevent the cytokines from being secreted. After overnight incubation, the cells were stained for CD3, CD4, CD8, TNF-α, and IFN-γ according to the manufacturer's protocol, and analyzed by flow cytometry. Each colored bar represents a T cell population and cytokine production. Monofunctional $CD4^+$ and $CD8^+$ T cells producing either TNF-α or IFN-γ were the most common in response to survivin mix.

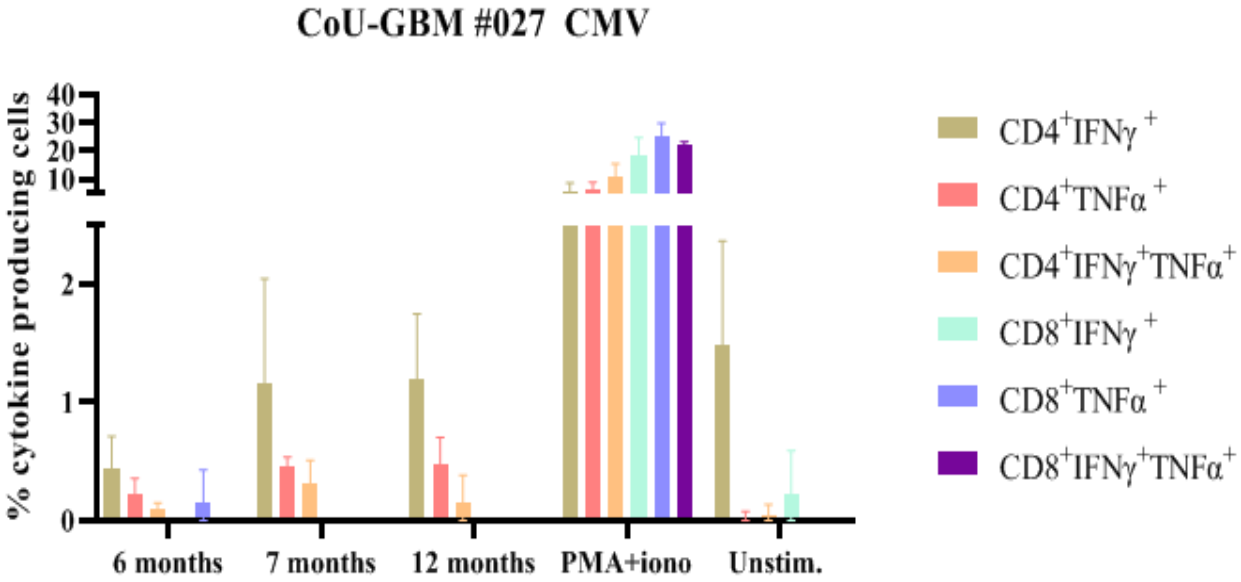

Figure 13 Intracellular cytokine staining of CMV-stimulated T cells from different time points from CoU-GBM #027. CMV stimulated T cells from three different time points were seeded in a 96-well plate with monocytes at an target:effector ratio of 2:1. T cells and monocytes alone, and T cells, monocytes, and PMA+ionomycin were used as negative and positive control, respectively. Protein transport inhibitors were added to the wells to prevent the cytokines from being secreted. After overnight incubation, the cells were stained for CD3, CD4, CD8, TNF-α, and IFN-γ according to the manufacturer's protocol, and analyzed by flow cytometry. Each colored bar represents a T cell population and cytokine production. In response to CMVpp65 protein, monofunctional $CD4^+$ T cells were the predominant cytokine producing T cell population.

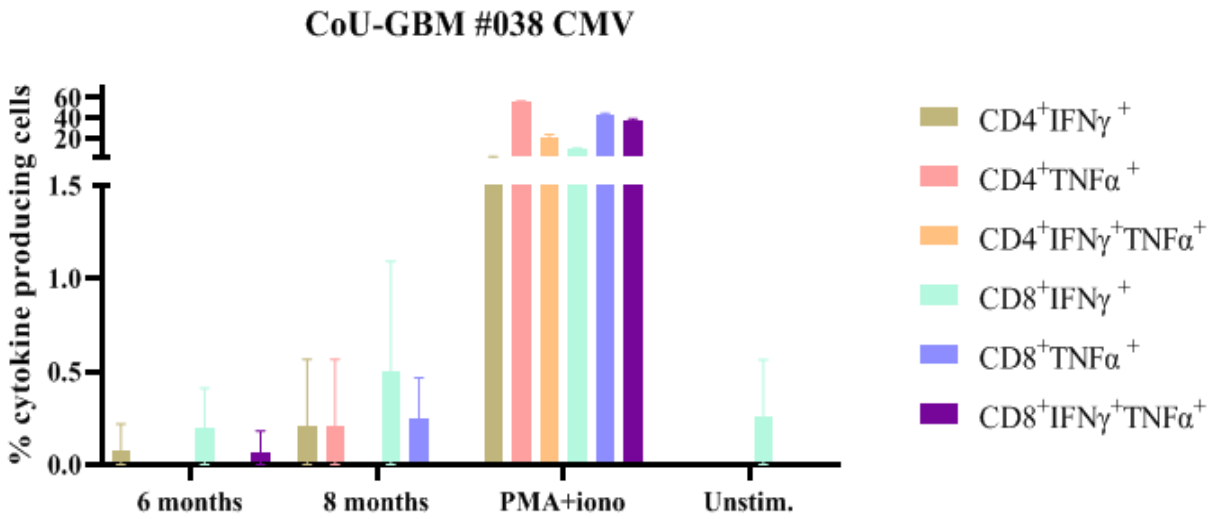

Figure 14 Intracellular cytokine staining of CMV-specific T cells from different time points from CoU-GBM #038. CMV stimulated T cells from two different time points were seeded in a 96-well plate with irradiated PBMCs at an target:effector ratio of 2:1. T cells and PBMCs alone, and T cells, PBMCs, and PMA+ionomycin were used as negative and positive control, respectively. Protein transport inhibitors were added to the wells to prevent the cytokines from being secreted. After overnight incubation, the cells were stained for CD3, CD4, CD8, TNF-α, and IFN-γ according to the manufacturer's protocol, and analyzed by flow cytometry. Each colored bar represents a T cell population and cytokine production. There were mainly monofunctional T cells that produced TNF-α or IFN-γ in response to CMVpp65 protein in patient #038.

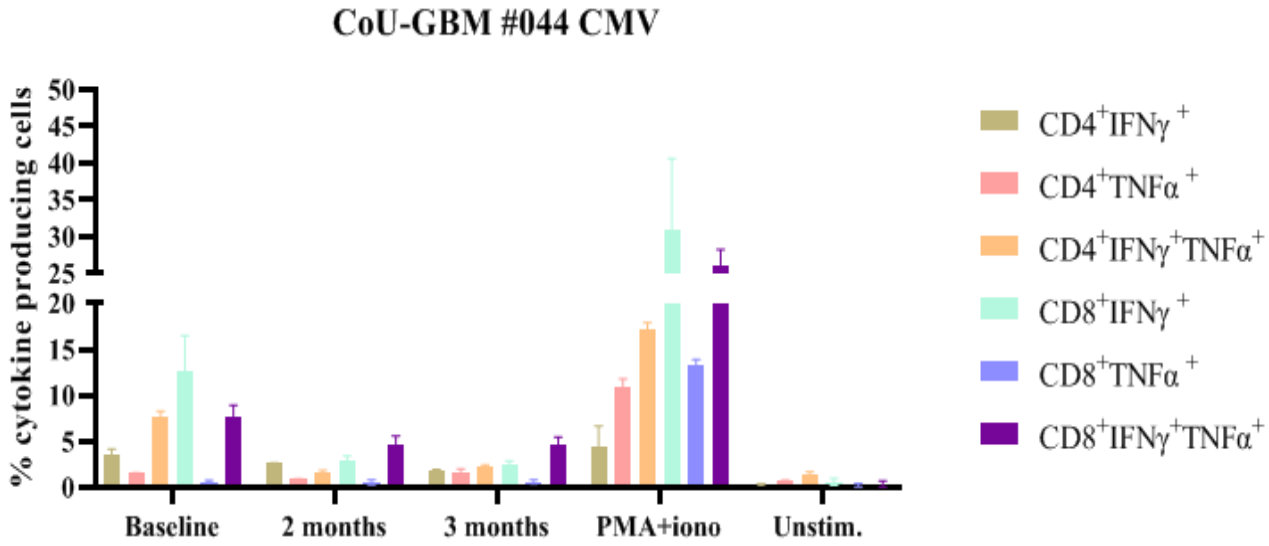

Figure 15 Intracellular cytokine staining of CMV-specific T cells from different time points from CoU-GBM #044. CMV stimulated T cells from 3 different time points were seeded in a 96-well plate with monocytes at an target:effector ratio of 2:1. T cells and monocytes alone, and T cells, monocytes, and PMA+ionomycin were used as negative and positive control, respectively. Protein transport inhibitors were added to the wells to prevent the cytokines from being secreted. After overnight incubation, the cells were stained for CD3, CD4, CD8, TNF-α, and IFN-γ according to the manufacturer's protocol, and analyzed by flow cytometry. Each colored bar represents a T cell population and cytokine production. Both monofunctional and polyfunctional $CD4^+$ and $CD8^+$ T cells were present in response to CMVpp65 protein in patient #044.

Mass cytometry of PBMCs and TILs

Flow cytometry is a useful and common tool used to profile multiple parameters of the immune system, but flow cytometry is limited by the number of parameters that can be analyzed at the same time. In flow cytometry, the antibodies are labelled with fluorophores. The fluorophores are excited by a laser to emit light that is captured by a detector in the flow cytometer. The emission spectra of these fluorophores overlap and must be compensated, and therefore limiting the number of fluorophores that can be used at the same time. Time-of-flight mass cytometry (CyTOF), however, uses antibodies conjugated to heavy metal isotopes that are normally not present in biological specimens. The time-of-flight of each metal depends on the atom's mass, and detection overlap and background is generally low because cells do not contain heavy metals. Because no fluorophores are used in CyTOF, a lot more markers can be used simultaneously compared to flow cytometry (Gadalla et al., 2019). This is especially favorable when limited material, as was the case here, is available.

To characterize the immune profile of the patients, PBMCs and TILs, where available, were analyzed by mass cytometry. One panel for PBMCs consisting of 37 extracellular markers (**Table 4**) and one panel for TILs consisting of 37 extracellular markers (**Table 5**) were used to stain the cells. The panels included lineage markers, differentiation markers, exhaustion markers, activation markers, and chemotaxis markers. PBMCs from CoU-GBM #027 and CoU-GBM #038, and TILs from CoU-GBM #027 and CoU-GBM #028 were stained for the 37 extracellular markers and acquired the following day using a Helios mass cytometer (Fluidigm). PBMCs from two time points were available from CoU-GBM #038, while PBMCs from 5 different time points were available from CoU-GBM #027. The gating strategy used to exclude calibration beads, dead cells, and doublets are shown in **Figure 19**. ViSNE plots with all the markers for both patients were generated in Cytobank and can be found in the supplementary material.

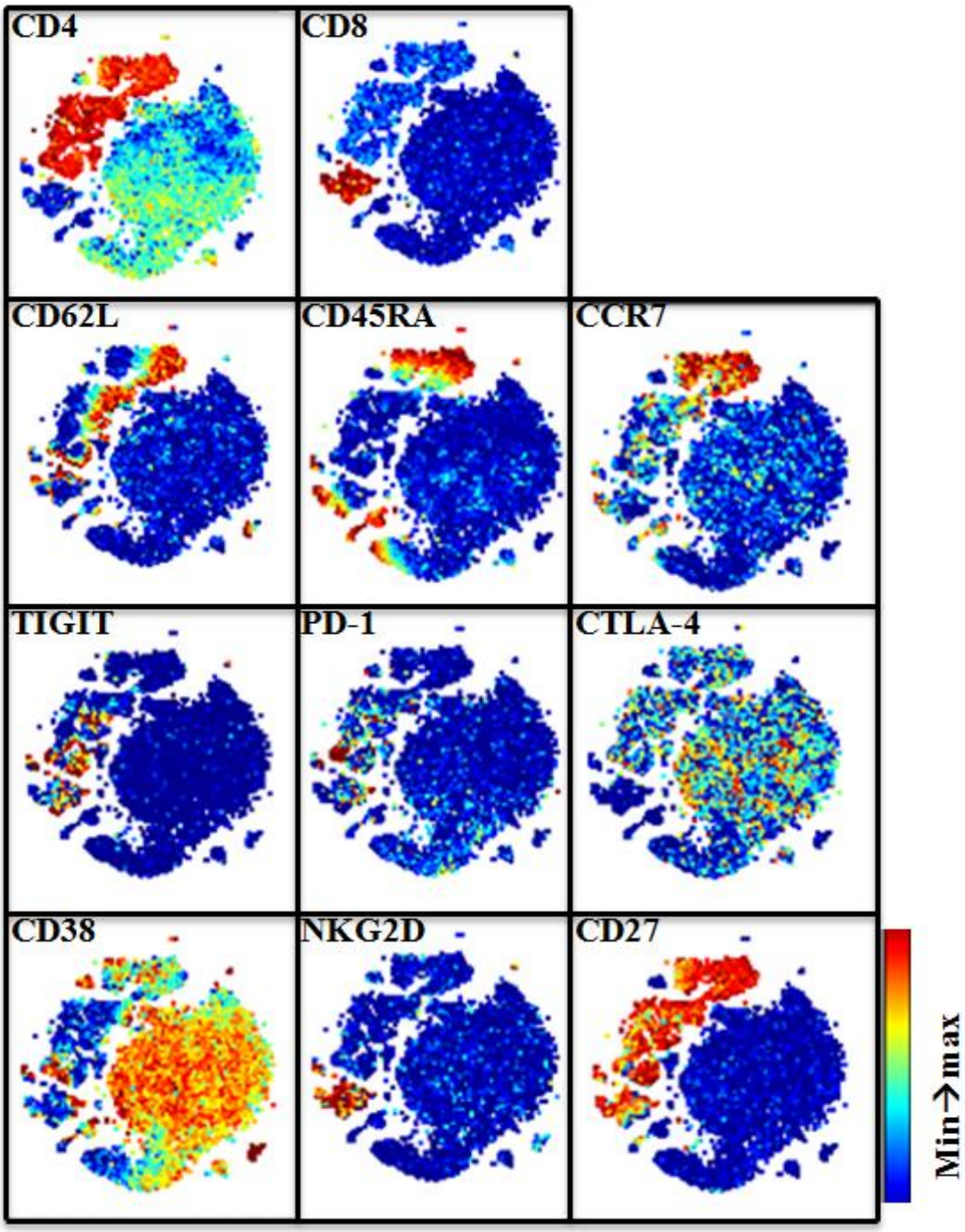

Figure 16 ViSNE plot of PBMCs from one time point from CoU-GBM #027. PBMCs were stained for 37 extracellular markers and acquired the following day using a Helios mass cytometer. ViSNE plots were generated in Cytobank. Lineage markers, differentiation markers, checkpoint markers, activation and co-stimulatory markers are shown.

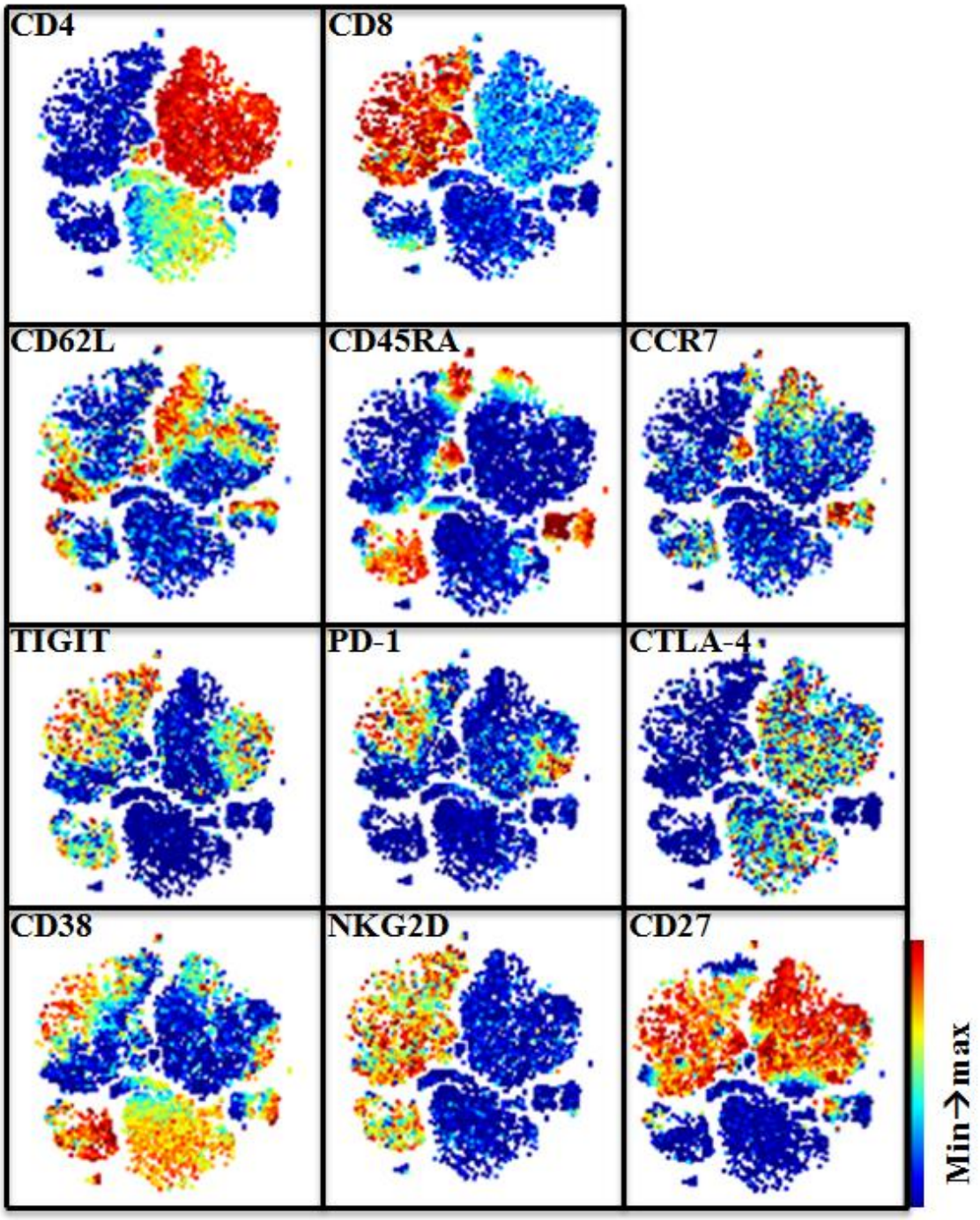

Figure 17 ViSNE plot of PBMCs from one time point from CoU-GBM #038. PBMCs were stained for 37 extracellular markers and acquired the following day using a Helios mass cytometer. ViSNE plots were generated in Cytobank. Lineage markers, differentiation markers, checkpoint markers, activation and co-stimulatory markers are shown.

Extracellular staining of PBMCs from CoU-GBM #027 showed that the population of $CD4^+$ T cells were much larger than the $CD8^+$ T cell population (**Figure 16**), in contrast to CoU-GBM #038, which had similar distribution of $CD4^+$ and $CD8^+$ T cells (**Figure 17**). That CoU-GBM #038 had more $CD8^+$ T cells was also found in the intracellular staining assay. CD45RA, CD62L, and CCR7 are markers commonly used in phenotyping of T cells for naïve and memory subsets. There were some $CD4^+$ naïve T cells in both patients, being $CD45RA^+CCR7^+CD62L^+$, but most of the T cells had a memory phenotype. Most of these memory T cells were effector memory T cells, with no expression of CD45RA and CCR7, and variable expression of CD62L. A small population of T_{TE} $CD8^+$ were present in CoU-GBM #038, being $CD45RA^+CD62L^-CCR7^-CD27^-$. The effector memory cells also expressed TIGIT, PD-1, CD38, CD27, and NKG2D for the $CD8^+$ T cells, indicating activation and prior antigenic exposure.

We also wanted to investigate if the different markers changed during the vaccination period. For CoU-GBM #027 PBMCs from five time points were available, from baseline to the last vaccination. 6 markers changed during the vaccination period; CD45RA, CD62L, CCR7, CD38, PD-1, and TIGIT (**Figure 18**). The expression of CD45RA, CD62L, and CCR7 decreased in both the $CD4^+$ and $CD8^+$ T cell populations, suggesting that the T cells gained more of a memory phenotype. The expression of CD38 and PD-1 increased from baseline (blue) and three months later (orange), while the expression of TIGIT decreased, indicating that the $CD8^+$ T cells were activated. The proliferation assay also showed a high response to CMVpp65 protein at this time point. The expression of CD38 and PD-1 then decreased at the later time points, in line with the decreased responses in the proliferation assay. No other changes in the expression of the markers by the T cell subsets were seen.

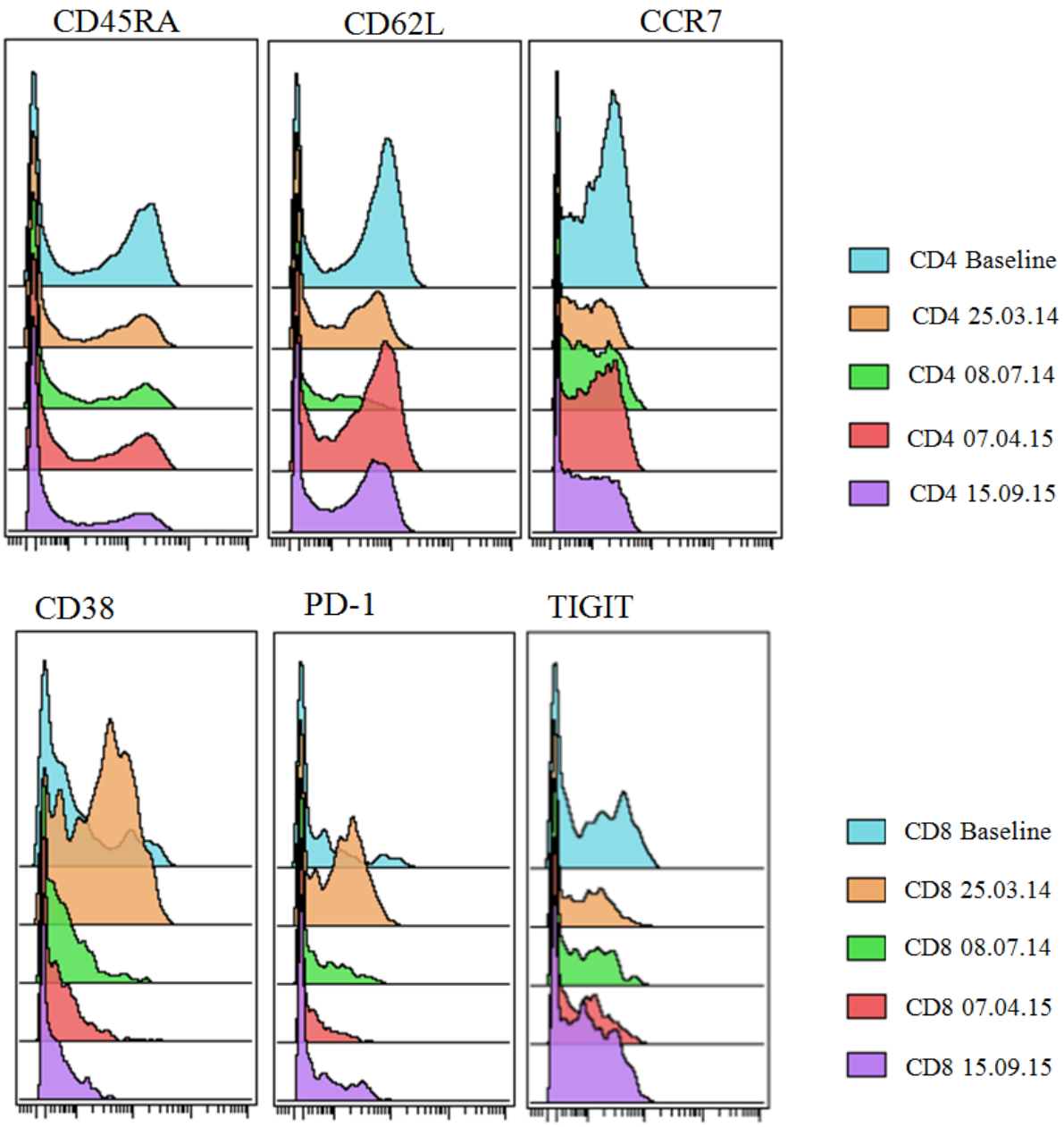

Figure 18 Histograms showing different expression of markers over time. CD4 population (top) and CD8 population (bottom) from PBMCs of CoU-GBM #027.

.

TILs CoU-GBM #027 and CoU-GBM #028

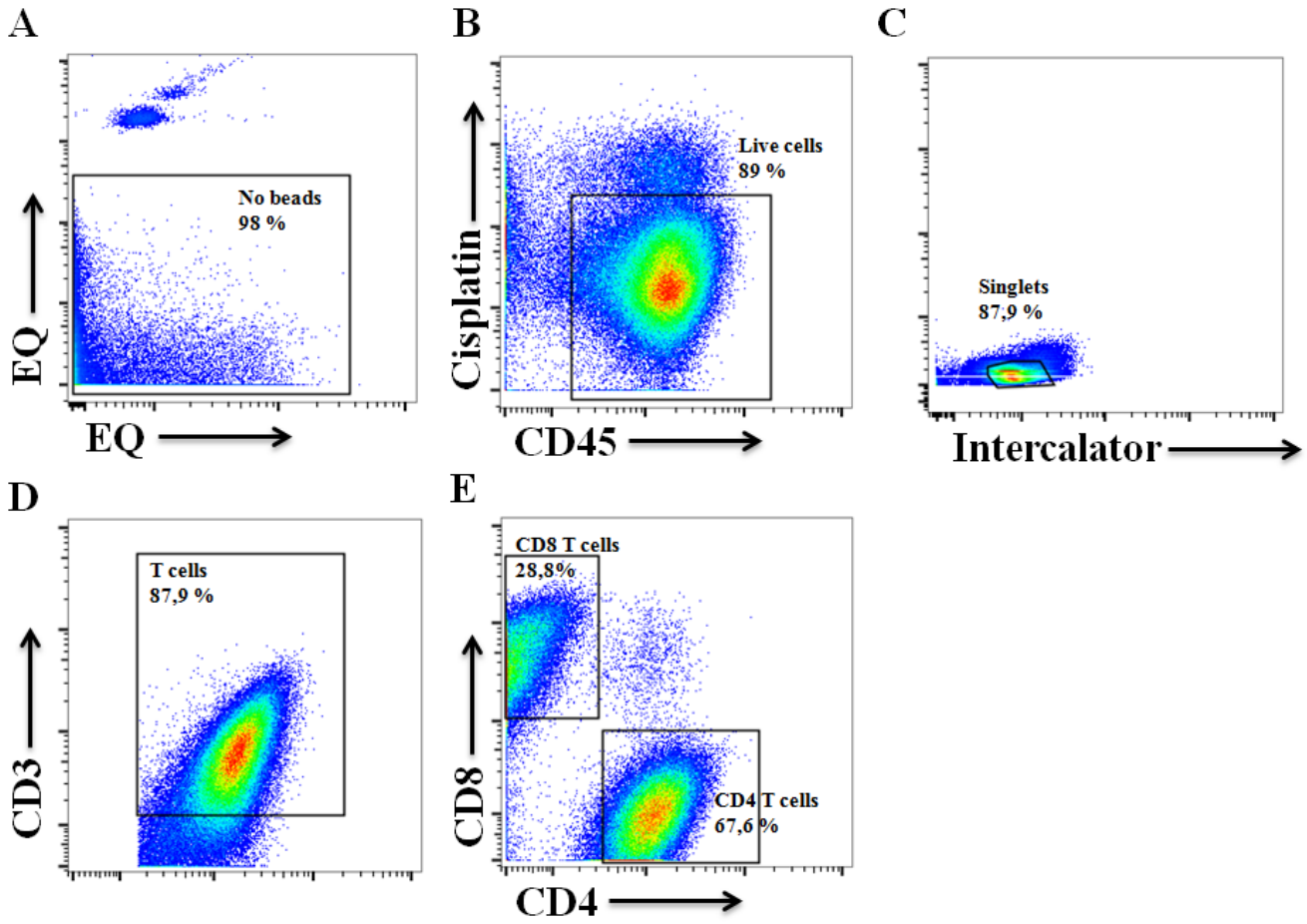

Figure 19 Gating strategy used to find the $CD4^+$ and $CD8^+$ populations in TILs from CoU-GBM #028. **A.** Beads were excluded by plotting EQ on both axes. **B** Dead cells were excluded by plotting CD45 vs. cisplatin, which enters dead cells. **C**. Exclusion of doublets, only single nucleated cells were chosen for further analysis. **D.** $CD3^+$ cells were included to find the T cells. **E**. $CD4^+$ T cells and $CD8^+$ T cells. Both $CD4^+$ and $CD8^+$ populations are present in the tumor infiltrating lymphocytes of this patient.

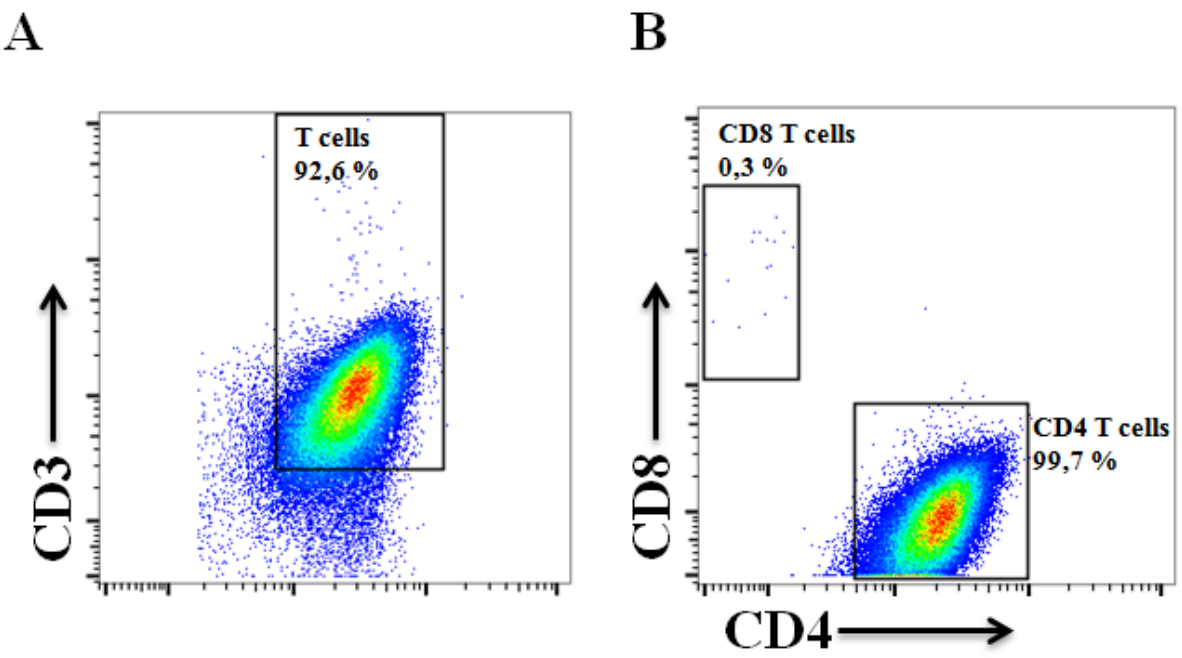

Figure 20 Same gating strategy, i.e. exclude beads, dead cells, and doublets, as in figure 16 were used to find the live, single cells. **A.** $CD3^+$ cells were included to find the T cells. **B.** $CD4^+$ and $CD8^+$ T cells. Only $CD4^+$ T cells were present in the TILs from CoU-GBM #027.

Next, we wanted to investigate the TILs from the two patients CoU-GBM #027 and #028 where TILs were available. First, an extracellular antibody panel consisting of 37 antibodies (**Table 5**) was used to stain the TILs before acquiring the samples on a Helios mass cytometer. Gating in FlowJo and ViSNE plots were used to examine the expression of the different extracellular markers.

The ViSNE plots with all of the rest of the markers are in the supplementary material. Gating as described in figure **Figure 19** was used before generating the ViSNE plots in Cytobank.

Extracellular staining of the TILs from CoU-GBM #027 and CoU-GBM #028 showed that CoU-GBM #027 only had $CD4^+$ infiltrating lymphocytes (**Figure 20,Figure 23 A**), while CoU-GBM #028 had both $CD4^+$ and $CD8^+$ infiltrating lymphocytes and a small population of double positive T cells (**Figure 19E, Figure 23B**). Although it was a small population, it was a very heterogeneous group of cells, with expression of markers like CD57, HLA-DR, CTLA-4, TIGIT, and CD69 (data not shown). Phenotyping of T cells infiltrating human GBM, showed that tumor-infiltrating $CD4^+$ and $CD8^+$ T cells from both patients demonstrated a predominantly effector memory T cell phenotype ($CD45RA^-CCR7^-CD62L^-$), reflecting prior antigenic exposure (**Figure 21B/C, Figure 22**). There was a small population, about 5 %, positive for CD62L, which may be early effector cells (Cieri et al., 2013), and the largest

proportion of these cells were positive for the co-stimulatory molecules CD27 and/or CD38 in CoU-GBM #027, indicating activation (**Figure 21D**).

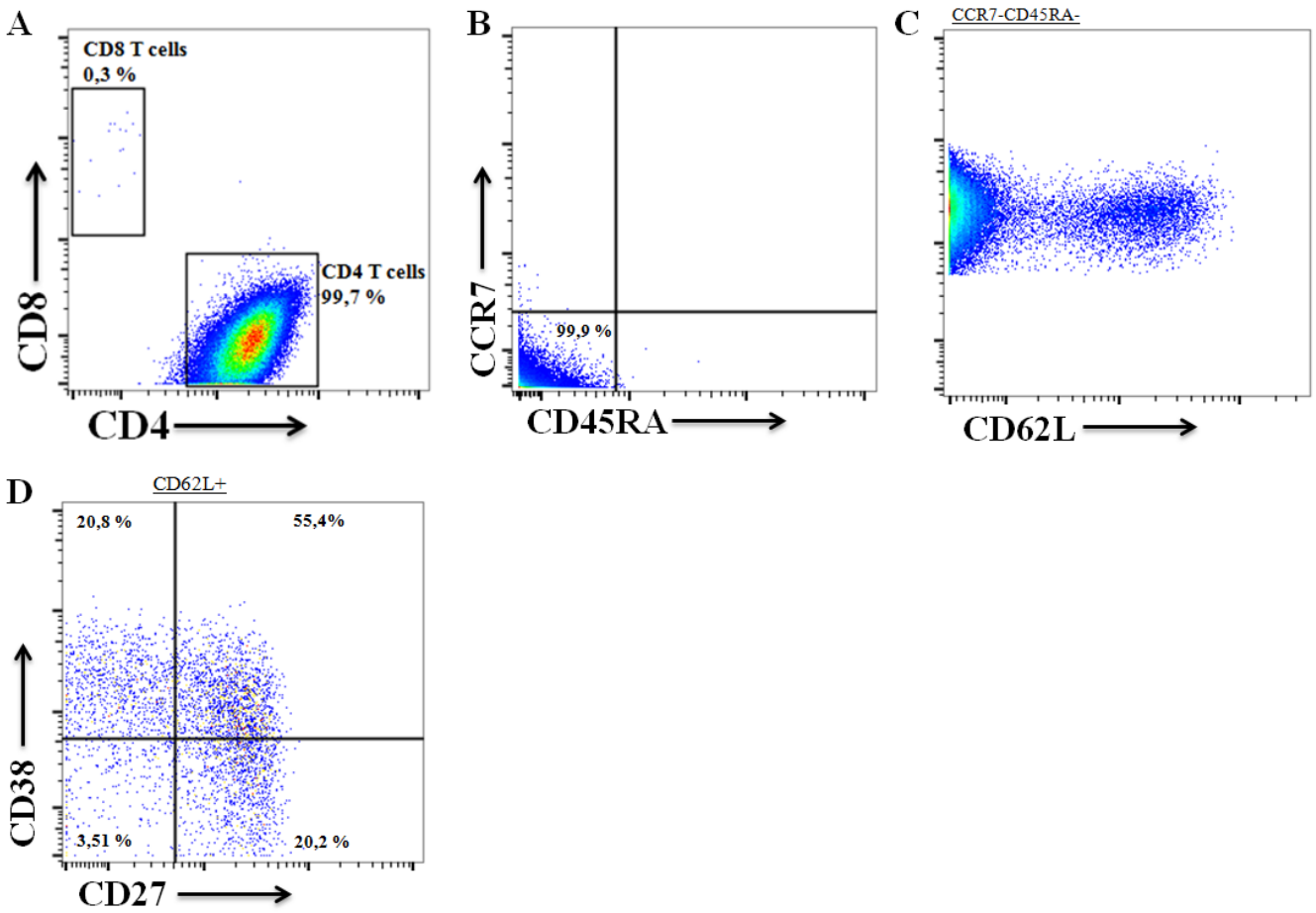

Figure 21 Phenotyping of TILs from CoU-GBM #027. **A.** Gating of the $CD4^+$ and $CD8^+$ T cells. **B and C**. Phenotyping of the $CD4^+$ T cell subset. **D.** Gating of $CD4^+$ $CD45RA^-CCR7^-CD62L^+$ based on expression of CD38 and CD27. The $CD4^+$ T cells had an effector memory phenotype ($CD45RA^-$ $CCR7^-CD62L^-$) , reflecting prior antigenic exposure. There was a small population positive for CD62L, which were positive for CD38 and/or CD27, suggesting that this population was activated.

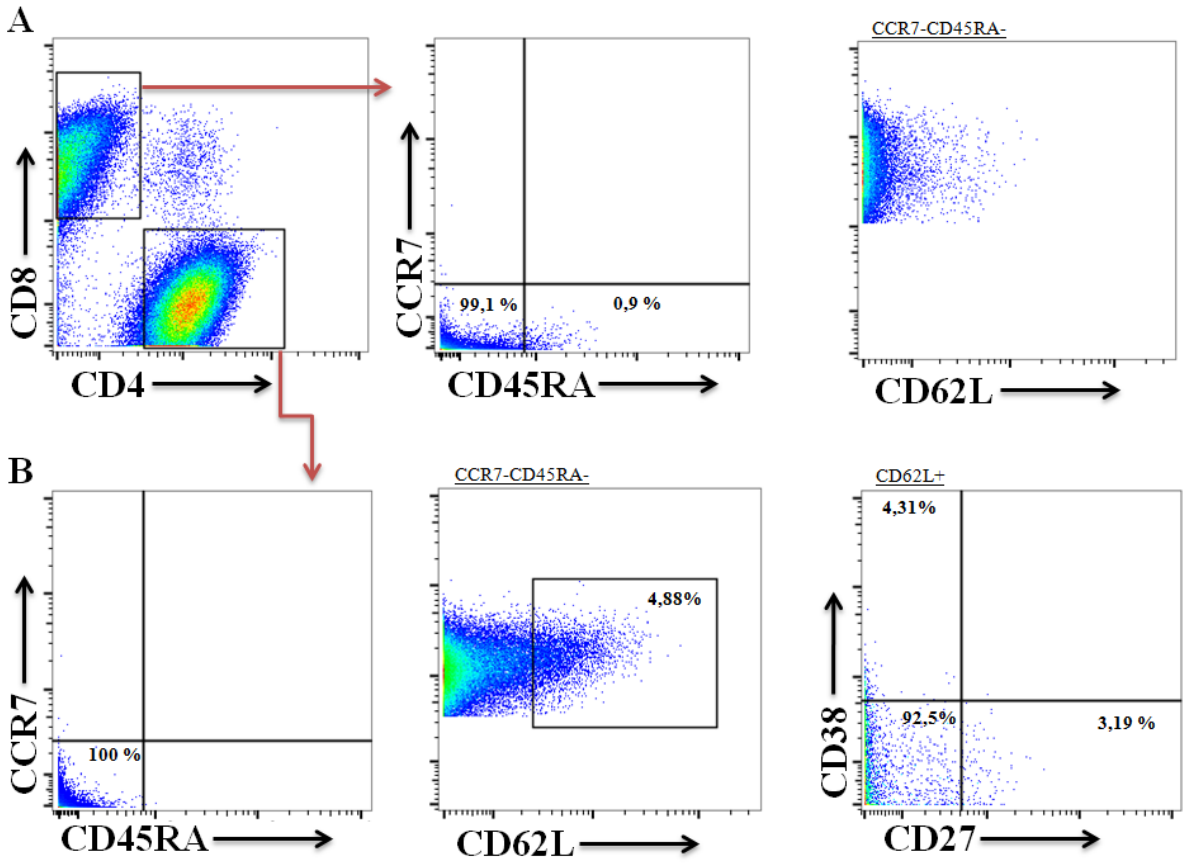

Figure 22 Phenotyping of TILs from CoU-GBM #028. **A.** Gating strategy used to phenotype the $CD8^+$ T cell population. **B**. Gating strategy used to phenotype the $CD4^+$ T cell population. Both the $CD4^+$ and $CD8^+$ T cells exhibited an effector memory phenotype.

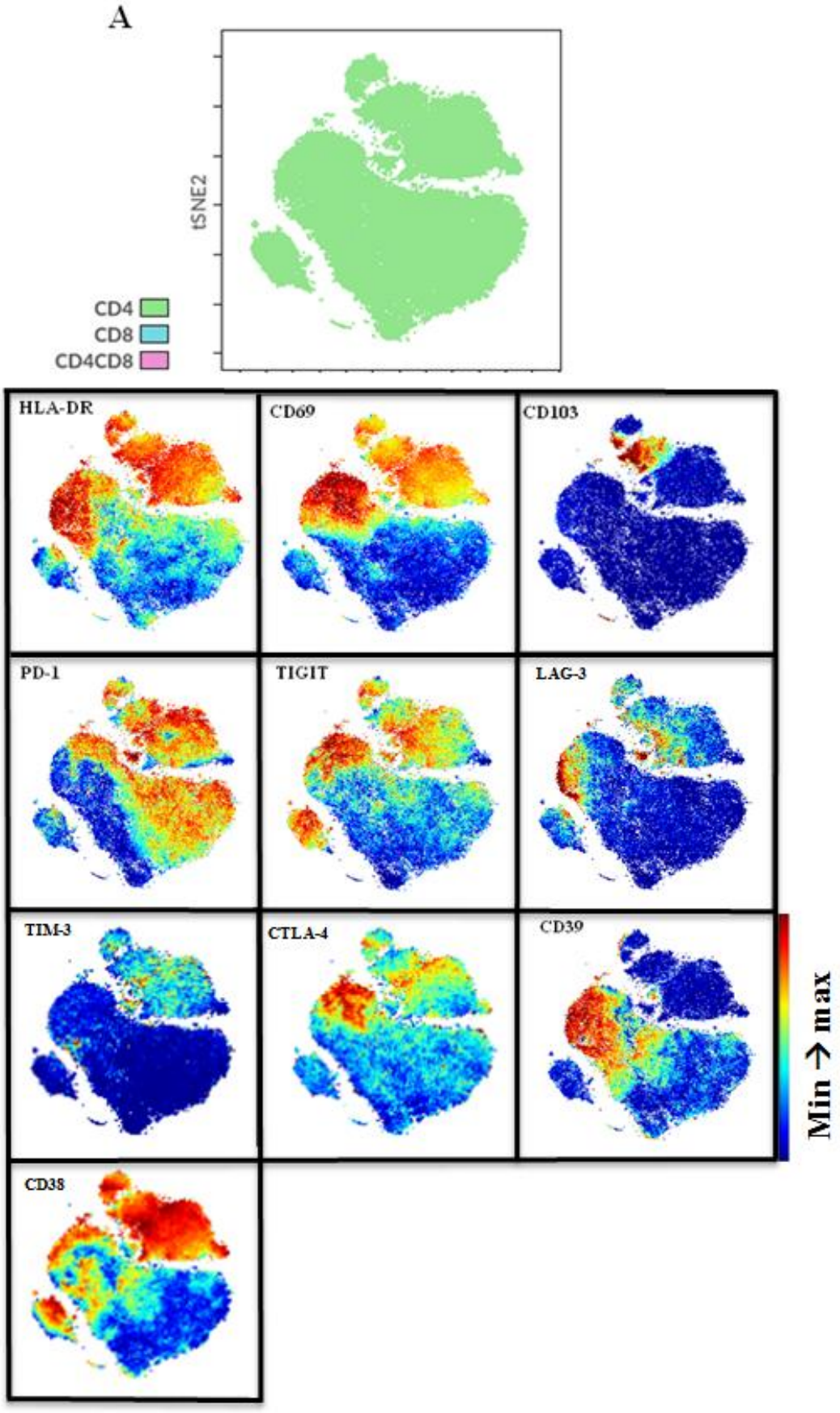
A
tSNE2
CD4
CD8
CD4CD8
HLA-DR
CD69
CD103
PD-1
TIGIT
LAG-3
TIM-3
CTLA-4
CD39
CD38
Min → max

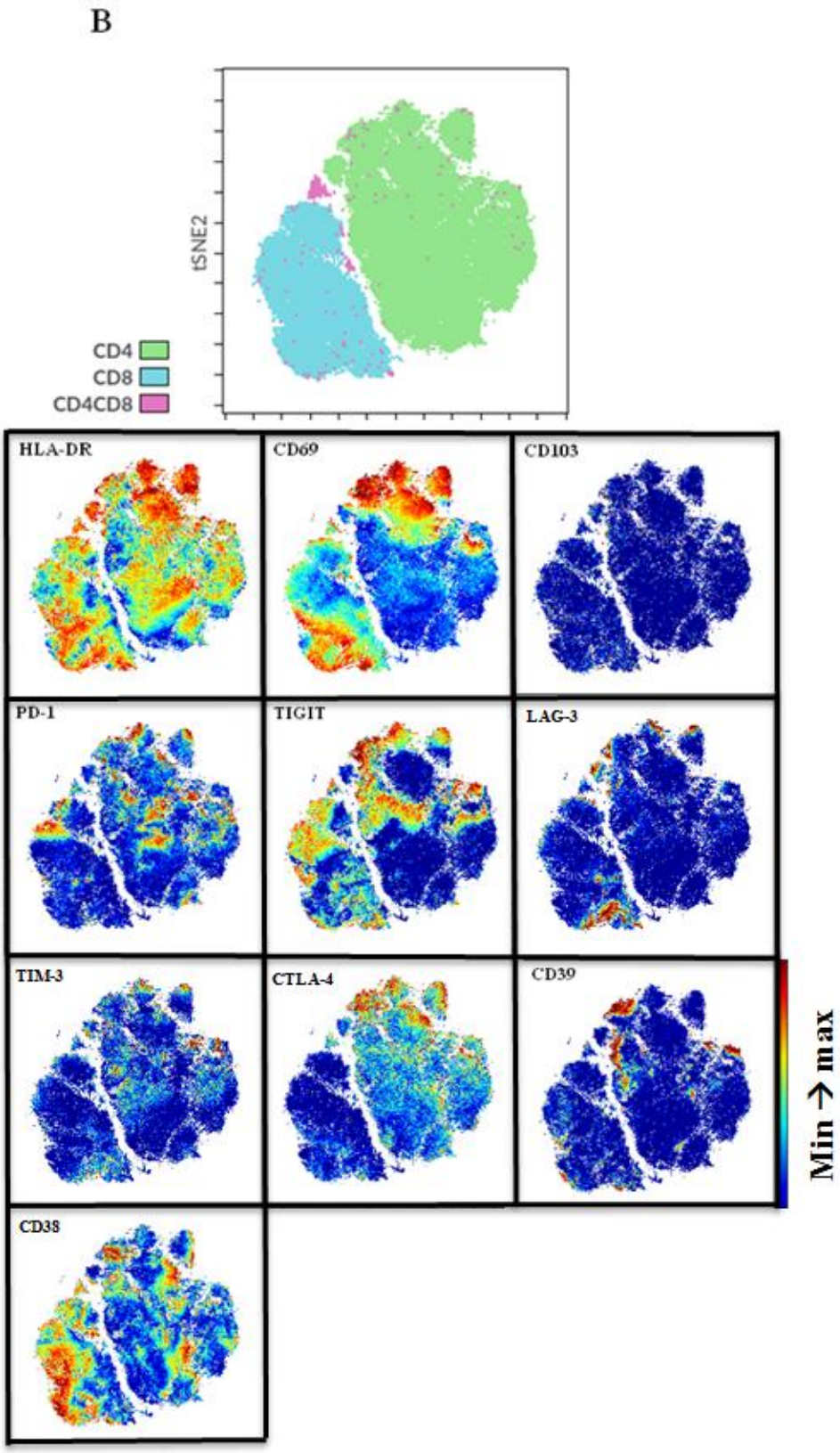

Figure 23 ViSNE plots of TILs from CoU-GBM #027 (**A**) and CoU-GBM #028 (**B**). CoU-GBM #028 had $CD4^+$, $CD8^+$ and double positive T cells in the TILs, and CoU-GBM #027 only had $CD4^+$ TILs. Expression of activation, tissue residency, and checkpoint molecules are shown. ViSNE plots were made in Cytobank.

Of all the T cells in the TILs from CoU-GBM #027, about 76% expressed PD-1. In CoU-GBM #028, about 29% expressed PD-1. 66% of the PD-1 expressing T cells also expressed TIGIT in CoU-GBM #027, while the percentage was 49% in CoU-GBM #028. A small percentage of the PD-1^{+}TIGIT^{+} T cells also co-expressed the checkpoints LAG-3, TIM-3, and CTLA-4, indicating that this population was exhausted, but the co-expression of HLA-DR, CD69, and CD38 indicate that there also were activated T cells present in the TILs. CoU-GBM #027 also had a highly activated CD103^{+}CD69^{+} T cell population, termed tissue resident T cells, which have shown to be the most potent cytokine producers in non-small cell lung cancer (Oja et al., 2018). There were also exhausted T cells present in both the CD4^{+} and CD8^{+} T cell compartments in CoU-GBM #028, being CD45RA^{-}CCR7^{-}CD62L^{-}CD57^{+}.

CoU-GBM #027 was the only patient where both PBMCs and TILs were analyzed by mass cytometry. Comparison of the TILs and the PBMCs from this patient showed some differences. There were few CD8^{+} T cells in the PBMCs and this population was absent in the TILs, meaning that only the CD4^{+} T cells infiltrated the tumor. The phenotype of the TILs was an effector phenotype, while in the PBMCs there was also a small population of naïve T cells. The major differences between the PBMCs and TILs were in the expression of the checkpoint molecules. Whereas the PBMCs had low expression of TIGIT, PD-1, CTLA-4, LAG-3, TIM-3, and CD39, the TILs had higher expression of all of these markers, except TIM-3. CD38 was also more expressed in the TILs, and co-expressed with the co-stimulatory molecule CD27.

The proliferation assays and the ELISpot assay on PBMCs showed that there were immune responses in the patients. We also wanted to investigate if the T cells infiltrating the tumor were responsive to the antigens in the vaccine. Due to limited material, only the CMVpp65 protein was tested against TILs from CoU-GBM #027 and CoU-GBM #028. CMV-stimulated TILs from both patients were tested for IFN-γ production in an ELISpot assay. CoU-GBM #028 showed a very good response and produced a lot of IFN-γ in response to CMVpp65, compared to the unstimulated cells (**Figure 24**). This result support the effector memory phenotype of the TILs - the T cells exerted an effector function when their cognate antigen was presented to them. This also indicated that CMVpp65 protein had been presented to these T cells by an APC, and that the T cells successfully had trafficked and infiltrated the tumor, or that CMV could be present in the tumor. The CMV-stimulated TILs from CoU-GBM #027, however, did not show as promising results in the ELISpot assay, but there were some cells

that produced IFN-γ (**Figure 24**). This means that the TILs from from patient #027 likely recognized other glioblastoma-associated antigens.

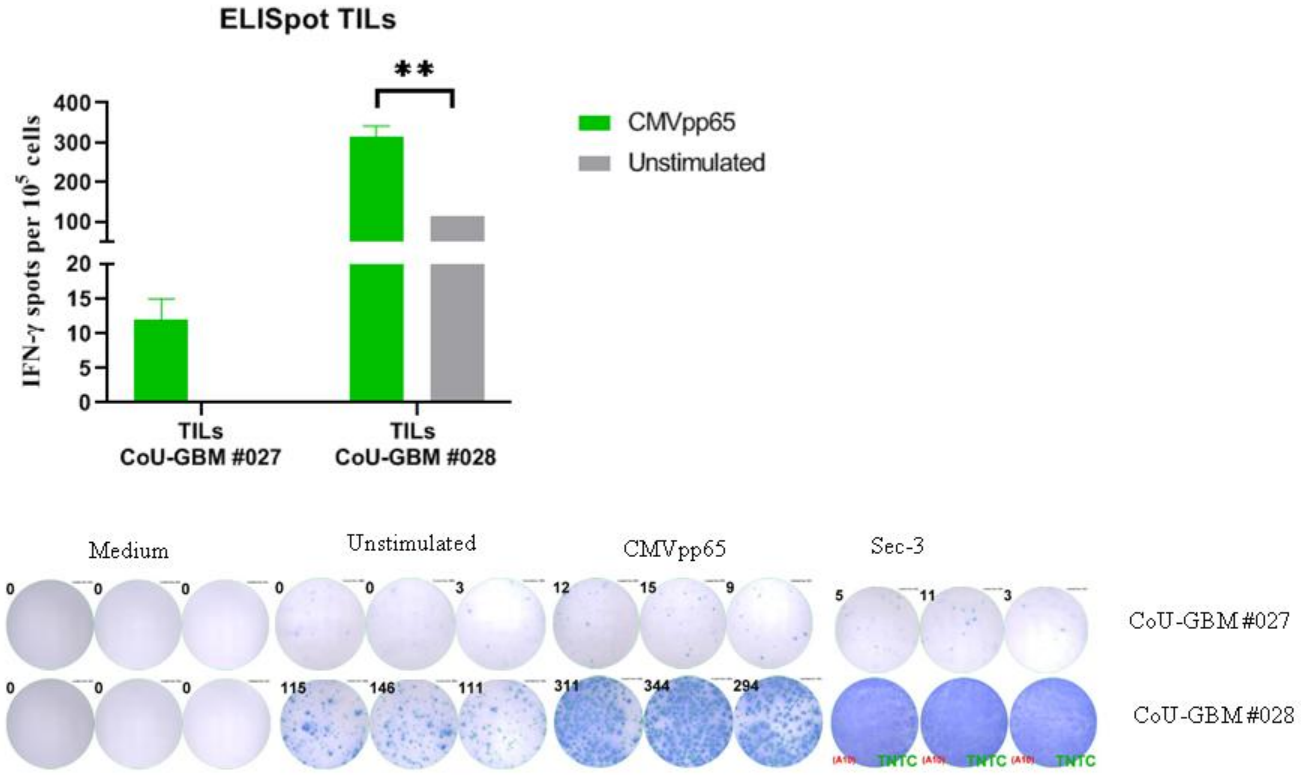

Figure 24 ELISpot of CMV-stimulated TILs from CoU-GBM #027 and CoU-GBM #028. T cells and autologous EBV-LCLs were seeded in a 96-well pre-coated ELISpot plate alone (background), with CMVpp65 (10µL/mL), or 0,1µg/mL sec-3 (positive control). Medium alone was used as negative control. The plate was incubated for 24 hours, followed by the procedure using the manufacturer's protocol. The plate was scanned and counted using an Immunospot analyzer. A two-tailed paired t test was done in GraphPad Prism using the values from the triplicates. The CMV-stimulated TILs from CoU-GBM #028 produced IFN-γ in response to CMVpp65 protein. **, P<0.002. *TILs*: tumor-infiltrating lymphocytes.

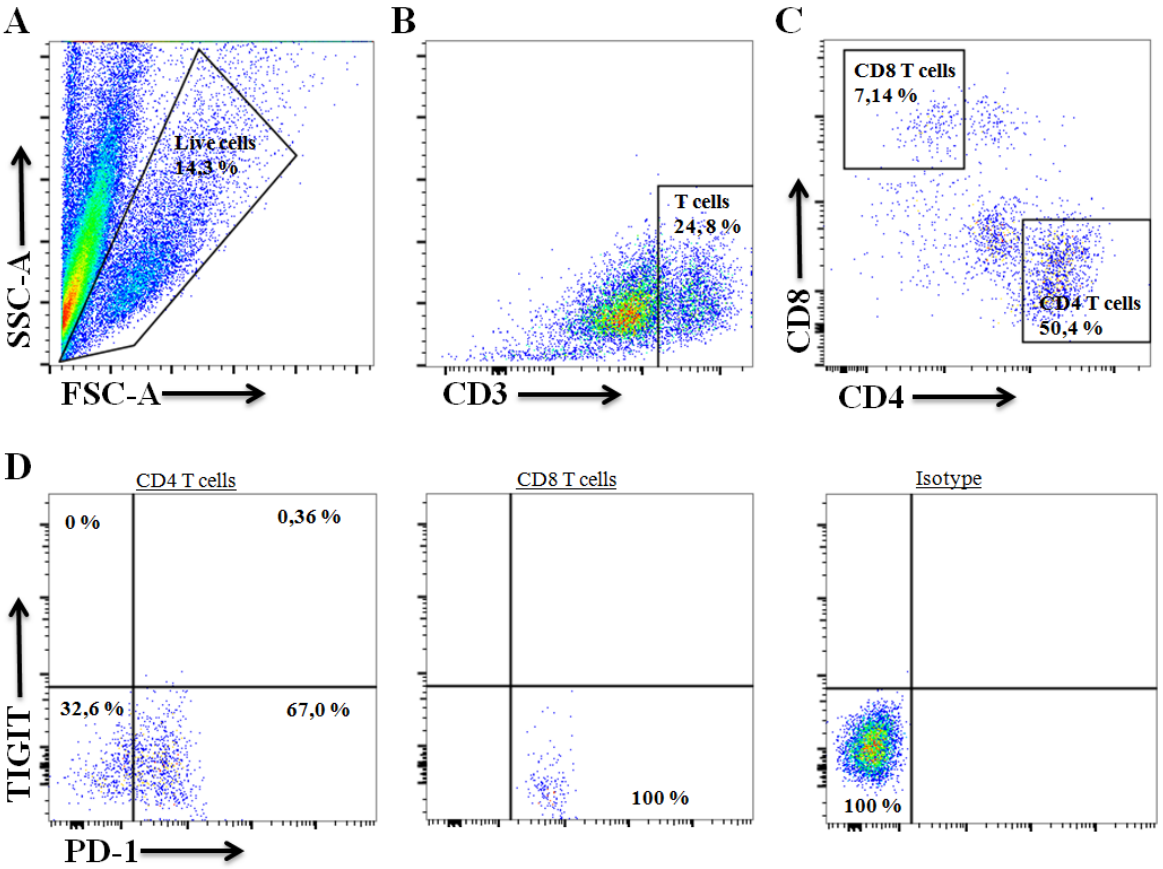

Figure 25 TIGIT and PD-1 staining of CMV-stimulated TILs from CoU-GBM #028. CMV-stimulated TILs were co-cultured with autologous EBV-LCLs at a target:effector ratio of 2:1. The EBV-LCLs were pre-incubated with CMVpp65 protein at a concentration of 10 µL/mL. After overnight incubation in 37°C, 5% CO_2, the cells were stained for CD3, CD4, CD8, PD-1, and TIGIT. Isotypes were included to see if there were unspecific binding of the antibodies. **A**. Gating of live cells. **B**. Gating of the T cells. **C.** $CD4^+$ and $CD8^+$ TILs. **D** TIGIT and PD-1 expression by $CD4^+$ TILs, $CD8^+$ TILs, and the isotype control.

We also wanted to see if the CMV-stimulated TILs expressed PD-1 and/or TIGIT. The CMV-stimulated TILs from CoU-GBM #027 were all used in the ELISpot assay, but CMV-stimulated TILs from CoU-GBM #028 were stained for CD3, CD4, CD8, TIGIT and PD-1. Both the $CD4^+$ and $CD8^+$ T cells were positive for PD-1 and negative for TIGIT (**Figure 25**).

5 DISCUSSION

Despite great success in many aspects of immunotherapy over the past 5 decades, improved outcomes for patients diagnosed with glioblastoma remain difficult to achieve. Checkpoint inhibitors targeted against PD-1 or CTLA-4, which have offered great responses and prolonged survival in patients with for example melanoma, have so far failed to offer significant survival benefit beyond the current median OS of 15 months after initial diagnosis (Smith et al., 2020).

The main goal of this thesis was to investigate if immune responses could be induced by autologous dendritic cells transfected with hTERT peptides, survivin peptides, and CMVpp65 protein in patients diagnosed with glioblastoma. PBMCs from 6 patients that received these DC vaccines in 2014-2016 were tested and immune responses were measured by proliferation assays, ELISpot, flow cytometry and mass cytometry. In addition, TILs from two of the patients were analyzed by ELIspot and mass cytometry.

PBMCs from different time points during the vaccination period were tested for proliferation in a proliferation assay. In 5 out of 6 patients we saw a positive response (SI ≥2) in response to either CMVpp65 protein, hTERT peptide mix, or survivin peptide mix (**Figure 6**). In 4 out of 6 patients, we saw responses against CMVpp65, and these were stronger than for the peptide mixes and they were clearly vaccine induced since the responses came after the vaccinations.

One reason for the stronger responses against CMVpp65 protein may be that CMVpp65 protein is a highly immunogenic foreign antigen that induce strong cytotoxic responses in CMV-specific cytotoxic T cells. hTERT and survivin are also immunogenic, however these antigens exist in the cells to some degree and strong responses towards hTERT and survivin may be suppressed. Also, in these experiments 6 different hTERT peptides and 4 different survivin peptides were used to stimulate the cells. These peptide mixes consist of the most immunogenic peptides reported in literature, however the patients may respond to other peptides not used here. The patients have not been HLA-typed and we are using long peptides that can be processed and presented for the optimal epitopes to be selected by each patient's immune system. Still, the vaccine contains full-length mRNA encoding the defined antigens and we could therefore miss epitopes as we do not cover the full protein with our peptide mixes. Another reason for the strong CMVpp65 protein responses compared to the tumor associated antigens may be that a high percentage of the population has been infected with

CMV, and the vaccine may boost strong, already existing memory T cell responses. CoU-GBM #038 had a response to CMVpp65 protein at baseline, which may be because that patient already had CMV-specific memory T cells. In addition, a high background value may have masked responses that were present. The SI value of the proliferation assay was calculated by dividing each value of the triplicates of stimulated cells by the mean of the background (unstimulated cells). So, if the background was very high, it was difficult to know if there may have been a response towards the peptides.

Responses against survivin and hTERT using cancer vaccines have been detected in several other malignancies. Responses against survivin peptides have been detected in recurrent malignant glioma and metastatic melanoma (Fenstermaker et al., 2016; Nitschke et al., 2017), and responses against hTERT peptides have been detected in non-small cell lung cancer (Brunsvig et al., 2006; Brunsvig et al., 2020), pancreatic cancer (Bernhardt et al., 2006), and melanoma (Inderberg-Suso et al., 2012). In all these trials, peptide vaccines were directly administered to the patients in combinations with adjuvant, not as transfected DCs. In general, it is easier to detect responses against peptide vaccines than against DC vaccines because of high background in assays, which has also been reported by others (Lam et al., 2015). As mentioned, this was also seen in the patients used in this thesis.

Proliferation assays measures the ability of T cells to proliferate in response to an antigen, which only happens if the T cells have been primed to that antigen. The ELISpot assay is a very sensitive assay that detects and measures the IFN-γ secretions by stimulated effector cells. To be able to do the ELISpot assay, there had to be T cells left after the proliferation assay set up. The number of cells available and the viability of the cells were very variable among the patients and between the different pre-stimulated T cells. The survivin pre-stimulated T cells were generally in a bad state with poor viability. Therefore, the ELISpot assay was only done on a few patients, time points, and pre-stimulated T cells.

The results from the ELISpot assays showed that both the CMVpp65 protein stimulated T cells and the hTERT peptide mix stimulated T cells secreted IFN-γ in response to their cognate antigen. Interestingly, some of these responses detected in the ELISpot assay were not detected in the proliferation assay, i.e. the hTERT peptide mix responses and the CMVpp65 protein responses in CoU-GBM #035 (**Figure 7**, **Figure 8**), and the CMVpp65 protein response in CoU-GBM #044 (**Figure 7**). The proliferation assay mostly detects proliferating $CD4^+$ T cells. However, the ELISpot assay detects IFN-γ secreted by both T_H1 cells and T_C $CD8^+$ T cells, so it is possible that the T cells that secreted the IFN-γ were $CD8^+$

and therefore not detected in the proliferation assay. Nonetheless, immune responses were detected in all patients when adding the results from the proliferation assays together with the ELISpot assay.

The TILs from CoU-GBM #028 also showed significant IFN-γ production in response to CMVpp65 protein, but CoU-GBM #027 did not. One possible reason for this may be that the CMV-stimulated TILs from patient #027 were pre-stimulated, frozen down, and then thawed before the assay, while the CMV-stimulated TILs from patient #028 were harvested directly from the pre-stimulated TILs. The freezing and thawing resulted in a decrease in viability with many dead cells. Another reason could be that the reactivity of the TILs in CoU-GBM #027 was mainly against other tumor antigens. A third explanation could be that the TILs in CoU-GBM #027 had higher expression of the checkpoint molecules PD-1, TIGIT, CTLA-4, CD39, and to some degree LAG-3 and TIM-3. This patient had the longest OS and there were probably good anti-tumor responses initially, however the expression of all these inhibitory checkpoints may have contributed to an ineffective anti-tumor response by exhausted T cells.

The pre-stimulated T cells were stained for the surface markers CD3, CD4 and CD8, and analyzed by flow cytometry. In addition, the cells were stained intracellularly to examine if the T cells also produced the cytokine TNF-α in response to their cognate antigen. As for the ELISpot assay, there had to be T cells left after the proliferation assay set up to do this. And in general, there were not enough viable cells to do both ELISpot and intracellular cytokine staining, except for the CMV-stimulated cells in CoU-GBM #038 and CoU-GBM #044.

There were big differences between the patients and between the peptide-stimulated T cells regarding which T cell population produced cytokines and which cytokine(s) they produced. For the hTERT- and CMV-stimulated T cells in CoU-GBM #027, it was mainly the $CD4^+$ T cells that produced IFN-γ, however for the survivin-stimulated T cells, it was mainly monofunctional TNF-α producing $CD4^+$ and $CD8^+$ T cells and some IFN-γ producing $CD8^+$ T cells. The CMV-stimulated T cells from CoU-GBM #038 consisted of monofunctional $CD4^+$ and $CD8^+$ T cells that produced IFN-γ or TNF-α, while in CoU-GBM #044 there were relatively high percentages of all populations, except TNF-α producing $CD8^+$ T cells. So why were not the responses detected in the proliferation assay for CoU-GBM #044, given these results and the fact that proliferation assay mostly detects $CD4^+$ proliferating T cells? In this patient there were a lot of $CD4^+$ T cells that could have given high SI values. One possible explanation is one mentioned previously, which is high background. This patient, in particular, had very high background in the proliferation assay (data not shown), making it

more difficult to determine a positive response. Another explanation could be that the T cells had high expression of checkpoint molecules, meaning they are exhausted, which may have a larger impact on the capacity to proliferate compared to secretion of cytokines (Wherry & Kurachi, 2015).

Immunotherapy in glioblastoma

In 2014 and 2015, the FDA approved the three first checkpoint inhibitors that target PD-1, pembrolizumab and nivolumab for unresectable or metastatic melanoma, and nivolumab for non-small-cell lung cancer. These checkpoint inhibitors block the interaction between PD-1 and PDL-1 and PDL-2, thereby preventing the inhibition of the antitumor response caused by PD-1, and have shown promising results in other malignancies, such as Hodgins lymphoma and renal cancer (Preusser et al., 2015). In 2014, the first large phase III clinical trial of nivolumab in recurrent glioblastoma, called the CheckMate 143, was initiated (NCT02017717). The purpose of the study was to compare the efficacy and safety of nivolumab versus Avastin, an anti-angiogenic monoclonal antibody. Unfortunately, it did not improve the overall survival compared to Avastin, although some subgroups can benefit from this (Bernstock et al., 2019; Reardon et al., 2020).

There is currently an on-going randomized trial, called DEN-STEM, of DC immunotherapy in patients with GBM (NCT03548571). The DCs are transfected with mRNA of survivin, hTERT, and autologous tumor stem cells, and the trial will investigate if the DC vaccines and immune responses provide a real survival benefit compared to standard treatment. As mentioned previously, 3-day DCs matured with the Münich cytokine cocktail were produced for vaccination in this current study. This resulted in strong inflammation in many of the patients, which led to steroid treatment. High doses of steroids are immunosuppressive and may have led to complete abrogation of the immune response (Giles et al., 2018; Papa et al., 1986). In the ongoing DEN-STEM study, however, 7-day DCs matured with the Jonuleit cocktail are used as these seem to induce immune responses, but limit inflammation and avoid use of higher doses of steroids due to inflammation and pseudo-progression unless there is real tumor progression.

CMV in glioblastoma

The detection of human CMV proteins and nucleic acids in a high percentage of low- and high grade malignant gliomas was first reported in 2002 by Cobbs et al. (Cobbs et al., 2002). Since then, there has been a lot of debate regarding the role and existence of CMV in gliomas.

Several clinical trials concerning immunotherapy and CMV in glioblastoma are ongoing or completed.

Smith et al. reported that CMV-specific T cells are a safe adjuvant immunotherapy for primary glioblastoma multiforme (Smith et al., 2020). 25 patients were treated with in-vitro expanded autologous CMV-specific T cells, and they demonstrated a median progression free survival of 10 months and overall survival of 21 months following diagnosis. From 2006 to 2019, 102 patients with newly diagnosed glioblastoma received Valganciclovir as an add-on therapy to standard therapy. Valganciclovir, an antiviral medication used to treat CMV infection, was shown to prolong the median overall survival (21.4 months vs 13.3 months in control group) and give a 2-year survival rate of 49.8%, compared to 17% in the control group (Stragliotto et al., 2020). A phase I clinical trial with glioblastoma patients receiving adoptive immunotherapy using CMV-specific T cells demonstrated prolonged progression free survival in some patients, however, only 11 patients were included in the study (Schuessler et al., 2014).

Hence, many clinical trials have demonstrated that immunotherapy targeting CMV is safe, and that it prolongs the overall survival and progression free survival in some glioblastoma patients. The patients in this thesis also showed responses to CMV, however, there are too few patients included in our study to conclude. All patients demonstrated an immune response against at least one of the vaccine antigens either in T cell proliferation assay or IFN-γ ELISpot assays. Our results indicate that stronger and prolonged vaccine-induced immune responses may contribute to enhanced survival. CoU-GBM #027 was the longest surviving patient who also received the highest number of vaccine doses (except CoU-GBM #019) and who demonstrated strong immune responses and upregulation of immune checkpoints on TILs. This is in line with previous research. However, further research must be done in a larger patient cohort.

Future directions

GBM is an especially difficult cancer to treat because of its location, its immunosuppressive environment, heterogeneity, and low mutational burden. Because of the poor prognosis in GBM, immunotherapy is an interesting therapeutic approach. To date, phase III clinical trials with ICIs and vaccine therapy for GBM have not shown as promising results as for other cancer types. Given the fact that GBM is highly immunosuppressive with many immune

evasion mechanisms, combinatorial strategies are being studied to overcome the therapy resistance seen in GBM (Medikonda et al., 2021).

Chimeric antigen receptor (CAR) T cell therapy is a relatively new approach which has been approved for B cell lymphoma and leukemia. CAR T cells are genetically modified T cells harvested from the patient, which are adoptively transferred back into the patient to elicit an anti-tumor immune response(Medikonda et al., 2021). CAR T cells against different antigens have been tested in patients with GBM (Ahmed et al., 2017; Brown et al., 2016; O'Rourke et al., 2017). One obstacle to CAR T therapy is the tumor heterogeneity both between patients and intratumorally, and CAR T cell targeting multiple antigens may be more efficacious (Bielamowicz et al., 2018).

Combinations of immunotherapies may be necessary to increase the therapeutic effficacy. Neoantigens for incorporation into a personalized vaccine to treat GBM have been detected (Johanns et al., 2019), and combining such a personalized vaccine with immune checkpoint inhibitors might improve the therapies by inducing or increasing the amount and effector functions of tumor-specific T cells in the tumor (Johanns et al., 2019). However, it is important to remember that the brain is sensitive to inflammation caused by the tumor, as well as by standard therapies and immunotherapies, because it increases the pressure in the brain. As mentioned previously, Medrol is often given to patients to treat edema and can suppress immune responses. Future studies will try to understand which immunotherapeutic strategies have the most promise when combined and if they are effective in patients (Woroniecka & Fecci, 2020).

7 REFERENCES

Ahmed, N., Brawley, V., Hegde, M., Bielamowicz, K., Kalra, M., Landi, D., Robertson, C., Gray, T. L., Diouf, O., Wakefield, A., et al. (2017). HER2-Specific Chimeric Antigen Receptor-Modified Virus-Specific T Cells for Progressive Glioblastoma: A Phase 1 Dose-Escalation Trial. *JAMA Oncol*, 3 (8): 1094-1101. doi: 10.1001/jamaoncol.2017.0184.

Alberts, B., Johnson, A., Lewis, J., Morgan, D., Raff, M., Roberts, K. & Walter, P. (2015). The Innate and Adaptive Immune Systems. In Wolfe, N. (ed.) *Molecular Biology of the Cell*, pp. 1324-1340. New York: Garland Science.

Alexandrov, L. B., Nik-Zainal, S., Wedge, D. C., Aparicio, S. A., Behjati, S., Biankin, A. V., Bignell, G. R., Bolli, N., Borg, A., Børresen-Dale, A. L., et al. (2013). Signatures of mutational processes in human cancer. *Nature*, 500 (7463): 415-21. doi: 10.1038/nature12477.

Badalamenti, G., Fanale, D., Incorvaia, L., Barraco, N., Listì, A., Maragliano, R., Vincenzi, B., Calò, V., Iovanna, J. L., Bazan, V., et al. (2019). Role of tumor-infiltrating lymphocytes in patients with solid tumors: Can a drop dig a stone? *Cell Immunol*, 343: 103753. doi: 10.1016/j.cellimm.2018.01.013.

Banchereau, J. & Steinman, R. M. (1998). Dendritic cells and the control of immunity. *Nature*, 392 (6673): 245-52. doi: 10.1038/32588.

Bernhardt, S. L., Gjertsen, M. K., Trachsel, S., Møller, M., Eriksen, J. A., Meo, M., Buanes, T. & Gaudernack, G. (2006). Telomerase peptide vaccination of patients with non-resectable pancreatic cancer: A dose escalating phase I/II study. *Br J Cancer*, 95 (11): 1474-82. doi: 10.1038/sj.bjc.6603437.

Bernstock, J. D., Mooney, J. H., Ilyas, A., Chagoya, G., Estevez-Ordonez, D., Ibrahim, A. & Nakano, I. (2019). Molecular and cellular intratumoral heterogeneity in primary glioblastoma: clinical and translational implications. *J Neurosurg*: 1-9. doi: 10.3171/2019.5.Jns19364.

Bielamowicz, K., Fousek, K., Byrd, T. T., Samaha, H., Mukherjee, M., Aware, N., Wu, M. F., Orange, J. S., Sumazin, P., Man, T. K., et al. (2018). Trivalent CAR T cells overcome interpatient antigenic variability in glioblastoma. *Neuro Oncol*, 20 (4): 506-518. doi: 10.1093/neuonc/nox182.

Brown, C. E., Alizadeh, D., Starr, R., Weng, L., Wagner, J. R., Naranjo, A., Ostberg, J. R., Blanchard, M. S., Kilpatrick, J., Simpson, J., et al. (2016). Regression of Glioblastoma after Chimeric Antigen Receptor T-Cell Therapy. *N Engl J Med*, 375 (26): 2561-9. doi: 10.1056/NEJMoa1610497.

Brune, W. & Andoniou, C. E. (2017). Die Another Day: Inhibition of Cell Death Pathways by Cytomegalovirus. *Viruses*, 9 (9). doi: 10.3390/v9090249.

Brunsvig, P. F., Aamdal, S., Gjertsen, M. K., Kvalheim, G., Markowski-Grimsrud, C. J., Sve, I., Dyrhaug, M., Trachsel, S., Møller, M., Eriksen, J. A., et al. (2006). Telomerase peptide vaccination: a phase I/II study in patients with non-small cell lung cancer. *Cancer Immunol Immunother*, 55 (12): 1553-64. doi: 10.1007/s00262-006-0145-7.

Brunsvig, P. F., Guren, T. K., Nyakas, M., Steinfeldt-Reisse, C. H., Rasch, W., Kyte, J. A., Juul, H. V., Aamdal, S., Gaudernack, G. & Inderberg, E. M. (2020). Long-Term Outcomes of a Phase I Study With UV1, a Second Generation Telomerase Based Vaccine, in Patients With Advanced Non-Small Cell Lung Cancer. *Front Immunol*, 11: 572172. doi: 10.3389/fimmu.2020.572172.

Chauvin, J. M. & Zarour, H. M. (2020). TIGIT in cancer immunotherapy. *J Immunother Cancer*, 8 (2). doi: 10.1136/jitc-2020-000957.

Chen, D. S. & Mellman, I. (2013). Oncology meets immunology: the cancer-immunity cycle. *Immunity*, 39 (1): 1-10. doi: 10.1016/j.immuni.2013.07.012.

Cieri, N., Camisa, B., Cocchiarella, F., Forcato, M., Oliveira, G., Provasi, E., Bondanza, A., Bordignon, C., Peccatori, J., Ciceri, F., et al. (2013). IL-7 and IL-15 instruct the generation of human memory stem T cells from naive precursors. *Blood*, 121 (4): 573-84. doi: 10.1182/blood-2012-05-431718.

Cobbs, C. S., Harkins, L., Samanta, M., Gillespie, G. Y., Bharara, S., King, P. H., Nabors, L. B., Cobbs, C. G. & Britt, W. J. (2002). Human cytomegalovirus infection and expression in human malignant glioma. *Cancer Res*, 62 (12): 3347-50.

Constantino, J., Gomes, C., Falcão, A., Cruz, M. T. & Neves, B. M. (2016). Antitumor dendritic cell-based vaccines: lessons from 20 years of clinical trials and future perspectives. *Transl Res*, 168: 74-95. doi: 10.1016/j.trsl.2015.07.008.

Crough, T., Beagley, L., Smith, C., Jones, L., Walker, D. G. & Khanna, R. (2012). Ex vivo functional analysis, expansion and adoptive transfer of cytomegalovirus-specific T-cells in patients with glioblastoma multiforme. *Immunol Cell Biol*, 90 (9): 872-80. doi: 10.1038/icb.2012.19.

Cuoco, J. A., Benko, M. J., Busch, C. M., Rogers, C. M., Prickett, J. T. & Marvin, E. A. (2018). Vaccine-Based Immunotherapeutics for the Treatment of Glioblastoma: Advances, Challenges, and Future Perspectives. *World Neurosurg*, 120: 302-315. doi: 10.1016/j.wneu.2018.08.202.

Dosset, M., Castro, A., Carter, H. & Zanetti, M. (2020). Telomerase and CD4 T Cell Immunity in Cancer. *Cancers (Basel)*, 12 (6). doi: 10.3390/cancers12061687.

Fenstermaker, R. A., Ciesielski, M. J., Qiu, J., Yang, N., Frank, C. L., Lee, K. P., Mechtler, L. R., Belal, A., Ahluwalia, M. S. & Hutson, A. D. (2016). Clinical study of a survivin long peptide vaccine (SurVaxM) in patients with recurrent malignant glioma. *Cancer Immunol Immunother*, 65 (11): 1339-1352. doi: 10.1007/s00262-016-1890-x.

Gadalla, R., Noamani, B., MacLeod, B. L., Dickson, R. J., Guo, M., Xu, W., Lukhele, S., Elsaesser, H. J., Razak, A. R. A., Hirano, N., et al. (2019). Validation of CyTOF Against Flow Cytometry for Immunological Studies and Monitoring of Human Cancer Clinical Trials. *Front Oncol*, 9: 415. doi: 10.3389/fonc.2019.00415.

Giles, A. J., Hutchinson, M. N. D., Sonnemann, H. M., Jung, J., Fecci, P. E., Ratnam, N. M., Zhang, W., Song, H., Bailey, R., Davis, D., et al. (2018). Dexamethasone-induced immunosuppression: mechanisms and implications for immunotherapy. *J Immunother Cancer*, 6 (1): 51. doi: 10.1186/s40425-018-0371-5.

Inderberg-Suso, E. M., Trachsel, S., Lislerud, K., Rasmussen, A. M. & Gaudernack, G. (2012). Widespread CD4+ T-cell reactivity to novel hTERT epitopes following vaccination of cancer patients with a single hTERT peptide GV1001. *Oncoimmunology*, 1 (5): 670-686. doi: 10.4161/onci.20426.

Jackson, C. M., Choi, J. & Lim, M. (2019). Mechanisms of immunotherapy resistance: lessons from glioblastoma. *Nat Immunol*, 20 (9): 1100-1109. doi: 10.1038/s41590-019-0433-y.

Johanns, T. M., Miller, C. A., Liu, C. J., Perrin, R. J., Bender, D., Kobayashi, D. K., Campian, J. L., Chicoine, M. R., Dacey, R. G., Huang, J., et al. (2019). Detection of neoantigen-specific T cells following a personalized vaccine in a patient with glioblastoma. *Oncoimmunology*, 8 (4): e1561106. doi: 10.1080/2162402x.2018.1561106.

Kim, N. W. (1997). Clinical implications of telomerase in cancer. *Eur J Cancer*, 33 (5): 781-6. doi: 10.1016/s0959-8049(97)00057-9.

Lam, T. S., van de Meent, M., Falkenburg, J. F. & Jedema, I. (2015). Monocyte-derived dendritic cells can induce autoreactive CD4(+) T cells showing myeloid lineage directed reactivity in healthy individuals. *Eur J Immunol*, 45 (4): 1030-42. doi: 10.1002/eji.201444819.

Lau, S. K., Chen, Y. Y., Chen, W. G., Diamond, D. J., Mamelak, A. N., Zaia, J. A. & Weiss, L. M. (2005). Lack of association of cytomegalovirus with human brain tumors. *Mod Pathol*, 18 (6): 838-43. doi: 10.1038/modpathol.3800352.

Lichtenegger, F. S., Schnorfeil, F. M., Rothe, M., Deiser, K., Altmann, T., Bücklein, V. L., Köhnke, T., Augsberger, C., Konstandin, N. P., Spiekermann, K., et al. (2020). Toll-like receptor 7/8-matured RNA-transduced dendritic cells as post-remission therapy in acute myeloid leukaemia: results of a phase I trial. *Clin Transl Immunology*, 9 (3): e1117. doi: 10.1002/cti2.1117.

Lin, B., Du, L., Li, H., Zhu, X., Cui, L. & Li, X. (2020). Tumor-infiltrating lymphocytes: Warriors fight against tumors powerfully. *Biomed Pharmacother*, 132: 110873. doi: 10.1016/j.biopha.2020.110873.

Lucas, K. G., Bao, L., Bruggeman, R., Dunham, K. & Specht, C. (2011). The detection of CMV pp65 and IE1 in glioblastoma multiforme. *J Neurooncol*, 103 (2): 231-8. doi: 10.1007/s11060-010-0383-6.

Mahnke, Y. D., Brodie, T. M., Sallusto, F., Roederer, M. & Lugli, E. (2013). The who's who of T-cell differentiation: Human memory T-cell subsets. *European Journal of Immunology*, 43 (11): 2797-2809. doi: https://doi.org/10.1002/eji.201343751.

Medikonda, R., Dunn, G., Rahman, M., Fecci, P. & Lim, M. (2021). A review of glioblastoma immunotherapy. *J Neurooncol*, 151 (1): 41-53. doi: 10.1007/s11060-020-03448-1.

Mousset, C. M., Hobo, W., Woestenenk, R., Preijers, F., Dolstra, H. & van der Waart, A. B. (2019). Comprehensive Phenotyping of T Cells Using Flow Cytometry. *Cytometry A*, 95 (6): 647-654. doi: 10.1002/cyto.a.23724.

Nitschke, N. J., Bjoern, J., Iversen, T. Z., Andersen, M. H. & Svane, I. M. (2017). Indoleamine 2,3-dioxygenase and survivin peptide vaccine combined with temozolomide in metastatic melanoma. *Stem Cell Investig*, 4: 77. doi: 10.21037/sci.2017.08.06.

O'Rourke, D. M., Nasrallah, M. P., Desai, A., Melenhorst, J. J., Mansfield, K., Morrissette, J. J. D., Martinez-Lage, M., Brem, S., Maloney, E., Shen, A., et al. (2017). A single dose of peripherally infused EGFRvIII-directed CAR T cells mediates antigen loss and induces adaptive resistance in patients with recurrent glioblastoma. *Sci Transl Med*, 9 (399). doi: 10.1126/scitranslmed.aaa0984.

Oja, A. E., Piet, B., van der Zwan, D., Blaauwgeers, H., Mensink, M., de Kivit, S., Borst, J., Nolte, M. A., van Lier, R. A. W., Stark, R., et al. (2018). Functional Heterogeneity of CD4(+) Tumor-Infiltrating Lymphocytes With a Resident Memory Phenotype in NSCLC. *Front Immunol*, 9: 2654. doi: 10.3389/fimmu.2018.02654.

Papa, M. Z., Vetto, J. T., Ettinghausen, S. E., Mulé, J. J. & Rosenberg, S. A. (1986). Effect of corticosteroid on the antitumor activity of lymphokine-activated killer cells and interleukin 2 in mice. *Cancer Res*, 46 (11): 5618-23.

Pennock, N. D., White, J. T., Cross, E. W., Cheney, E. E., Tamburini, B. A. & Kedl, R. M. (2013). T cell responses: naive to memory and everything in between. *Adv Physiol Educ*, 37 (4): 273-83. doi: 10.1152/advan.00066.2013.

Preusser, M., Lim, M., Hafler, D. A., Reardon, D. A. & Sampson, J. H. (2015). Prospects of immune checkpoint modulators in the treatment of glioblastoma. *Nat Rev Neurol*, 11 (9): 504-14. doi: 10.1038/nrneurol.2015.139.

Reap, E. A., Suryadevara, C. M., Batich, K. A., Sanchez-Perez, L., Archer, G. E., Schmittling, R. J., Norberg, P. K., Herndon, J. E., 2nd, Healy, P., Congdon, K. L., et al. (2018). Dendritic Cells Enhance Polyfunctionality of Adoptively Transferred T Cells That Target Cytomegalovirus in Glioblastoma. *Cancer Res*, 78 (1): 256-264. doi: 10.1158/0008-5472.Can-17-0469.

Reardon, D. A., Brandes, A. A., Omuro, A., Mulholland, P., Lim, M., Wick, A., Baehring, J., Ahluwalia, M. S., Roth, P., Bähr, O., et al. (2020). Effect of Nivolumab vs Bevacizumab in Patients With Recurrent Glioblastoma: The CheckMate 143 Phase 3 Randomized Clinical Trial. *JAMA Oncol*, 6 (7): 1003-1010. doi: 10.1001/jamaoncol.2020.1024.

Richardson, J. R., Schöllhorn, A., Gouttefangeas, C. & Schuhmacher, J. (2021). CD4+ T Cells: Multitasking Cells in the Duty of Cancer Immunotherapy. *Cancers (Basel)*, 13 (4). doi: 10.3390/cancers13040596.

Sabado, R. L., Balan, S. & Bhardwaj, N. (2017). Dendritic cell-based immunotherapy. *Cell Res*, 27 (1): 74-95. doi: 10.1038/cr.2016.157.

Santana, M. A. & Esquivel-Guadarrama, F. (2006). Cell Biology of T Cell Activation and Differentiation. *International Review of Cytology*, 250: 217-274. doi: 10.1016/S0074-7696(06)50006-3.

Schuessler, A., Smith, C., Beagley, L., Boyle, G. M., Rehan, S., Matthews, K., Jones, L., Crough, T., Dasari, V., Klein, K., et al. (2014). Autologous T-cell therapy for cytomegalovirus as a consolidative treatment for recurrent glioblastoma. *Cancer Res*, 74 (13): 3466-76. doi: 10.1158/0008-5472.Can-14-0296.

Seder, R. A., Darrah, P. A. & Roederer, M. (2008). T-cell quality in memory and protection: implications for vaccine design. *Nat Rev Immunol*, 8 (4): 247-58. doi: 10.1038/nri2274.

Sharpe, A. H. & Pauken, K. E. (2018). The diverse functions of the PD1 inhibitory pathway. *Nat Rev Immunol*, 18 (3): 153-167. doi: 10.1038/nri.2017.108.

Shojaei, F., Yazdani-Nafchi, F., Banitalebi-Dehkordi, M., Chehelgerdi, M. & Khorramian-Ghahfarokhi, M. (2019). Trace of survivin in cancer. *Eur J Cancer Prev*, 28 (4): 365-372. doi: 10.1097/cej.0000000000000453.

Smith, C., Lineburg, K. E., Martins, J. P., Ambalathingal, G. R., Neller, M. A., Morrison, B., Matthews, K. K., Rehan, S., Crooks, P., Panikkar, A., et al. (2020). Autologous CMV-specific T cells are a safe adjuvant immunotherapy for primary glioblastoma multiforme. *J Clin Invest*, 130 (11): 6041-6053. doi: 10.1172/jci138649.

Stragliotto, G., Pantalone, M. R., Rahbar, A., Bartek, J. & Söderberg-Naucler, C. (2020). Valganciclovir as Add-on to Standard Therapy in Glioblastoma Patients. *Clin Cancer Res*, 26 (15): 4031-4039. doi: 10.1158/1078-0432.Ccr-20-0369.

Subklewe, M., Geiger, C., Lichtenegger, F. S., Javorovic, M., Kvalheim, G., Schendel, D. J. & Bigalke, I. (2014). New generation dendritic cell vaccine for immunotherapy of acute myeloid leukemia. *Cancer Immunol Immunother*, 63 (10): 1093-103. doi: 10.1007/s00262-014-1600-5.

Uematsu, M., Ohsawa, I., Aokage, T., Nishimaki, K., Matsumoto, K., Takahashi, H., Asoh, S., Teramoto, A. & Ohta, S. (2005). Prognostic significance of the immunohistochemical index of survivin in glioma: a comparative study with the MIB-1 index. *J Neurooncol*, 72 (3): 231-8. doi: 10.1007/s11060-004-2353-3.

van Willigen, W. W., Bloemendal, M., Gerritsen, W. R., Schreibelt, G., de Vries, I. J. M. & Bol, K. F. (2018). Dendritic Cell Cancer Therapy: Vaccinating the Right Patient at the Right Time. *Front Immunol*, 9: 2265. doi: 10.3389/fimmu.2018.02265.

Vik-Mo, E. O., Nyakas, M., Mikkelsen, B. V., Moe, M. C., Due-Tønnesen, P., Suso, E. M., Sæbøe-Larssen, S., Sandberg, C., Brinchmann, J. E., Helseth, E., et al. (2013). Therapeutic vaccination against autologous cancer stem cells with mRNA-transfected dendritic cells in patients with glioblastoma. *Cancer Immunol Immunother*, 62 (9): 1499-509. doi: 10.1007/s00262-013-1453-3.

Wang, X. F., Kerzerho, J., Adotevi, O., Nuyttens, H., Badoual, C., Munier, G., Oudard, S., Tu, S., Tartour, E. & Maillère, B. (2008). Comprehensive analysis of HLA-DR- and

HLA-DP4-restricted CD4+ T cell response specific for the tumor-shared antigen survivin in healthy donors and cancer patients. *J Immunol*, 181 (1): 431-9. doi: 10.4049/jimmunol.181.1.431.
Wherry, E. J. (2011). T cell exhaustion. *Nat Immunol*, 12 (6): 492-9. doi: 10.1038/ni.2035.
Wherry, E. J. & Kurachi, M. (2015). Molecular and cellular insights into T cell exhaustion. *Nat Rev Immunol*, 15 (8): 486-99. doi: 10.1038/nri3862.
Wilcox, J. A., Ramakrishna, R. & Magge, R. (2018). Immunotherapy in Glioblastoma. *World Neurosurg*, 116: 518-528. doi: 10.1016/j.wneu.2018.04.020.
Wirsching, H. G., Galanis, E. & Weller, M. (2016). Glioblastoma. *Handb Clin Neurol*, 134: 381-97. doi: 10.1016/b978-0-12-802997-8.00023-2.
Woroniecka, K. & Fecci, P. E. (2020). Immuno-synergy? Neoantigen vaccines and checkpoint blockade in glioblastoma. *Neuro Oncol*, 22 (9): 1233-1234. doi: 10.1093/neuonc/noaa170.
Zanetti, M. (2017). A second chance for telomerase reverse transcriptase in anticancer immunotherapy. *Nat Rev Clin Oncol*, 14 (2): 115-128. doi: 10.1038/nrclinonc.2016.67.
Zhang, Y. & Zheng, J. (2020). Functions of Immune Checkpoint Molecules Beyond Immune Evasion. *Adv Exp Med Biol*, 1248: 201-226. doi: 10.1007/978-981-15-3266-5_9.

SUPPLEMENTARY

Supplementary table 1. Overview of the amount of cells and the viability of the cells after thawing. One-two vials were thawed.

Sample ID	Number of cells	Viability
CoU-GBM #019		
20.04.15	$34{,}8*10^6$	92%
25.06.15	$13{,}8*10^6$	77%
27.08.15	$22{,}5*10^6$	87%
28.10.15	$31{,}5*10^6$	94%
23.12.15	$19{,}64*10^6$	87%
09.02.15	$3{,}34*10^7$	81%
26.04.16	$22{,}2*10^6$	93%
02.12.14	$29{,}4*10^6$	89%
08.05.17	$12{,}88*10^6$	76%
Monocytes	$9{,}4*10^6$	89%
CoU-GBM #027		
14.01.14	$10{,}24*10^6$	94%
04.12.13	$13{,}12*10^6$	92%
18.02.14	$6{,}54*10^6$	95%
25.03.14	$17{,}78*10^6$	90%
29.04.14	$8{,}22*10^6$	85%
03.06.14	$14{,}88*10^6$	95%
08.07.14	$15{,}42*10^6$	86%
05.08.14	$22{,}23*10^6$	91%
02.09.14	$2*10^6$	71%
30.09.14	$7{,}35*10^6$	69%
28.10.14	$14{,}04*10^6$	87%
25.11.14	$18{,}09*10^6$	94%
05.01.15	$16{,}75*10^6$	89%
02.02.15	$42{,}25*10^6$	91%
02.03.15	$16{,}45*10^6$	92%
07.04.15	$18{,}9*10^6$	93%
05.05.15	$16{,}64*10^6$	95%
01.06.15	$26*10^6$	95%
29.06.15	$8*10^6$	78%
15.09.15	$14*10^6$	93%
TILs 16.10.15	$2{,}82*10^6$	90%
TILs 13.11.15	$8{,}5*10^6$	70%
TILs 20.11.15	$5*10^6$	92%
Monocytes	$6*10^6$	89%
CMV stimulated 03.06.14	$8{,}45*10^5$	65%
CMV stimulated 08.07.14	$9{,}01*10^5$	59%
CMV stimulated 25.11.14	$8{,}72*10^5$	53%
CMV stimulated TILs	$2{,}6*10^6$	49%
CoU-GBM #028		
16.01.14	$15{,}62*10^6$	95%
17.02.14	$18{,}38*10^6$	94%
18.06.14	$4{,}88*10^6$	94%
07.11.14	$20{,}6*10^6$	95%
17.03.14	$12{,}9*10^6$	92%
20.05.14	$13{,}8*10^6$	87%
16.07.14	$11{,}3*10^6$	94%
14.08.14	$17{,}3*10^6$	93%
08.10.14	$5{,}54*10^6$	85%
TILs 20.06.14	$3{,}64*10^6$	90%
TILs 20.06.14	$10{,}5*10^6$	73%
CoU-GBM #035		
09.02.15	$29{,}7*10^6$	91%
16.03.15	$17{,}45*10^6$	82%

13.04.15	$18*10^6$	78%
11.05.15	$13*10^6$	88%
06.07.15	$7{,}1*10^6$	58%
CoU-GBM #038		
21.01.15	$19{,}48*10^6$	90%
04.03.15	$2{,}14*10^7$	95%
08.04.15	$2{,}98*10^7$	91%
06.05.15	$13{,}08*10^6$	92%
03.06.15	$12{,}34*10^6$	91%
01.07.15	$14{,}96*10^6$	92%
29.07.15	$12{,}7*10^6$	93%
26.08.15	$12{,}4*10^6$	92%
23.09.15	$12{,}2*10^6$	94%
CMV stimulated 23.09.15	$9*10^5$	68%
CMV stimulated 29.07.15	$9{,}5*10^5$	72%
CoU-GBM #044		
16.06.16	$15{,}6*10^6$	94 %
01.08.16	$14{,}6*10^6$	96 %
26.09.16	$9{,}6*10^6$	97%
21.11.16	$11{,}5*10^6$	86%
CMV stimulated 16.06.16	$1{,}5*10^6$	63%
CMV stimulated 01.08.16	$1{,}48*10^6$	55%
CMV stimulated 26.09.16	$9{,}78*10^5$	58%
Monocytes	$5{,}82*10^6$	86%

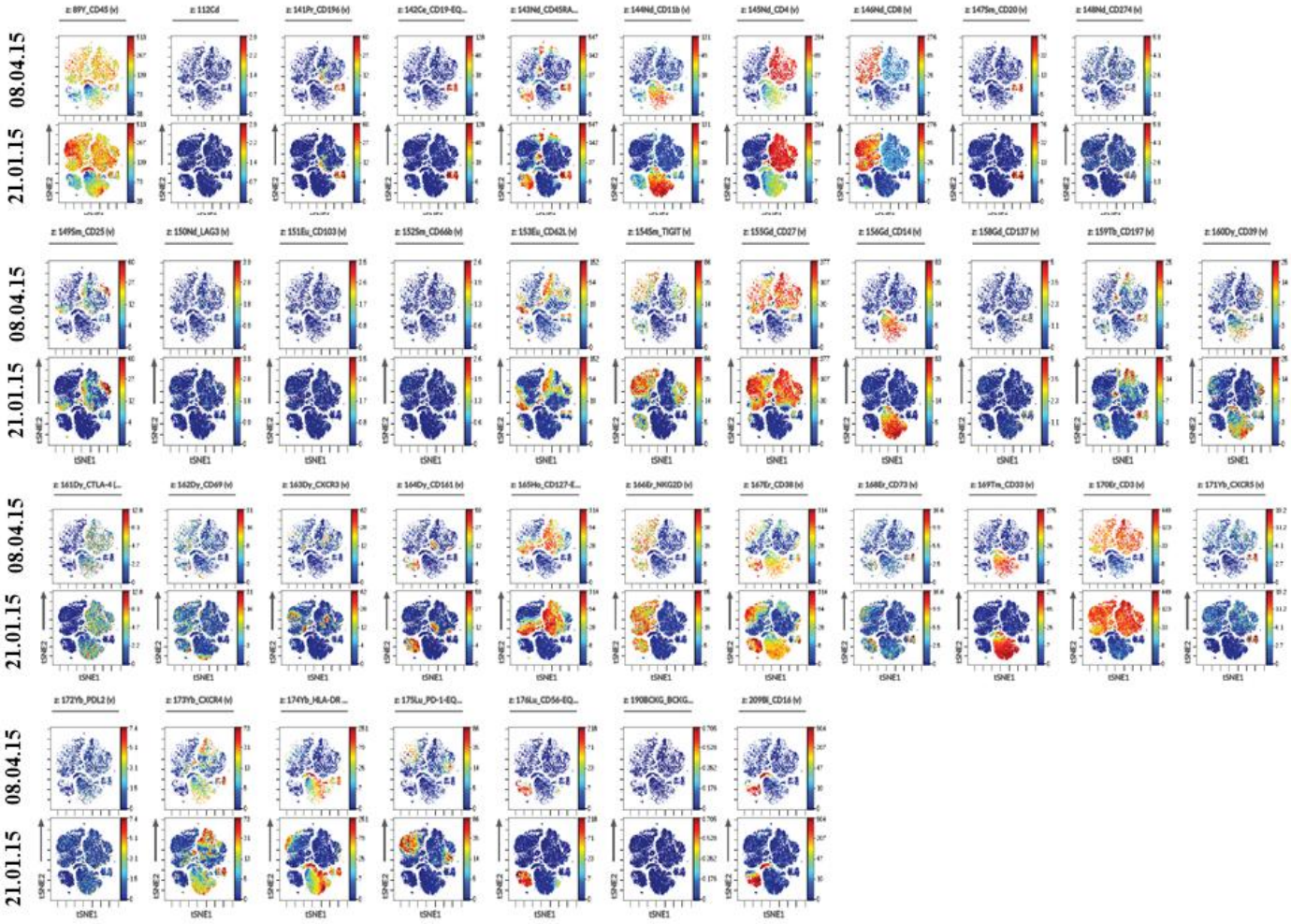

Supplementary figure 1. ViSNE plots of PBMCs from CoU-GBM #038

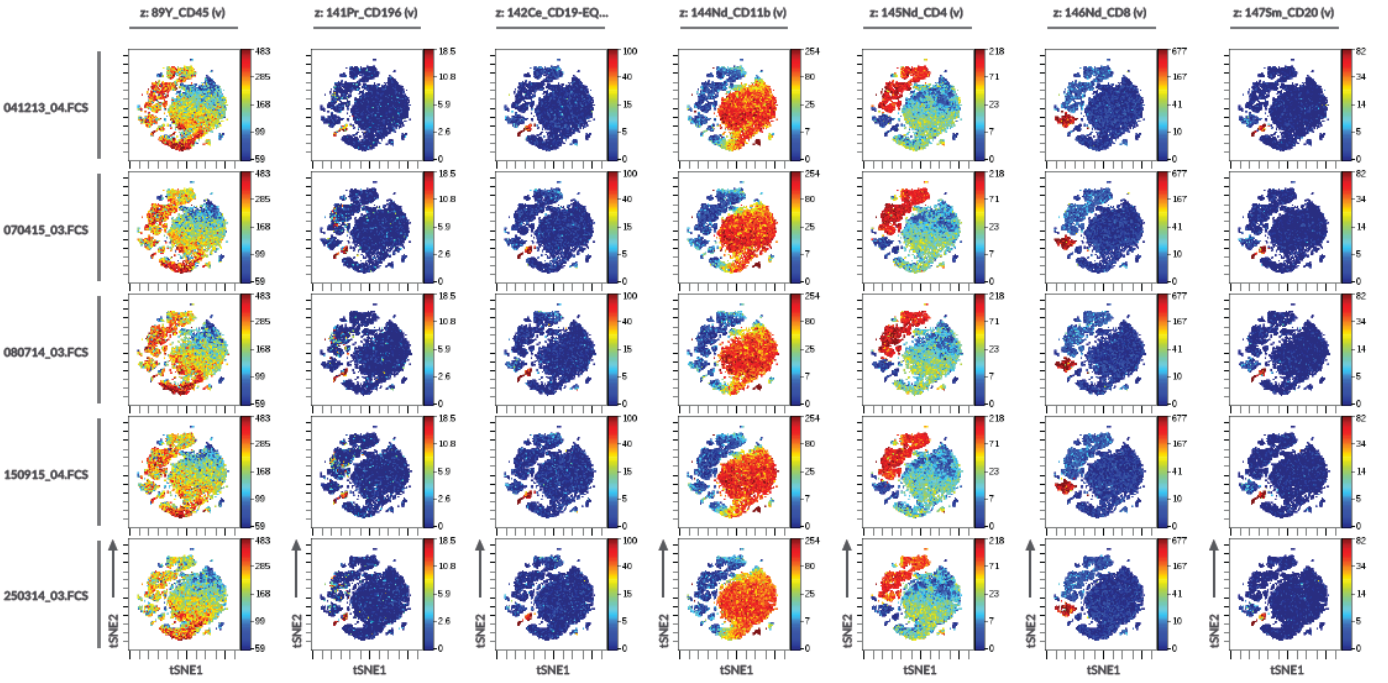
z: 89Y_CD45 (v)
z: 141Pr_CD196 (v)
z: 142Ce_CD19-EQ...
z: 144Nd_CD11b (v)
z: 145Nd_CD4 (v)
z: 146Nd_CD8 (v)
z: 147Sm_CD20 (v)
041213_04.FCS
070415_03.FCS
080714_03.FCS
150915_04.FCS
250314_03.FCS
tSNE1
tSNE2

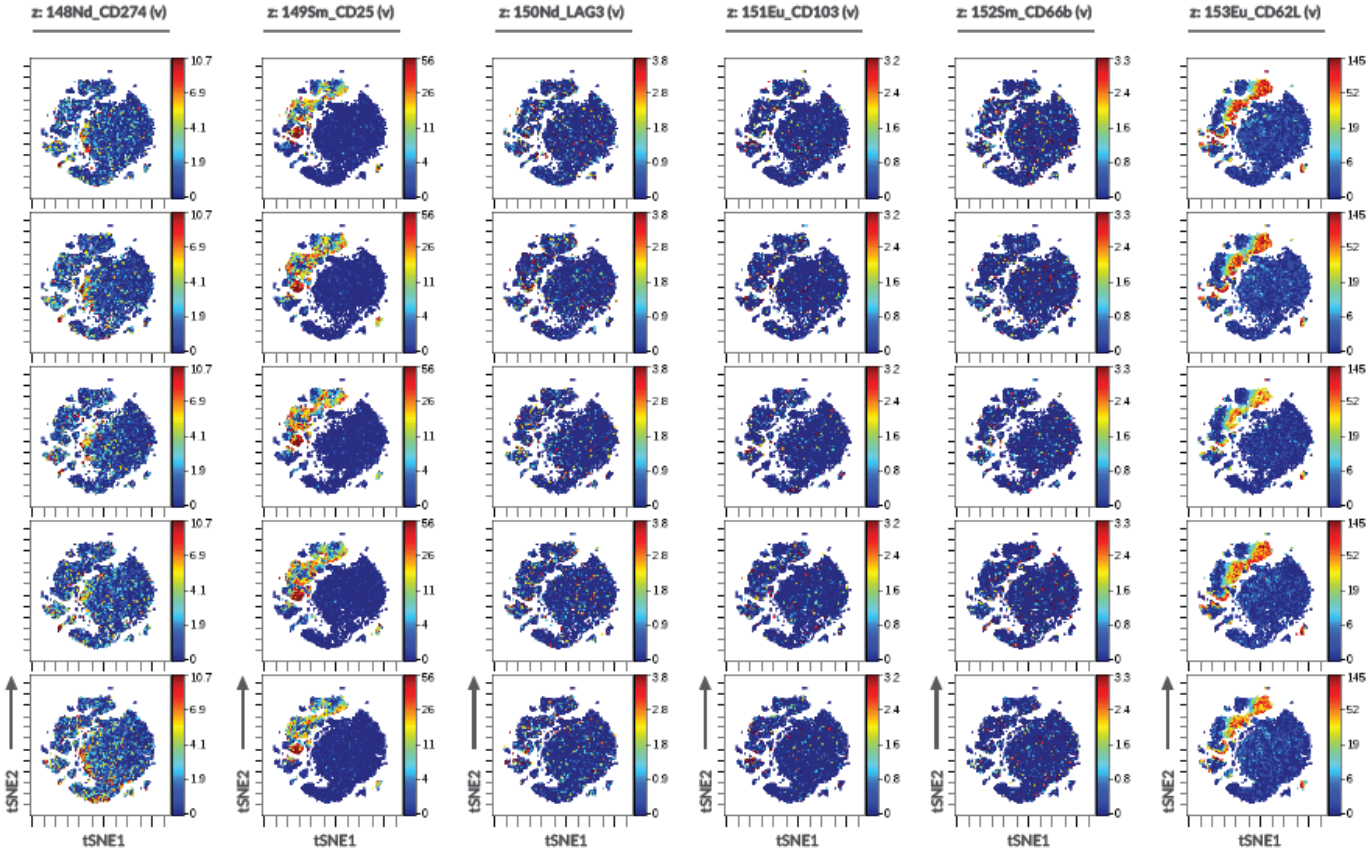
z: 148Nd_CD274 (v)
z: 149Sm_CD25 (v)
z: 150Nd_LAG3 (v)
z: 151Eu_CD103 (v)
z: 152Sm_CD66b (v)
z: 153Eu_CD62L (v)
tSNE1
tSNE2

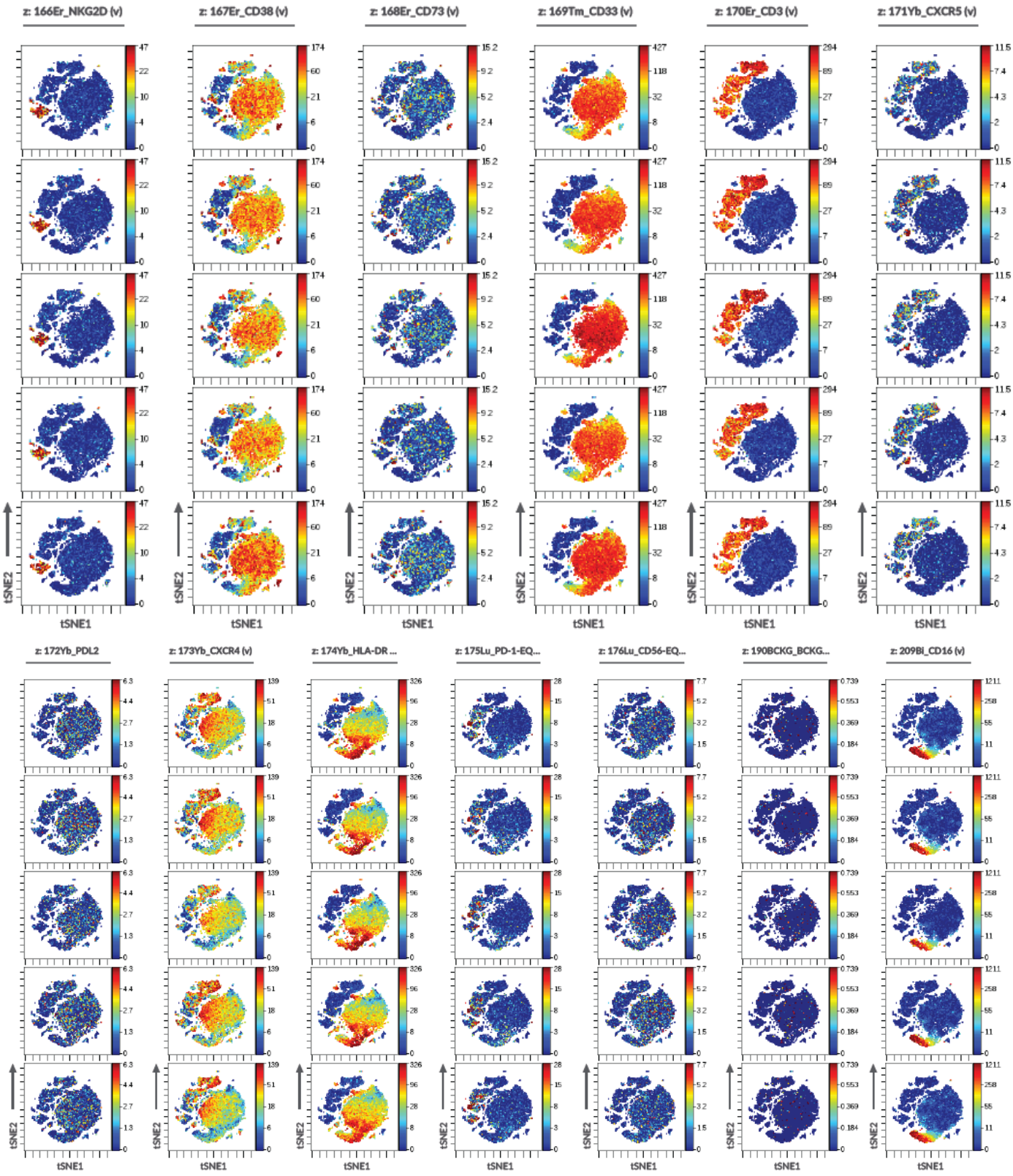
z: 166Er_NKG2D (v)
z: 167Er_CD38 (v)
z: 168Er_CD73 (v)
z: 169Tm_CD33 (v)
z: 170Er_CD3 (v)
z: 171Yb_CXCR5 (v)
z: 172Yb_PDL2
z: 173Yb_CXCR4 (v)
z: 174Yb_HLA-DR ...
z: 175Lu_PD-1-EQ...
z: 176Lu_CD56-EQ...
z: 190BCKG_BCKG...
z: 209Bi_CD16 (v)
tSNE1
tSNE2

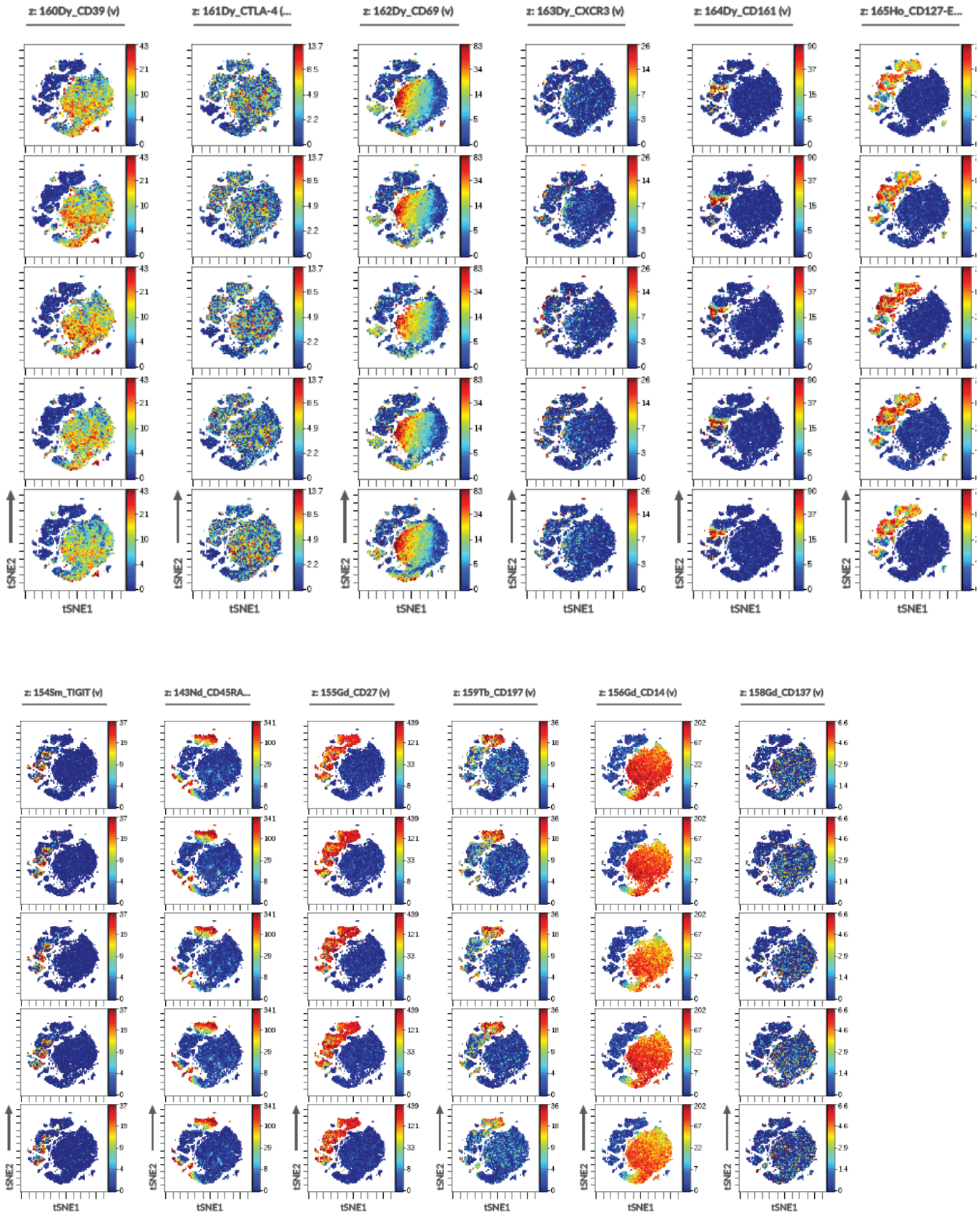

Supplementary figure 2. ViSNE plots of PBMCs from CoU-GBM #027

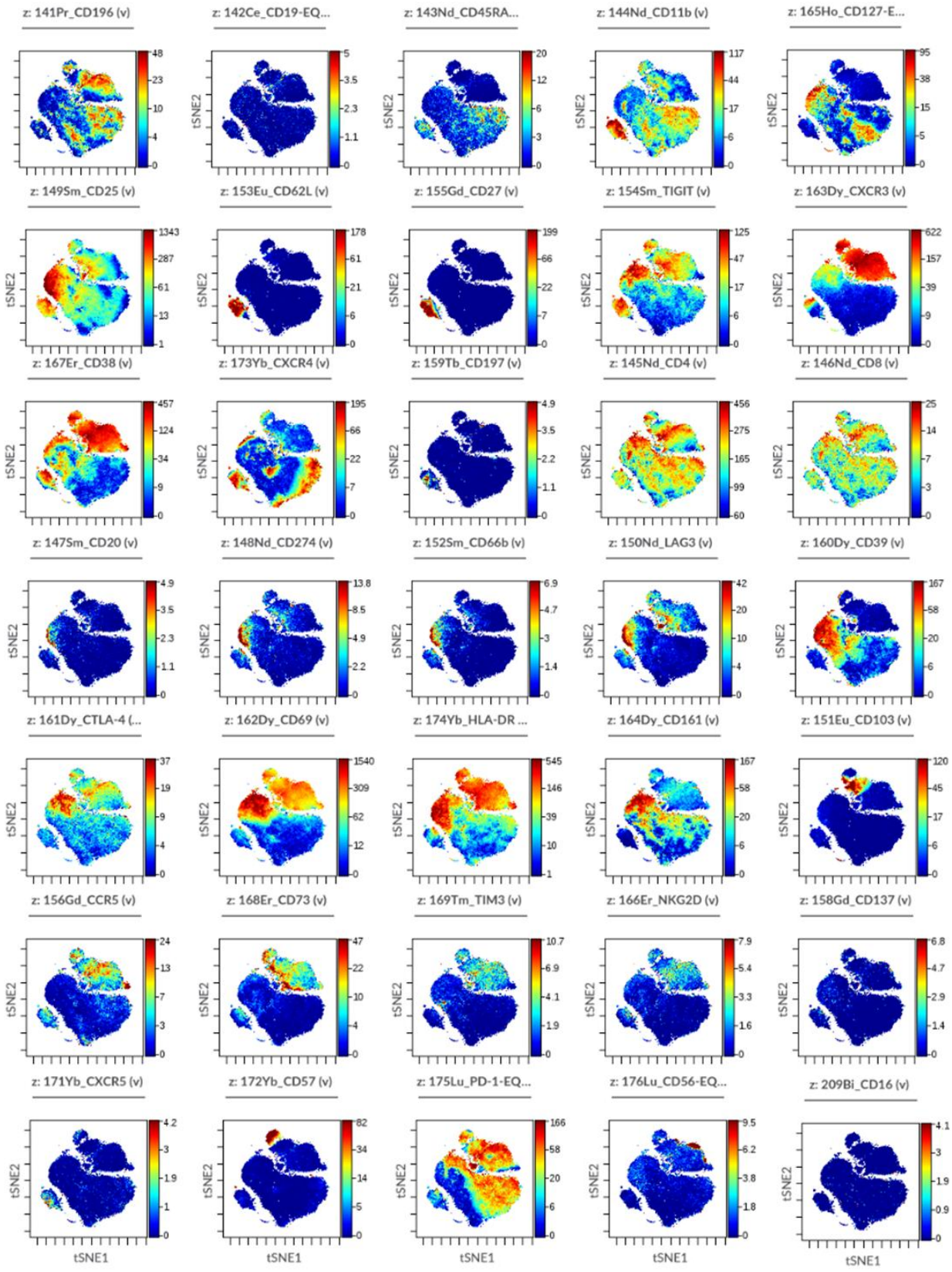

Supplementary figure 3. ViSNE plots of TILs from CoU-GBM #027

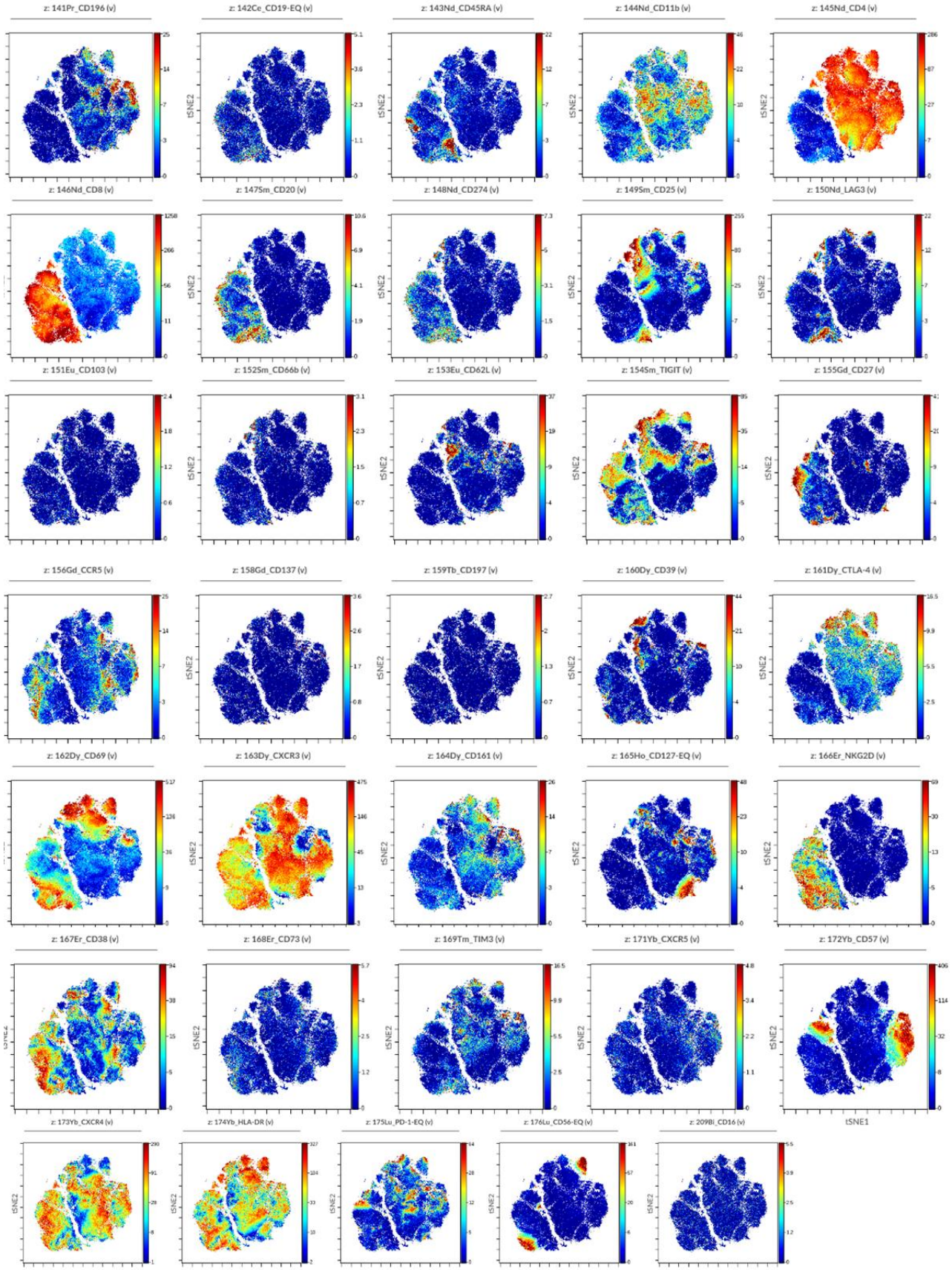

Supplementary figure 4. ViSNE plots of TILs from CoU-GBM #028

Norges miljø- og biovitenskapelige universitet
Noregs miljø- og biovitskapelege universitet
Norwegian University of Life Sciences

Postboks 5003
NO-1432 Ås
Norway